Università degli Studi di Padova

Sede Amministrativa: Università degli Studi di Padova

Dipartimento di Salute della Donna e del Bambino – SDB

SCUOLA DI DOTTORATO DI RICERCA IN:

MEDICINA DELLO SVILUPPO E SCIENZE DELLA PROGRAMMAZIONE

INDIRIZZO: Ematooncologia, immunologia e genetica

CICLO XXVI

SET UP OF DIFFERENT STRATEGIES TO SELECTIVELY TARGET GLIOBLASTOMA CELLS

Direttore della Scuola: Ch.mo Prof. Giuseppe Basso

Coordinatore d'indirizzo: Ch.mo Prof. Giuseppe Basso

Supervisore: Dott. Luca Persano

Dottoranda: Sara Bianco

A tutti Coloro

che mi hanno permesso

di arrivare fino a QUI

Infinite Grazie

Table of contents

SUMMARY

Glioblastoma Multiforme (GBM) is the most common malignant brain tumor in adults, displaying fast growth, vascular proliferation, diffuse infiltrative nature into the brain parenchyma and necrosis areas. Despite optimal multimodal therapeutical treatment including surgical resection followed by radiotherapy and chemotherapy, the prognosis of patients remains still dismal, with a median survival of 14 months. One hypothesis seems to be related to the existence in the brain of the Cancer Stem Cells (CSCs). These cells are so-called Glioma Stem Cells (GSCs) and are described as a sub population of undifferentiated tumor-cells with stem-like properties, self-renewal, multi-lineage differentiation ability, maintained proliferation and highly tumorigenic potential in immune-deficient mice. GSCs seem to be play a key role in GBM initiation and progression, contributing to chemotherapy and radiotherapy resistance and tumor recurrence.

Therefore, there is an urgent need to develop novel therapeutic approaches, to selectively target GSCs.

In this study, we focus on two different therapeutical approaches:

- the use of Mesenchymal Stem Cells (MSCs) as delivery vehicles for brain tumor therapy, exploiting their inherent tumor-tropism probably related to the effect of cytokines and chemokines, secreted by infiltrated tissues.
- Virotherapy, employing the R3616 as neuroattenuated Herpes Simplex Virus type1. R3616 is a HSV1 mutant deleted for both copies of the gene γ34.5, important for viral replication and neurovirulence. The effect of these deletions inhibits autophagy, blocks virus-induced host protein shutoff, and attenuate virus replication in GSCs, minimizing neurotoxicity.

GSCs employed for this study have been isolated from GBM specimens obtained during surgical procedures of tumor removal and cultured in adhesion under normoxic and hypoxic conditions or in suspension as neurospheres under normoxic conditions. Neuropheres were phenotypically characterized for some of stemness markers, such as CD133, Nestin, Sox2 and CD44.

In order to choose the best cell candidate for cell delivery experiments, we investigated between hMSCs isolated from human bone marrow of healthy donors (BM-MSCs) and glioma patients adipose tissue (AT-MSCs) obtained during GBM surgical resection. hMSCs from both sources were phenotypically characterized and cultured under hypoxic and normoxic conditions in order to mimic the peculiar and heterogeneous GBM microenvironment towards cells would be further delivered. The BM-MSCs retained: a.) faster growth, b.) a greater *in vitro* multilineage differentiative potential and c.) increased migratory ability than AT-MSCs, especially in hypoxic conditions; thus suggesting to be the most suitable vehicles for our future analyses.

Moreover, we evaluated BM-MSCs tropism to GBM derived cells modulated by oxygen levels or by the presence and absence of soluble factors shown to be able to stimulate astro-glial and neuronal differentiation, such as BMP2 and WNT3a respectively. Indeed, BMPs are members of the Transforming Growth Factor-β (TGF-β) Superfamily shown to stimulate both proliferation and mitotic arrest, to promote astro-glial differentiation reducing cell growth and increasing portion of $GFAP^+$ cells. Wnt3a ligand mediates neuronal differentiation and proliferation inhibition of GBM cells and this phenomenon is enhanced under hypoxic conditions.

hMSCs tropism was assessed both when primary GBM –derived cells were pre-treated alternatively with BMP2 or WNT3a and when such factors were delivered towards GBM cells. Our data demonstrated pro-differentiating molecules as enhancing agents of hMSCs migratory properties, especially in hypoxia.

Experiments involving viruses were performed both on HSV1 wild type and R3616 to test the ability to replicate in and to kill GSCs. As expected for a neuroattenuated virus, R3616 replication in GSCs was widely impaired and the killing ability were decreased compared to the wild type. Both viruses were also employed to test their replication capacity and cytotoxicity in BM-MSCs. Compared to HSV1 wild type, R3616 retained impaired replication efficiency and attenuated killing ability in hMSCs.

BM-MSCs inherent tropism was also investigated in GSCs infected with HSV1 wild type or R3616. Interestingly, we found that GSCs R3616 infected significantly increased the migratory properties of BM-MSCs.

In conclusion, these findings support the use of BM-MSCs as a promising cell vehicle candidate for tumor-specific delivery and open the way to the development of engineered BMPs-expressing MSCs to further assays in GBM -derived cells.

Additionally, the R3616 ability to kill GSCs encourages next efforts to combine both methods to obtain an efficient strategy to selectively target GSCs. Our preliminary data have already demonstrated that co-treatment of R3616 and BMP2 increases the differentiation markers expression. Accordingly, BM-MSCs retained a preferential inherent homing towards more differentiated cells.

SOMMARIO

Il Gliobalstoma multiforme (GBM) è il più comune e maligno dei tumori cerebrali nell'adulto, caratterizzato da una rapida crescita, proliferazione vascolare e diffusa infiltrazione nel parenchima cerebrale. Nonostante negli ultimi anni siano stati fatti notevoli progressi terapeutici che includono la rimozione chirurgica della massa, seguita da radioterapia e chemioterapia, la prognosi ancora oggi permane particolarmente infausta con una sopravvivenza media di circa 14 mesi dalla diagnosi. Ciò pare sia associato anche all'esistenza nel cervello di una popolazione di cellule definita "Cancer Stem Cells" (CSCs). Tali cellule vengono definite Glioma Stem Cells (GSCs) e, al pari delle normali cellule neuronali staminali, sono caratterizzate da capacità di auto-rinnovamento, sono multipotenti, nonché tumorigeniche *in vivo*.

Inoltre, le GSCs sembrano svolgere un ruolo importante nell'insorgenza e la progressione del GBM, contribuendo appunto alla resistenza alla chemioterapia e alla radioterapia, oltre ad essere responsabili delle recidive di tale tumore. A fronte di tutto ciò, si rende quindi necessario più che mai lo sviluppo di nuove strategie terapeutiche che siano particolarmente selettive e mirate a colpire la popolazione delle GSCs. In questo lavoro di tesi, abbiamo posto la nostra attenzione in particolare a due strategie:

- L'uso delle Cellule Staminali Mesenchimali (MSCs) come sistemi di delivery cellulari per composti attivi contro i tumori cerebrali sfruttando il loro intrinseco tropismo per il letto tumorale per effetto di citochine e chemochine rilasciate dai tessuti infiltrati.
- L'utilizzo di un virus oncolitico di tipo herpetico, R3616, ingegnerizzato per colpire selettivamente le cellule tumorali e non causare neurovirulenza, essendo stato deleto dei geni γ34.5 responsabili dell'insorgenza di encefalite. L'effetto di queste delezioni inoltre comporta inibita autofagia e attenuata replicazione anche nelle stesse GSCs.

Le GSCs utilizzate per i nostri esperimenti sono state derivate da biopsie di pazienti affetti da GBM e coltivate in adesione al 21% che al 2% di O_2 o in sospensione al 21% di O_2 come neurosfere secondo i parametri previsti da protocolli accettati in letteratura.

Le cellule cresciute come neurosfere sono state caratterizzate fenotipicamente con alcuni dei più comuni marcatori di staminalità, tra cui il CD133, la Nestina, Sox2 e il CD44.

Per gli esperimenti di delivery cellulari sono state inizialmente valutate le hMSCs isolate dai campioni di midollo osseo derivanti da donatori sani (BM-MSCs) e da tessuto adiposo (AT-MSCs) cerebrale prelevato durante l'intervento di rimozione chirurgica di GBM dello stesso paziente. Le MSCs appartenenti ad entrambe le fonti sono state immuno-fenotipicamente caratterizzate e coltivate in ipossia e in normossia al fine di valutarne la capacità e l'efficienza di crescita ricreando il tipico microambiente del GBM verso cui poi le cellule dovrebbero essere fatte migrare. Saggi a.) di crescita, b.) di differenziamento *in vitro* e c.) di migrazione hanno evidenziato come le BM-MSCs migrino in maniera più efficiente e selettiva delle AT-MSCs verso le cellule tumorali, specie in condizioni ipossiche. Pertanto, le BM-MSCs sono state scelte come modello di delivery cellulare per proseguire i nostri esperimenti. Inoltre abbiamo visto come questa migrazione avvenga anche verso cellule tumorali pre-trattate con fattori morfogeni ad effetto pro-differenziativo nei gliomi, quali BMP2 e WNT3a. Le BMPs sono membri della Famiglia del Transforming Growth Factor-β (TGF-β), e sono in grado a livello cerebrale di portare ad arresto del flusso mitotico, blocco della proliferazione cellulare e ad un'azione di differenziamento in senso gliale aumentando la percentuale di cellule a fenotipo $GFAP^+$. Il Wnt3a è noto essere invece un ligando in grado di promuovere il differenziamento in senso neuronale e inibire la proliferazione cellulare, specie in ipossia.

Per gli esperimenti di Virotherapy si è innanzitutto valutata la capacità di replicazione e di morte cellulare del virus deleto R3616 paragonandola all' efficienza dell'HSV1 wild type nelle GSCs. R3616 ha dimostrato un'efficienza di replicazione e di uccisione attenuata rispetto all'HSV1 wild type. Entrambi i virus sono stati poi testati per valutare la capacità di replicazione e di killing nelle BM-MSCs. Rispetto all' HSV1 wild type, R3616 ha riportato una minore citotossicità e compromessa capacità di replicazione.

L'efficienza di migrazione delle BM-MSCs è stata poi valutata in GSCs infettate sia con HSV1 wt, sia con R3616. In entrambi i casi è trovato un aumentato tropismo delle BM-MSCs, specie quando le GSCs erano state infettate con R3616.

In conclusione in questo lavoro, proponiamo l'utilizzo di cellule staminali mesenchimali come veicolo per trattare il Glioblastoma con molecole fisiologiche ad azione pro-differenziativa così da aumentarne la risposta agli attuali trattamenti chemioterapici.
Inoltre, l'aumentata efficienza di migrazione insieme alla capacità di uccisione selettiva delle GSCs riscontrata nell'utilizzo di R3616, incoraggiano a un trattamento di combinazione dei due possibili approcci. Risultati preliminari hanno già evidenziato come GSCs infettate con R3616 e trattate con BMP2 siano in grado di aumentare l'espressione dei canonici marcatori di differenziamento cellulare e ciò incoraggia a valutare se tale effetto possa stimolare ulteriormente l'efficienza e aumentare la selettività di migrazione delle BM-MSCs.

1. INTRODUCTION

1.1 CLASSIFICATION OF BRAIN TUMORS

Primary Brain Tumors are a heterogeneous group of malignancies that originate and reside within the Central Nervous System (CNS) (Germano et al., 2010).

In Europe, about 27,700 new CNS tumors are diagnosed (Crocetti et al., 2012). The incidence of primary CNS cancers ranges from 4.5 to 11.2 cases per 100,000 men and from 1.6 to 8.5 per 100,000 women according to the data provided by the Surveillance of Rare Cancers in Europe (RARECARE; www.rarecare.eu) (Crocetti et al., 2012). The peak of incidence is 18.5/100,000 among people over 65 years (Crocetti et al., 2012) with the 5-year survival rate of 17% for males and 19% for females (Sant et al., 2009) and differences across European regions (Crocetti et al., 2012).

Among CNS tumors, gliomas are the most common primary malignancies. They arise from the constituent glial cells of the brain (Masui et al., 2012). that supply nutrients, oxygen and maintain the physiological homeostasis. According to their morphological appearance gliomas are defined as astrocytomas, composed predominantly of astrocytes, oligodendrogliomas, composed predominantly of oligodendrocytes, and tumors containing a mixtures of various glial cells (i.e. oligoastrocytomas) and ependymal cells (i.e. ependymomas) (Dolecek et al., 2012).

Among them, astrocytomas are the most common CNS tumors, with an incidence rate of 4.8 per 100,000 per year in Europe (Crocetti et al., 2012).

The World Health Organization (WHO) grading system further classifies gliomas into four different grades (I–IV) based on the degree of malignancy, as determined by histopathological criteria (Louis et al., 2007):

- grade I: pilocytic astrocytoma,
- grade II: diffuse astrocytoma,
- grade III: anaplastic astrocytoma,
- grade IV: Glioblastoma Multiforme.

Grade I astrocytomas (pilocytic astrocytomas) are slow-growing, relatively circumscribed and benign tumors.
Grade II (diffuse astrocytomas), so-called low grade astrocytomas, are histologically characterized by moderate cellularity, mild nuclear atypia, rare or absent mitotic figures and they are moderately proliferative and invasive. Conversely, grade III (anaplastic astrocytomas) and IV (glioblastoma multiforme) astrocytomas are defined as high-grade gliomas (Nager et al., 2012).
Grade III (anaplastic astrocytoma) tumors are characterized by increased cellularity, nuclear atypia, and mitotic activity. These tumors are more proliferative and infiltrative compared with grade II gliomas.
Grade IV astrocytomas display uncontrolled cellular proliferation, diffuse infiltration, robust angiogenesis, necrotic tissue and hypoxic areas (Westphal and Lamszus, 2011).

1.2 GLIOBLASTOMA MULTIFORME (GBM)

Glioblastoma Multiforme (GBM) is the most aggressive and highly lethal form of primary brain tumor in adults. In industrialized countries, the annual incidence of GBM is 2-3 cases per 100,000 people (Louis et al., 2007) (Wen and Kesari, 2008), with a median survival of 14.6 months after diagnosis (Dolecek et al., 2012) (Stopschinski et al., 2013) (Germano et al., 2010) (Nager et al., 2012).

No underlying causes have been identified for GBMs. There are few known risk factors, such as the exposure to ionizing radiation (Wen and Kesari, 2008) and the exposure to electromagnetic fields (Crocetti et al., 2012); no preventive strategies and no practical methods for screening (Dirks, 2010). Only about the 5% of patients present family history of gliomas, but in most of these familial cases no common genetic aberrations have been currently identified (Wen and Kesari, 2008). GBM affects preferentially men than women and it is more common in whites than in blacks. The median age of patients at the time of diagnosis is approximately 64 years (Wen and Kesari, 2008) (Fisher et al., 2007). Most common symptoms are headache, nausea, focal neurological deficits (visual impairment), alterations in mental status or epileptic seizures depending on the localization of the tumor, intracranial pressure and grade of infiltration into the brain parenchyma (Louis et al., 2007).

GBM is usually located in the cerebral hemispheres (Robert and Wastie, 2008). It can grow quickly and become very large before producing symptoms. About 50% of identified GBMs occupy more than one lobe of a hemisphere, or are expanded bilaterally (Ohgaki and Kleihues, 2005a) (Robert and Wastie, 2008). GBMs may even extend to the meningeal or ventricular wall and only rarely malignant cells may spread to the spinal cord. Extracranial metastasis of GBM beyond the CNS is extremely rare event, with a reported frequency of only 0.44% (Robert and Wastie, 2008).

In **Figure 1.** is shown an example of the Magnetic Resonance Imaging (MRI) scan in a patient affected of GBM at the left hemisphere (Dirks, 2008).

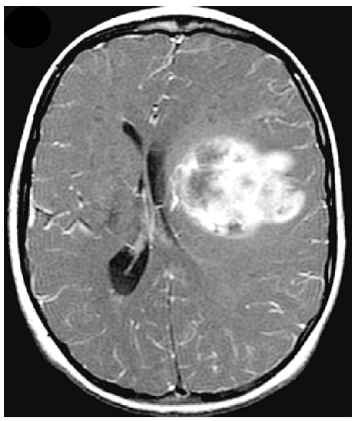

Figure 1. Magnetic Resonance Imaging (MRI) of GBM-affected patient at the left-hemisphere (Dirks, 2008)**.**

GBM can occur as *"primary"* or *"secondary"* tumors based on clinical characteristics (Nager et al., 2012) (Westphal and Lamszus, 2011):

- *primary* or "*de novo*" GBM, representing the majority of GBM cases, arise without any prior evidence of a lower-grade precursor lesion and it is detected more commonly in older patients (mean age of 62 years);
- *secondary* GBM, develops progressively from a lower-grade glioma and typically occur in younger patients (median age of 45 years), generally over a period of 5–10 years.

Such distinction also reflects mutations and perturbed signaling pathways important for GBM progression (Ohgaki and Kleihues, 2005b); nonetheless, primary and secondary GBMs remain morphologically indistinguishable and respond similarly to currently conventional therapies (Wen and Kesari, 2008).

The majority of GBM present genetic alterations that occur through epigenetic modifications, point mutations, translocations, amplifications, or deletions leading to a deregulated signaling pathway and contributing to a so heterogeneous and aggressive tumorigenesis (Chen et al., 2012).

On the base of gene expression profile data, The Cancer Genome Atlas (TCGA) classified GBM into four different molecular subgroups (Nigro et al., 2005): (a.) *Proneural*, (b.) *Neural*, (c.) *Classical* and (d.) *Mesenchymal* (Stopschinski et al., 2013) (Sulman et al., 2009) (Lei et al., 2011) (Parsons et al., 2008).

Interestingly, each of these subtypes shown an enrichment of gene expression signatures from distinct neural lineages, implying that the expression patterns of the different subtypes may reflect the phenotype of their specific cells of origin (Noushmehr et al., 2010). These molecular signatures were associated with tumor aggressiveness and disease progression and could be related to the different signaling pathways implicated in the gliomagenesis.

Notably, *proneural* GBM comprised patients with primary diagnosis, younger age and better clinical outcome; *mesenchymal* GBM showed older patients and patient with tumor relapse (Stopschinski et al., 2013).

1.3 GBM TREATMENTs

The standard of care for newly diagnosed GBM involves surgical resection, radiotherapy (60 Gy over a period of 6 weeks) with concomitant chemotherapy with Temozolomide (Temodal ^{TM}) (75 mg per square meter of body-surface area per day for 6 weeks) followed by adjuvant chemotherapy with Temozolomide (TMZ), (150 to 200 mg per square meter per day for 5 days every 28 days for 6 cycles), according to The European Organization for Research and Treatment of Cancer (EORTC) and the

National Cancer Institute of Canada (NCIC) regime published by Stupp in 2005 (Stupp et al., 2005) (Stopschinski et al., 2013).

As reported by Stupp et al. (Stupp et al., 2005) (Stupp et al., 2009a), the combination of radiotherapy and TMZ had an acceptable side-effect profile and, compared with radiotherapy alone treatment (60 Gy over a period of 6 weeks), increased the median survival from 12.1 to 14.6 months (Stupp et al., 2009a) (Wen and Kesari, 2008) (Weller et al., 2010). In addition, the survival rate at 2 years among the patients who received radiotherapy plus TMZ was significantly greater than the rate among the patients who received radiotherapy alone (27.2% vs. 10.9%).

Beyond the standard of care treatment, another chemotherapeutic approach for GBM involves the implantation of biodegradable polymers (wafers) containing Carmustine (Gliadel Wafers, MGI Pharma), at the time of surgical resection of the tumor. Wafers are implanted in the surgical cave and positioned in tight contact with the brain surface infiltrated by the tumor. Each wafer, 1.45 cm in diameter and 200 mg weight, contains 7.7 mg of Carmustine (Fleming and Saltzman, 2002).

The aim of the treatment with these polymers, which release Carmustine gradually over the course of several weeks, is to kill residual tumor cells.

In a randomized, placebo-controlled trial that investigated the use of Carmustine polymers in patients with newly diagnosed malignant gliomas, median survival increased from 11.6 months to 13.9 months at 2 years (Wen and Kesari, 2008) (Westphal et al., 2003).

TMZ and Carmustine are two alkylating agents. TMZ is administered orally as a prodrug that at physiological pH hydrolyzes spontaneously to its active metabolite: the 5-(3-metyltriazen-1-yl)imidazole-4-carboxamide (MTIC). MTIC causes DNA damage by metilating the O6- position of guanine, resulting in a mismatch with thymine in double-strand DNA and activation of the mismatch repair system for cytotoxic effect (Weller et al., 2010) (Stopschinski et al., 2013).

The efficacy of TMZ has been reported (Hegi et al., 2005) (Stupp et al., 2009a) to be dependent on the methylation status of the promoter for O6-methylguanine-DNA methyltransferase (MGMT), a DNA repairing enzyme that neutralizes the toxic effects of TMZ by removing alkyl groups from DNA. If the promoter is methylated, the MGMT gene is silenced, thus the response to therapy will be greater and prolong patient survival (Stupp et al., 2009a) (Darefsky et al., 2012).

Carmustine (1,3-bis 2-chloroethyl)-1-nitrosourea or BCNU) belongs to the nitrosureas family that, by a cross-linking to guanine and adenine bases, cause DNA strand breaks during mitosis.

Despite all therapeutics advances, GBM still remains a lethal disease. Indeed, the majority of GBMs rapidly recur within 2–3 cm of the original tumor site, giving rise to relapses with an even more aggressive and resistant phenotype, unequivocally affecting patient's outcome (Wen and Kesari, 2008).

These failures reflect the highly infiltrative nature of GBM, the heterogeneous cytoarchitecture consisting in normoxic and hypoxic cells and necrotic areas. In addition, Blood Brain Barrier (BBB) protects the CNS, preventing many systemically administered chemotherapics to reach tumor sites.

Among all these features, increasing evidences indicate the existence of a fraction of cancer cells with stem-like properties in GBM (Ignatova et al., 2002) (Hemmati et al., 2003) (Galli et al., 2004) (Singh et al., 2004a; Singh et al., 2004b); this hypothesis has already been described for leukemia (Bonnet and Dick, 1997), breast (Al-Hajj et al., 2003), pancreas (Esposito et al., 2002) and colon (Ricci-Vitiani et al., 2007) cancers.

These cells are called GBM stem cells (GSCs) and are characterized by the self-renewal capacity, tumorigenicity, stem cell markers expression and ability to escape to conventional therapies.

1.4 "CANCER STEM CELLS HYPOTHESIS"

The "cancer stem cells hypothesis" suggests that only a distinct sub population of tumor cells, named cancer stem-cell (CSCs) are able to reconstitute the cellular heterogeneity typical of the original tumor (Maugeri-Sacca et al., 2013) (Stopschinski et al., 2013).

Resembling normal stem cells, CSCs are characterized by: (a.) asymmetric cell division, (b.) infinite growth, (c.) multipotency, (d.) the capability to differentiate into proliferating progenitor-like and more differentiated cells and (e.) tumorigenicity (Reya et al., 2001) (Bao et al., 2006a; Bao et al., 2006b) (Visvader and Lindeman, 2008).

This connotation implies a "hierarchical model", organized in a pyramidal manner with few CSCs at the apex representing the founders of the entire population (**Figure 2.A.**)

(Maugeri-Sacca et al., 2013) (Stopschinski et al., 2013). Nowadays, growing evidences support a more plastic "clonal-hierarchical" model where CSCs and their progeny may retain or acquire stem-like properties under the microenvironmental stimuli including hypoxia, low pH and exposure to paracrine-acting signals (**Figure.2.B.**) (Maugeri-Sacca et al., 2013).

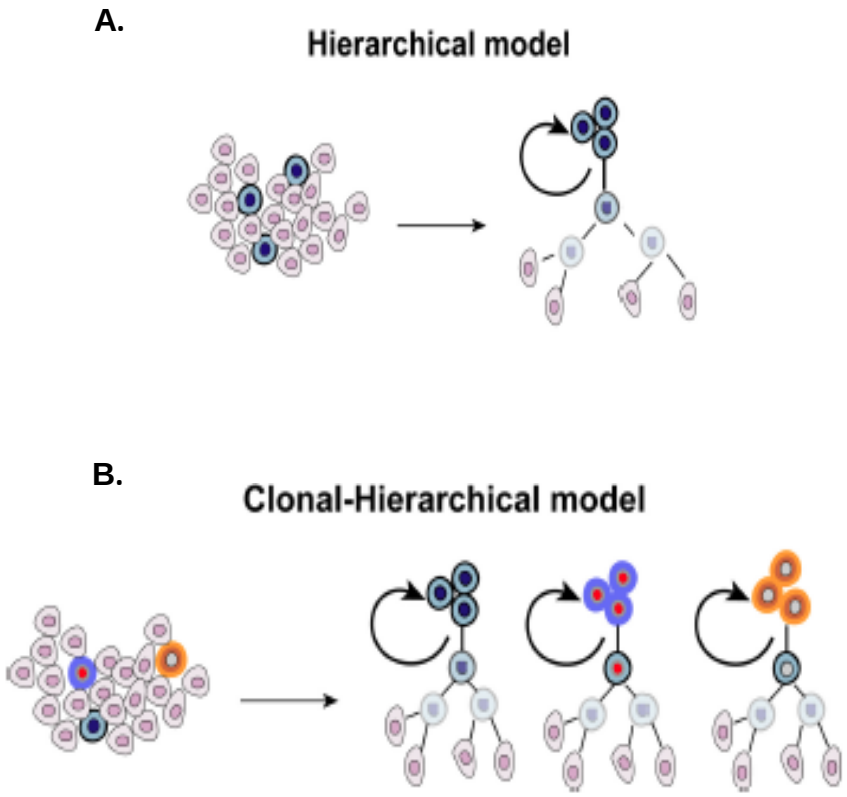

Figure 2. Models proposed to explain the origin and evolution of cancer. The "Hierarchical CSCs" model originally postulated that a stem-like cell located at the apex of the tumor pyramid is the precursor of the whole tumor population (Panel **A.**). The combined "Clonal-Hierarchical stem cell" model suggests that CSCs could undergo clonal evolution, and therefore multiple CSC clones coexisted within the tumor (Maugeri-Sacca et al., 2013) (Stopschinski et al., 2013) (Panel **B.**).

To date, there are increasing evidence suggesting the presence of stem cell-like tumor cells within GBM, thus so-called Glioblastoma stem cells (GSCs) share several properties with their Neural Stem Cells (NSCs) counterparts (Dirks, 2008).

NSCs are pluripotent cells located in the dentate gyrus of the hippocampus and in the sub-ventricular zone (SVZ) of the forebrain lateral ventricles (Weiss et al., 1996) (Gage,

1998) (Curtis et al., 2007) (Sanai et al., 2004). According to the stem cells hypothesis, GSCs are thought to be able of giving rise to cells that express markers of primary neurons and glial cells, such as astrocytes and oligodendrocytes, as well as being able to self-renew (Galli et al., 2004).

Unlike NSCs counterparts (**Figure 3. A.**), GSCs function in a dysregulated manner and are thereby able to repopulate all the cell-types contributing to glioma proliferation (Gursel et al., 2011), to create heterogeneity and to promote invasion (Persano et al., 2013) (**Figure3. B.**).

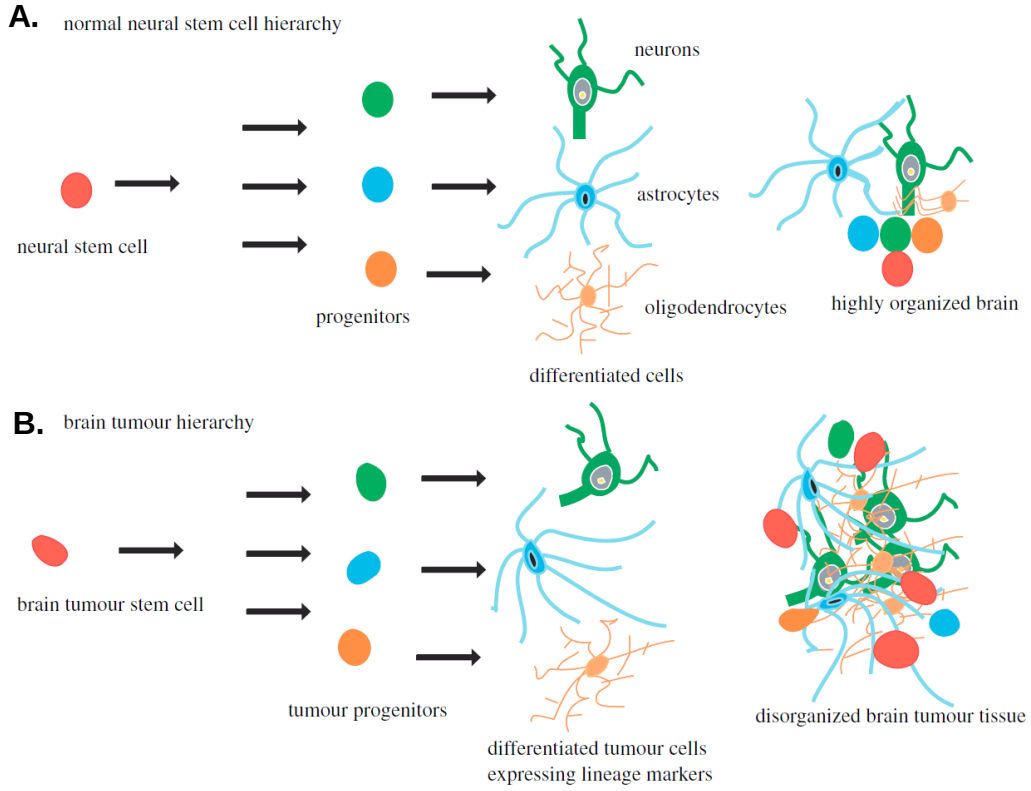

Figure. 3. Stem cell hierarchy in normal brain (Panel **A.) and brain tumors (**Panel **B.)** (Dirks, 2008)**.** Rare stem cells in the brain are able to self-renew to maintain themselves and also generate progenitors that proliferate and differentiate into mature cells that form the highly organized brain parenchyma. The hierarchy remains poorly defined in terms of markers that unequivocally define stem cells from progenitor cells. Brain tumors are also organized as a hierarchy based on cancer stem cells. Cancer stem cells are dysregulated in terms of self-renewal and proliferation and they aberrantly differentiate into cells that form the bulk of the disorganized cancer tissues.

Strict criteria have been necessary to identify GSCs, such as (Vescovi et al., 2006):

a.) **Expression of a repertoire of markers common to stem cells.** CD133 (Prominin-1 surface antigen) expression, originally broadly investigated for GSCs characterization and targeting (Uchida et al., 2000), appears to date not the unique hallmark for GSCs identification (Singh et al., 2004a) (Beier et al., 2007). The validation of novel stem markers and their combined use might add a further level of reliability to current isolation protocols (Dirks, 2008). This repertoire include for example: Nestin (Tohyama et al., 1992) (Dahlstrand et al., 1992), the sex determining region Y box 2 transcription factor (Sox2) (Cai et al., 2002) (Hemmati et al., 2003), BMI1 (Hayry et al., 2008) and CXCR4 (Zheng et al., 2012).

b.) The **ability to self-renew** and **to differentiate into multiple lineages** (i.e. neurons, astrocytes and oligodendrocytes) (Reynolds and Weiss, 1992) is a hallmark of stem cells. Self-renewal of stem cells is *in vitro* determined through neurosphere-forming ability when a single cell is grown in serum free medium supplemented with EGF and FGF as growth factors (Galli et al., 2004) (Gursel et al., 2011). Indeed, by definition, a neurosphere represents a clonal single cell-derived floating cluster of proliferating cells (Reynolds and Weiss, 1992) (Reynolds and Weiss, 1996) (Tropepe et al., 1999).

c.) **Tumorigenicity of GSCs**: capability to recapitulate the tumor of patient from which the cells were derived upon injection into immune-compromised mice (Galli et al., 2004) (Dirks, 2008).

1.5 GLIOBLASTOMA STEM-LIKE CULTURES

Primary GBM derived cells can be cultured:

a.) in adhesion (Conti et al., 2005) (Sun et al., 2008), on laminin (Pollard et al., 2009) or fibronectin-coated plates (Pistollato et al., 2011);
b.) in neurosphere suspension conditions (Reynolds and Weiss, 1992) (Reynolds and Weiss, 1996).

In **Figure 4.** is represented an example of GBM stem-like cells grown in adhesion (Panel **A.**) or as neurospheres (Panel **B.**) (Pollard et al., 2009).

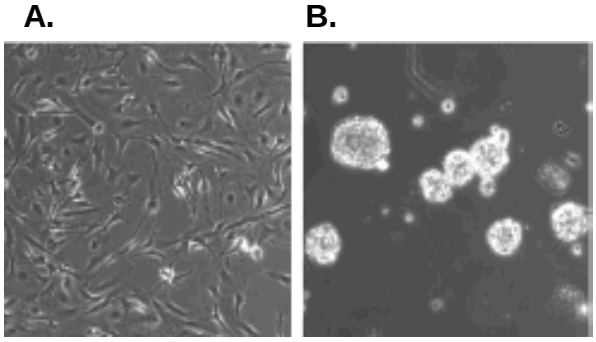

Figure 4. GBM stem like cells cultured in adhesion (Panel **A.) and in suspension as neurospheres (**Panel **B.)** (Pollard et al., 2009)**.**

GBM-derived cells can be grown in suspension as neurospheres in serum-free media supplemented with EGF and FGF growth factors (Galli et al., 2004) (Reynolds and Weiss, 1992) (Reynolds and Weiss, 1996). The neurosphere represents, by definition, a clonal single cell-derived floating cluster of proliferating cells (Reynolds and Weiss, 1992) (Reynolds and Weiss, 1996) (Tropepe et al., 1999).
The advantage of this modeling is a greater preservation of the native phenotype, genotype and karyotype; not preserved in adherent cells modeling due to the aberrations they can accumulate over the several passages (Gursel et al., 2011) (Gunther et al., 2008) (Chen et al., 2012). However, it has been recently proposed by Pollard an adaptation to the neurosphere model (Pollard et al., 2009) to facilitate high-throughput

screening and to also overcome some of the issues of neurosphere culture, such as inadvertent fusion among spheres and the lack of access to nutrients within the sphere (Pollard et al., 2009) (Reynolds and Rietze, 2005) (Singec et al., 2006) (Suslov et al., 2002). Moreover, neurospheres might contain more differentiated progeny and regions of cell death due to their inherent condensed structure, which would hinder the diffusion of the growth factors to the innermost cells (Woolard and Fine, 2009). This could be achieved by culturing cells on laminin -coated flasks (Pollard et al., 2009). In this way, cells that would normally form neurospheres, grow as an adherent culture, which allows of all the cells equal access to growth factors. Additionally, such cells grown in adhesion seem to be less heterogeneous than neurosphere cultures, and almost all of them seem to express canonical stem cell markers, such as Sox2, Nestin, CD133 with minimal expression of differentiation markers (Pollard et al., 2009). An additional issue in suspension culture might be represent by the mechanical and chemical dissociation that could entailed the introduction of cellular debris and increased cells death (Gursel et al., 2011). Nevertheless, it is also important to remind that it has been demonstrated that calf serum or serum substitute (Pistollato et al., 2011) as well as trypsin treatment to detached cells grown in adhesion induce cell differentiation (Singh et al., 2004b).
Although GSCs culture grown as spheres represent the ideal modeling for the *in vitro* study (Reynolds and Weiss, 1992); isolation, maintenance and experimentation on these cells may be pursued culturing cells both in adhesion and in suspension conditions.
However, there are experimental criteria widely recognized as necessary to define GSCs, that cannot exclude the self-renewal capacity, tumorigenicity (Galli et al., 2004) (Reynolds and Weiss, 1992), likewise the presence of the markers common to stem cells (Dirks, 2008) (Gursel et al., 2011).

In our experiments we used both protocols, following the guidelines designed by Dr. Pistollato and co-workers (Pistollato et al., 2011) for the data obtained in the Laboratory of Oncohematology (Dept. of Woman and Child, University of Padova); whereas, for results collected in the Laboratory of Microbiology and Virology (Dept. of Molecular Medicine, University of Padova) cells were grown as spheres under suspension conditions (Reynolds and Weiss, 1992).

1.6 THERAPEUTIC TARGETING OF GSCS

All features outlined above highlight the urgent need to develop novel and more effective therapies based on the specific targeting of GSCs, while sparing normal neural cells. Moreover, growing evidence indicates GSCs are less vulnerable to chemo and radiotherapy due to their ability to correct genetic lesions generated by DNA alkylating agent such as TMZ (Bao et al., 2006a) (Maugeri-Sacca et al., 2013).

Thus, it is possible that GSCs contribute to tumor repopulation after conventional therapies.

During last years several approaches have been investigated to selectively target GSCs population. Remarkable advances in the genetics and biology of gliomas, have contributed to our understanding of tumor development and progression and have given rise to novel therapeutic approaches. Gene therapy has been one area of focus, using vectors, often viruses, to insert immune-stimulating or drug-susceptibility genes (Boviatsis et al., 1994). Virotherapy employed genetically engineered viruses, such as HSV type 1 (HSV1), to establish productive infection only in dividing tumor cells without injuring adjacent normal brain tissue (Martuza et al., 1991).

However, taking into account the heterogeneity identified in GBMs, new therapeutical approaches cannot exclude genomic abnormalities and the peculiar tumor microenvironment. Such microenvironment, formed by supporting cells, extracellular matrix components, and other factors that maintain GSCs in a self-renewing, stem-like state, resembles *the stem cell niche* (Calvi et al., 2003) (Dirks, 2008).

Thus, therapeutical strategies that target GBM microenvironment or force GSCs to differentiate into lineage specific progenitors and mature astrocytes may be worthy pursued.

1.6.1 TARGETING GSCS BY INDUCING DIFFERENTIATION
Focus on Bone Morphogenetic Proteins (BMPs)

Therapy forcing GSCs to differentiate into a more commitment lineage might be a promising and non-cytotoxic strategy for GSCs targeting. In this regard, in our study we have focused our attention to BMPs. BMPs are members of the Transforming Growth Factor-β (TGF-β) Superfamily of secreted ligands. The prototypic receptors for BMP in mammals are the type II receptor, BMPR2, and type I receptors, BMPR1A and BMPR1B (Shou et al., 2002). BMP2 and BMP4, binding to BMPR1A, can act as neuroepithelial proliferation signals at very early stages of embryonic central nervous system development. Later, in development, they induce neuronal and astrocytic differentiation of NSCs and this event coinciding with the increased expression of BMPR1B (Shou et al., 2002). The most common TGF-β signal transduction pathway involves SMAD proteins (Heldin et al., 1997) and begins when a TGF-β or BMP family member, such as BMP2 or BMP4, bind to the BMPRI and then recruit the BMPRII. Activation of the receptor complex leads to phosphorylation of the receptors and subsequent phosphorylation of Smad1, Smad5, or Smad8 (receptor regulated SMAD proteins), allowing them to form a complex with Smad4 (coSMAD). This heteromeric complex translocates to the nucleus, to target BMP-regulated genes through interaction with co-activators or repressors. Smad 6 and Smad7 may act similarly to inhibit the BMP pathway through interactions with the receptor complex and thus inhibiting R-Smad activation. TGF-β and BMP pathways induce the expression of proteins involved in proliferation, differentiation, survival and apoptosis (Massague et al., 2005). In **Figure 5.** is reported a schematic model of the BMPs pathway.

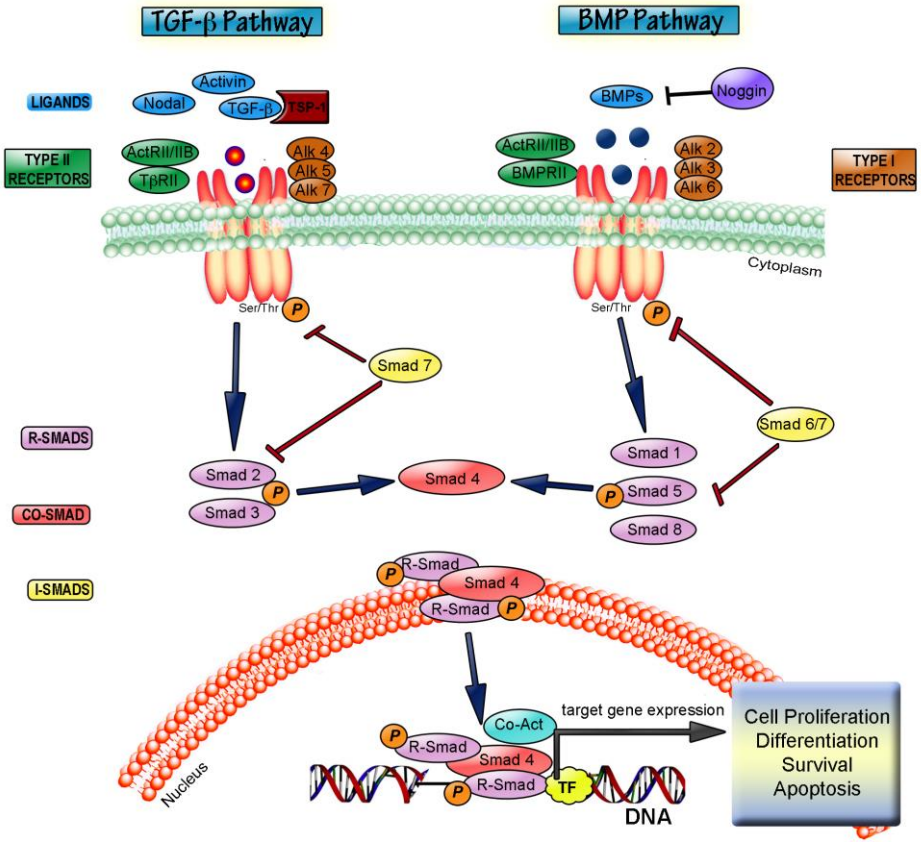

Figure 5. BMP Signaling Pathway (Villapol, DOI: 10.5772/53941). BMP2 and BMP4, bind to their type I receptor BMPRI before recruiting the type II receptor BMPRII. Activation of the receptor complex leads to phosphorylation of the receptors and subsequent phosphorylation of Smad1, Smad5, or Smad8, allowing them to form a complex with Smad4. This heteromeric complex translocates to the nucleus, to target BMP-regulated genes through interaction with co-activators or repressors. Smad6 and Smad7 may act similarly to inhibit the BMP pathway through interactions with the receptor complex and thus inhibiting R-Smad activation. TGF-β and BMP pathways induce the expression of proteins involved in proliferation, differentiation, survival and apoptosis.

BMP2 (Pistollato et al., 2009a), BMP4 (Piccirillo et al., 2009) (Piccirillo et al., 2006) and BMP7 (Tate et al., 2012) have been already employed as pro-differentiating factors for GBM treatment demonstrating *in vitro* cell growth arrest and astro-glial differentiation and promoting *in vivo* tumor growth inhibition (Piccirillo et al., 2009) (Piccirillo et al., 2006) (Kolenda et al., 2011). Nevertheless, almost the 20% of GBMs display epigenetic silencing of BMPR1B. Since these patients should not be affected by BMP pro-differentiating effects the therapeutic promise of BMPs treatment must be view with caution and proposed only for a subset of selected GBM patients expressing BMPR1B (Persano et al., 2013).

1.6.2 Focus on Wingless Type (WNT) proteins

Another way of forcing GSCs to differentiate into a more commitment lineage seem to be related to the Wingless type (WNT) protein pathway. Wnt factors are a family of 19 secreted glycoproteins of around 40 kDa in size (Li et al., 2012). During embryonic development Wnt critically contributes to the establishment of the body axis and organ development. In adult organs, the canonical Wnt signaling pathway displays important functions, including cell fate determination, cell proliferation, and stem cell maintenance (Valenta et al., 2012). It has been recently reported that Wnt activation promotes neuronal differentiation of GBM cancer cells under hypoxia by upregulating the pro-neuronal genes and by inhibiting the stemness-related pathways (Rampazzo et al., 2013). Nevertheless, the role of Wnt activation in regulating brain tumor phenotype remains currently controversial and the interaction between Wnt pathway and hypoxic signalling in brain tumours remain to be still elucidated.

1.7 The GBM hypoxic niche

Hypoxia is known to control transcription of many genes that are pivotal in many aspects of cancer biology (Heddleston et al., 2009) angiogenesis (Bao et al., 2006b), cell survival, genomic instability (Koshiji et al., 2005), invasion (Harris, 2002), chemotherapy and radiation resistance (Vaupel, 2004) (Amberger-Murphy, 2009) and glucose metabolism (Semenza, 2010) (Pistollato et al., 2010b) (**Figure 6.**).

Hypoxic area of the brain report an oxygen level less than 2.5%; conversely, healthy brain tissues have a range between 12.5% to 2.5% O_2 (Erecinska and Silver, 2001) (Evans et al., 2008). The close connection to oxygen levels and stem cells has been widely demonstrated (Bar, 2011) (Heddleston et al., 2009) (Keith and Simon, 2007) (Pistollato et al., 2007). Indeed, hypoxia prevents the differentiation of NSCs and promotes the self-renewal of CSCs (McCord et al., 2009) (Heddleston et al., 2009). Similarly, hypoxic niches are involved in maintaining the stem-like status of GSCs (Seidel et al., 2010) (Li et al., 2009)

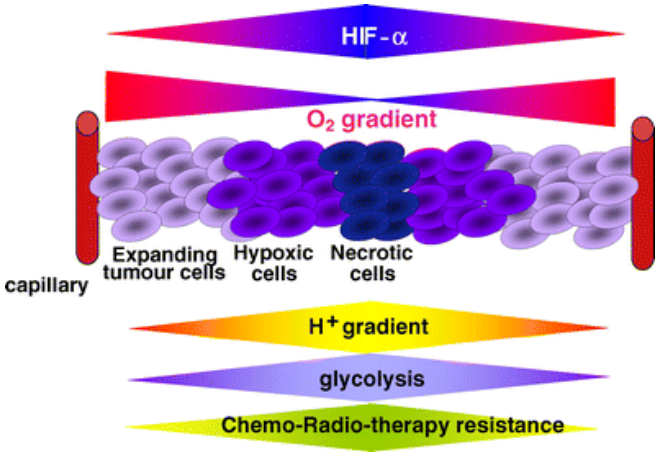

Figure 6. The characteristics of a hypoxic tumor mass (Vaupel P. et al. 2004).

The key intracellular molecular system of the hypoxic response is modulated by the Hypoxia Inducible Factor (HIF) (Semenza et al., 1995). Three members have been recognized: HIF1α, HIF2α and HIF3α.

HIF1α is ubiquitously expressed and it seem to be induced in both GSCs and non-stem cells, whereas HIF2α seem to be up regulated only in GSCs suggesting that its inhibition might spare NSCs. Inhibition of HIF factors in GBMs has been shown to be extremely effective. Reducing HIF-1α, using siRNA, inhibited the hypoxic response and attenuated GBM growth *in vitro* and *in vivo* (Gillespie et al., 2007). Similarly, targeting either HIF-1α or HIF-2α, reported reduction of VEGF expression in GSCs, and most importantly reduced the clonogenicity of CD133-positive cells *in vitro* and *in vivo* (Heddleston et al., 2009). This point is important as any potential therapy targeting HIF activity may not only target hypoxic cancer cells but may target normoxic cancer cells as well.

On this scenario, it is clear how the disruption of a such particular microenvironment may provide a new approach for selectively targeting GSCs (Pistollato et al., 2009b).

Moreover, lowered oxygen levels may repress the differentiative effect of BMPs (Pistollato et al., 2007) {Piccirillo, 2009 #378}. Previous studies indicate that distinct BMP signaling pathways able to promote differentiation and apoptosis in normal stem cells at low oxygen levels, *via* HIF-1α, de-sensitize GBM cells to BMP activation leading to a reduction in canonical SMAD1/5/8 activation (Pistollato et al., 2007) (Piccirillo et al., 2009). Importantly, re-exposure at 21% O_2 levels resulted in rapid loss

of HIF-1α, activation of SMAD1/5/8, and induced differentiation within at least 48h of reoxygenation (Pistollato et al., 2007) (Pistollato et al., 2009a).

Additionally, BMPRs genes are up-regulated in cells cultured under high oxygen tensions. Thus, the strongest BMP2 mediated effect at 21% O_2 correlate also with an increased expression of its receptor. These finding highlight the possibility of BMPs molecules to be used as pro-differentiating therapies for GBM, but open the way to study pro-differentiating molecules able to modulate GBM cells phenotype also in their physiological hypoxic microenvironment (Persano et al., 2013) (Piccirillo et al., 2009).

Another aspect to take into account is the hypoxia-mediated GSCs resistance to radiotherapy (Vaupel, 2004) and chemotherapy (Kolenda et al., 2011) highlighted by an increased proliferation and a decreased apoptotic potential (Pistollato et al., 2010a). Understanding the interactions between GCSs and the microenvironment balance of the niches where they reside will be fundamental to unveil the role of this controversial population in tumor initiation, progression, invasion and therapeutic resistance.

1.8 The three-layer concentric model of GBM

During last years, the role of hypoxic niche and how such lowered oxygen gradient could modulate GSCs proliferation, phenotype and differentiation have been extensively investigated by Dr. Persano and coworkers. By sampling multiple intratumoral areas through radiological imaging and image guided surgery, they unraveled a GBM phenotypic correlation to the hypoxic gradient, defining a *"tumor stem cell concentric model niche"* **(Figure 7.)**.

Based on the distance from the anoxic central core, three different layers have been identified (Pistollato et al., 2010a) (Persano et al., 2011): a.) the internal core, b.) the intermediate, and c.) the peripheral layers.

The inner core is highly hypoxic and characterized by more immature stem cells expressing Nestin and with low proliferation index.

The intermediate portion is a mildly hypoxic and thin transition area between the partially necrotic core and the peripheral layer, with immature and proliferating tumor precursor cells.

The peripheral layer appears the most vascularized and oxygenated area predominantly expressing committed/differentiated cells (Pistollato et al., 2010a).

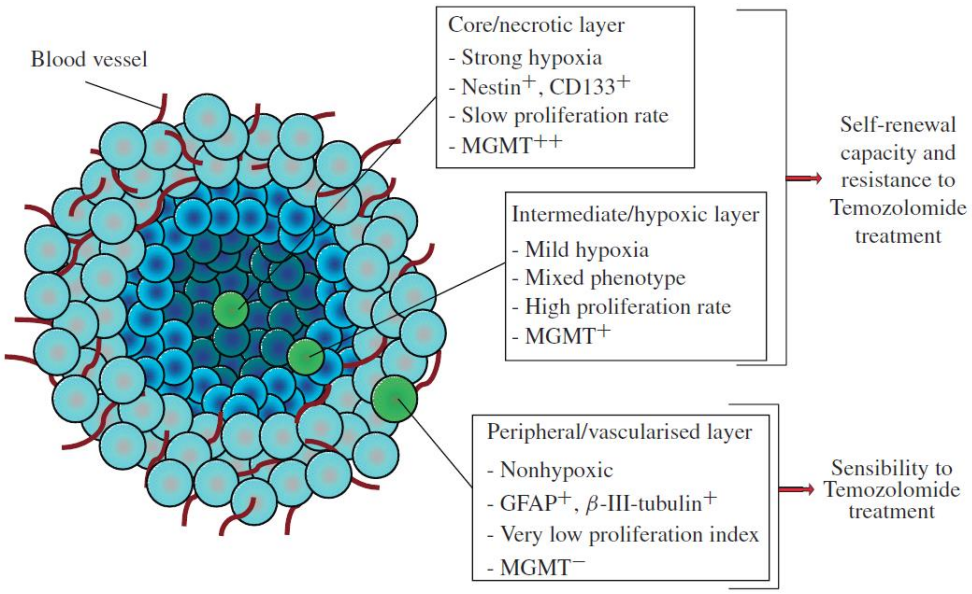

Figure 7.: Graphic representation summarizing the phenotypic and molecular of the three concentric layers model of GBM. Inner portions of tumor mass display more immature cancer cells (Nestin$^+$) and account for the highest percentages of cancer stem cells identified by CD133 staining. This identified stem cell population is resistant to alkylating agents-based chemotherapy *in vitro*. Peripheral GBM cells show a more differentiated phenotype (GFAP$^+$, βIII-tubulin$^+$) with low levels or absence of CD133$^+$ cells. These peripheral tumor cells are highly sensitive to Temozolomide (TMZ) (Persano et al., 2011).

According to the three concentric layers model, the highest percentage of CD133$^+$ cells were identified in the inner portion. These cells overexpressed MGMT enzyme and shown to be *in vitro* resistant to TMZ treatment. Conversely, peripheral GBM cells displayed a more differentiated phenotype with lower levels or absence of CD133$^+$ cells and they resulted highly sensitive to TMZ treatment (Persano et al., 2011). The existence of two types of cancer stem cells within different regions of the same human GBM was firstly been reported also by other groups (Piccirillo et al., 2009). Thus, the concentric distribution of GBM cells within the tumor mass might have important implications in the GBM treatment and both diagnostic and therapeutic methods might be improved.

1.9 STEM CELLS AS DELIVERING STRATEGIES IN GBM

Another approach for targeting GSCs uses stem cells to efficiently deliver therapeutic genes and their products to brain tumors.

Stem cells have several characteristics which make them suitable delivery tools. In the context of gliomas, three types of stem cells have been explored: a.) embryonic, b.) neural and c.) mesenchymal. Moreover, GBM have been reported to attract implanted and injected Neural Stem Cells (NSCs) and Mesenchymal Stem Cells (MSCs) (Aboody et al., 2000) (Benedetti et al., 2000) (Ehtesham et al., 2002a) (Ehtesham et al., 2002b). Due to their origin, NSCs are more suitable as therapeutic delivery vehicles for brain tumors than MSCs. Although the experimental results about NSCs are promising (Aboody et al., 2008), it is difficult to obtain NSCs from human brains because of practical and ethical problems, and there is the inevitable potential of immunological incompatibility in allogeneic transplantation.

MSCs might be used as a practical alternative stem cell source, easy to obtain and to engineered (Bexell et al., 2013) (Mundra et al., 2013). The feasibility of using autologous MSCs as cell carries appears very attractive because it allows to avoid discussion of allograft rejection altogether. Therefore, MSCs represent a promising gene or virus delivery vehicle for gliomas.

1.9.1 *Focus on Mesenchymal Stem Cells as potential therapeutical strategy for GBM*

MSCs are non-hematopoietic adult multipotent stem cells: they usually express CD73, CD90, CD105 and CD271 surface markers; whereas do not express hematopoietic lineage markers such as CD14 and CD45 (Bexell et al., 2013) (Keung et al., 2013) (Altaner, 2008). They can be isolated from bone marrow (Bruder et al., 1997), umbilical cord blood (Erices et al., 2000), adipose tissue (Zuk et al., 2002) (Zuk et al., 2001), peripheral blood and dental pulp (Pierdomenico et al., 2005) (Kern et al., 2006). Despite the origin site, MSCs are defined by their ability to (a) remain plastic adherent; (b.) self-renew and (c.) to undergo adipogenic, osteogenic, and chondrogenic differentiation (mesenchymal lineages) when maintained under standard culture

conditions (Mundra et al., 2013) (Dominici et al., 2006) (Keung et al., 2013) (Chamberlain et al., 2007).

Among MSCs, Adipose Tissue- (AT-MSCs) and Bone Marrow- derived MSCs (BM-MSCs) have extensively evaluated over last years since both of them offer the most accessible source of MSCs for use in research. Although bone marrow is the major source of MSCs, adipose tissue is less invasive, less expensive than bone marrow to obtain (Locke et al., 2011) (Yoo et al., 2009) and AT-MSCs demonstrated a more oncogenic resistance than BM-MSCs when injected in *in vivo* models (Momin et al., 2010).

Once intracranially or intravenously administered, MSCs easily cross the BBB and migrate throughout normal brain parenchyma, preferentially towards the injured sites. This is possible due to their own inherit homing ability toward tumor site (Doucette et al., 2011) (Sasportas et al., 2009) (Nakamizo et al., 2005) and mediated at least in part by chemokines and other specific tumor-derived growth factors such as the vascular endothelial growth factor-A (VEGF-A) and interleukin-8 (IL-8) (Birnbaum et al., 2007) (Nakashima et al., 2010) (Doucette et al., 2011) (Nakamizo et al., 2005).
Moreover, it has been shown that hypoxia increases the *in vitro* migration capacity of MSCs through a number of direct or indirect mechanisms, including modification of local factors involved in the maintenance of MSCs within BM or other tissues (Rochefort et al., 2006).
Moreover, compared with all other stem cells employed for cell delivery, MSCs have the clinical advantage to be acquired from patients and auto-transfused without fear of immune rejection and they are free of ethical concerns (Doucette et al., 2011) (Nakamizo et al., 2005) (Mundra et al., 2013) (Ahmed et al., 2011) (Kosztowski et al., 2009) (Ehtesham et al., 2002a) (Ehtesham et al., 2002b) as well.
Mesenchymal stem cells have been used to deliver a plethora of therapeutic agents to glioma including prodrugs, viruses, cytokines and antibodies (Lamfers et al., 2009) (Huang et al., 2010).
Gene-engineered MSCs producing interleukin-18, interleukin-2 and interleukin-12 infected by Adenoviral vector showed inhibition of glioma growth and prolonged the survival of glioma-bearing rats (Nakamura et al., 2004) (Xu et al., 2009) (Hong et al.,

2009). MSCs transfected with tumor necrosis factor related apoptosis-inducing ligand (TRAIL) induced apoptotic activity *in vitro* and *in vivo* (Yang et al., 2009) (Choi et al., 2011). Moreover, in the field of suicide gene therapy, intratumoral injection of MSCs transduced with herpes simplex virus-thymidine kinase gene (HSVtk) followed by Ganciclovir administration demonstrated a reduction of the tumor size and a significant survival prolongation (Amano et al., 2009).

Further studies are needed to improve both the safety therapeutical window and the migration capability of MSCs towards GBM. Indeed, there was no evidence of long-distance MSCs migration through normal brain tissue towards distant gliomas (Bexell et al., 2013). Conflicting data suggested how MSCs may play a role in the formation of new tumor blood vessels promoting the invasive nature of the GBMs (Schichor et al., 2012) or to fuse and transdifferentiate into tumor cells (Schichor et al., 2012). Other studies reported a MSCs inhibitory effect on the growth of the tumor (Schichor, et al., 2012) (Uccelli et al., 2008) (Ramasamy et al., 2007).

Despite all these controversies, MSCs hold the promising prospect of being ideal targeted therapeutic agents as well as cellular carrier in the treatment of GBM.

1.10 VIRO-THERAPY STRATEGIES IN GBM

Virotherapy is defined as the delivery of oncolytic viruses for cancer therapy (Stopschinski et al., 2013).

Oncolytic viruses (OVs) are genetically engineered viruses able to replicate in dividing cells but are severely impaired for replication in non-dividing cells (Martuza et al., 1991). Indeed, malignant glioma cells are a dividing tumor cell population, whereas, the surrounding normal brain is composed mostly of neurons and glia (Martuza et al., 1991)

One of the first genetically engineered OV was an oncolytic Herpes Simplex Virus (oHSV) (Martuza et al., 1991).

Herpes Simplex Virus 1 (HSV1) represents a suitable candidate to engender oncolytic activity because it infects most cell types in a broad range of species and it is cytolitic (Mullen and Tanabe, 2002). In addition, its genome is very large and stable with many non-essential genes that contribute to pathogenicity and replication in non-dividing cells (Whitley and Roizman, 2001). Thus, HSV genes associated with virulence can be

modified, deleted, and replaced with multiple therapeutic transgenes (i.e. immune-stimulatory molecules (Markert et al., 2012) and prodrug-activating enzymes (Braidwood et al., 2009) (Tyminski et al., 2005) without affecting the virus capacity to replicate and destroy tumor cells during its lytic phase. Further details about HSV1 will be discussed at paragraph **1.11**.

Early generation oHSVs, such as R3616 and 1716 HSVs, were improved by introducing multiple deletions and/ or mutations to prevent the reversion to wild-type HSV. Nowadays, different oHSVs such as 1716 (Papanastassiou et al., 2002), G207 (Hunter et al., 1999) (Mineta et al., 1995) and G47Δ and other several virus species, like adenovirus (ONYX-015) (Chiocca et al., 2004), reovirus (REOLYSIN) (Forsyth et al., 2008), Newcastle disease virus (Freeman et al., 2006), Seneca Valley virus and measles virus (Allen et al., 2013) (Todo et al., 2001) have already undergone in clinical trials (Senzer et al., 2009).

Clinical trials based on vaccinia virus for treating malignant gliomas are also ongoing (Liu et al., 2007).

To date, no serious adverse effects imputable to oHSV alone have been reported in the clinical trials, even when viruses were administered by intracranial injections in the case of glioma treatment. However, despite all promising results, further efforts should be done to improve the efficiency of OVs.

Moreover, two hurdles remain preventing the advancement of OV based therapies:

a.) the host antiviral immune response. Both innate and acquired anti-HSV immunity can clear oHSV prematurely to also limit oHSV replication and spread (Wakimoto et al., 2003).

b.) The inefficient viral distribution away from the tumor site. Physical barriers such as the extracellular matrix can restrict initial oHSV distribution and subsequent spread of virus in the tumor mass, allowing tumor cells to ‘outgrow’. Direct intra-tumoral injection of oHSVs has been the preferred route of administration, and this limits delivery to accessible tumor sites (Kanai et al., 2010).

1.10.1 *Focus on Oncolytic viruses and hypoxia relationship*

As above mentioned, hypoxia plays a fundamental role in GBM invasion, aggressiveness and standard therapies resistance (Bar, 2011) (Keith and Simon, 2007) (Li et al., 2009) (Seidel et al., 2010).

The decreased effectiveness of chemo and radiotherapy is in part due to:

a.) the distally located hypoxic cells, less exposed to systemically administered therapies;
b.) the HIF transcriptional pathways (Amberger-Murphy, 2009).

Thus, the development of new therapeutic strategies to counteract the hypoxia enhanced pathological potency of GSCs became crucial.

Oncolytic viruses, being selected to kill tumor cells, might represent a promising strategy for treating GBM. In particular, recent studies employed two oHSVs, already demonstrated safety in clinical trials (Markert et al., 2000): G207 (Aghi et al., 2009) and G47Δ (Sgubin et al., 2012).
Interestingly, the G207 ($\gamma34.5^-$, $ICP6^-$) exhibited enhanced replication in hypoxic environments compared to the wild-type HSV strain F in U87MG glioma cell lines (Aghi et al., 2009).
Furthermore, the G47Δ virus ($\gamma34.5^-$, $ICP6^-$, $ICP47^-$) retained the ability to infect, replicate in and to kill GSCs in hypoxic conditions *in vitro* and *in vivo* and importantly, counteracted the hypoxia-enhanced stem cell-like properties of GSCs, even if hypoxia promoted the $CD133^+$ GSC population (Sgubin et al., 2012).
Treatment with G47Δ should be an effective strategy to eliminate hypoxic GSCs resistant to conventional therapies and to improve therapeutic outcomes for GBM patients.
Nevertheless, the HIF response to oHSV infection and mechanisms involving infectivity and cytotoxicity in hypoxic conditions needed to be further investigated (Friedman et al., 2012).

1.11 *Herpes simplex virus (HSV)*

1.11.1 *Virus structure*

Herpes simplex virus type 1 (HSV1) is a human natural pathogen responsible for localized mucocutaneous lesions and encephalitis (Whitley and Roizman, 2001). HSV1 belongs to the *alpha-Herpesviridae* subfamily of herpesviruses. *Alpha-Herpesviruses* are characterized by a broad host range, rapid proliferation, visible cytopathic effects and latency phase in neuronal cells.

HSV1 is an enveloped, double-stranded DNA (dsDNA) virus. The mature virus particles, 120-300 nm size, consist of different components: a.) an external envelope, b.) a tegument, c.) an icosahedral nucleocapsid (100 nm size) and d.) a viral genome (Whitley and Roizman, 2001) (Mackem and Roizman, 1982) (**Figure 8.**).

The envelope contains a host-cell derived trilaminar lipid layer in which are embedded 13 different glycoproteins responsible for host cell recognition and entry (Mackem and Roizman, 1982) (Batterson and Roizman, 1983). The tegument is an amorphous layer, containing at least 20 different proteins with structural and regulatory roles at different stages of the virus life cycle. Its contains proteins such as virus protein 16 (VP16), VP22, virus shut-off *(vhs)* proteins that are collectively important for viral gene expression (Mackem and Roizman, 1982) (Batterson and Roizman, 1983) degradation of host cell mRNA (Kwong and Frenkel, 1989), viral particle assembly and inhibition of innate immune responses that can repress virus gene expression. The icosahedral capsid is composed of 162 capsomers, multiple structural proteins organized in 150 extravalent and 12 pentavalent, that encapsidate the viral genome (Newcomb et al., 1999).

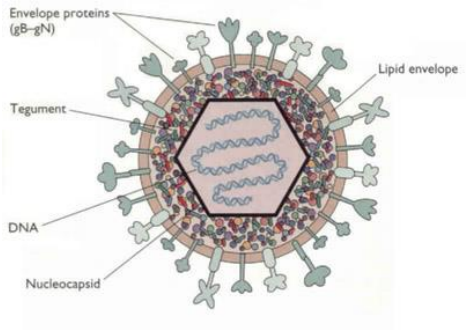

Figure 8. Schematic structure of HSV-1 (www.wisc.edu).

The HSV1 genome consists of a 153 kb linear double stranded DNA (Kieff et al., 1971) arranged as long (L) and short (S) unique (U) sequences (U_L and U_S) covalently linked and flanked by large inverted repeats, the L (R_L) and the S (R_S) repeat (**Figure 9.**) (Whitley and Roizman, 2001). HSV1 gene nomenclature is based upon the position of the gene within the long and short segments. Genes within the long segments are designed as U_L 1 to U_L 56 and genes in the short segments are designed as U_S 1 and U_S 12. The U_L region comprises the 82% of the genome (108 kb); the U_S region is 13 kb. Unique region genes are present as single copy; those in the repeated segments are present in two copies. In the middle of the U_L region is an origin of replication, ORI_L; whereas, two origin of replication are found in the R_S regions. The HSV1 DNA encodes about 90 genes; 84 of these transcriptional units encode proteins, divided in essential and non-essential functions (at least 47) (Whitley and Roizman, 2001).

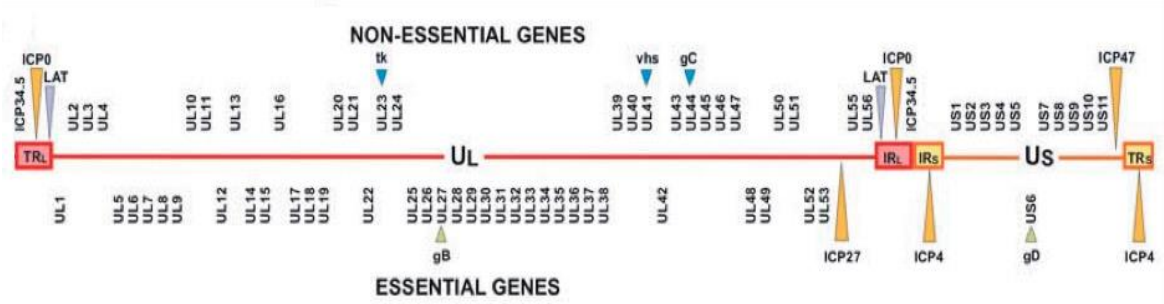

Figure 9. The genome of HSV1 has a unique long (U_L) and a unique short (U_S) regions, flanked by inverted repeated sequences, named LTR. The number of copies of LTRs repeat may vary and the repeats allow rearrangements of the unique regions and HSV exists as a mixture of four isomers.

1.11.2 *HSV Pathogenesis*

HSV1 can establish either a lytic infection or an asymptomatic, latent, infection in sensory neurons and, upon reactivation, causes lesions at or near point of entry into the body (Whitley and Roizman, 2001). The lytic cycle of the virus typically causes orofacial painful vesicular lesions and, in the most serious cases, encephalitis. Encephalitis is an inflammation of the brain that can be asymptomatic or characterized by flu-like symptoms, such as fever or severe headache, as well as confused thinking, seizures, or problems with senses or movement (Whitley and Roizman, 2001). In most cases, people with relatively mild illness recover within a few weeks with no long-term complications.

Nevertheless, severe cases of encephalitis can be life-threatening (Whitley and Roizman, 2001). The resulting complications can affect almost all areas of the CNS, causing meningitis, myelitis, but also respiratory distress syndrome and acute broncospasm (Whitley and Roizman, 2001).

1.11.3 *Viral infection*

During primary infection in epidermis and dermis cells, HSV1 replicates its DNA and produces the viral progeny.

HSV1 enters into the host cells by two different ways: endocytosis and fusion at the plasma membrane. To initiate infection, HSV attaches to at least three different classes of cell surface receptor. Once virus fused its envelope with the plasma membrane the capsid is transported to the nucleus where the DNA is released and a lytic replication cycle initiates. HSV replicates by three rounds of transcription that yield:

a.) α immediate early (α IE) proteins that mainly regulate viral replication;

b.) β early (β E) proteins that synthesize and package DNA;

c.) γ late (L) proteins. Among them structural there are virion proteins, glycoproteins and tegument proteins (Whitley and Roizman, 2001). L genes are divided into two classes: γ_1 and γ_2. Differently from γ_2, γ_1 genes do not require DNA replication and they are expressed also in presence of replication

inhibitors (Zhang and Wagner, 1987). L gene expression peaks around 12-13 hours post infection.

After the expression of L genes, viral core and capsid are assembled in the cellular nucleus. Viral DNA is reeled into the capsid. Capsids emerge from the nucleus into the perivascular space and acquire the tegument proteins (Turcotte et al., 2005).

1.11.4 *Latent infection*

After an initial lytic replication in epithelial cells of the primary lesion, HSV1, as a neurotropic virus, enters sensory neurons of the affected area to initiates a lytic replication or to undergo a latent infection characterized by minimal gene expression and the inability to detect infectious virus. During latency genetically intact genome persists in an inactive, but stable nucleosome-associated extrachromosomal state expressing only nucleosome-associated transcript (LAT) (Cohrs and Gilden, 2001) (Wagner and Bloom, 1997). The virus can remain in this state until an environmental or a physiological stress stimulus, such as fever, UV-light, anxiety, weariness, immune-suppression, causes some changes that can trigger transcription (**Figure 10.**). Activated HSV undergoes *de novo* protein synthesis and viral replication (Wagner and Bloom, 1997). Progeny virus travels down the nerve axon by anterograde transport back to the primary site of infection ad re-established infection (Wagner and Bloom, 1997).

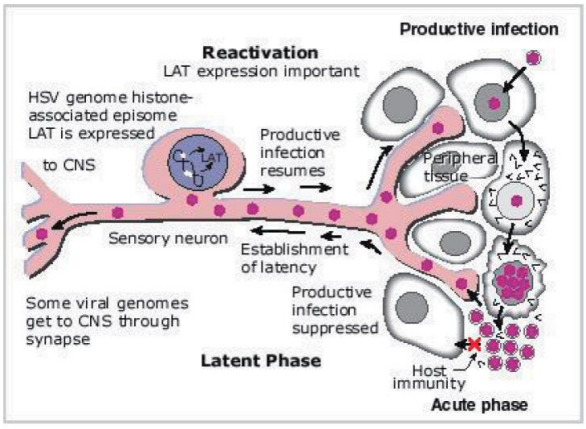

Figure 10. Schematic representation of HSV1 latent phase.

1.11.5 *Focus on Herpes virus and Virotherapy*

Since wild-type HSV causes potentially life-threatening encephalitis, attenuation is a prerequisite of OVs development. Of considerable interest in connection with this disease are the genes that confer upon the virus the capacity to replicate in the central nervous system (CNS) tissue. The diploid γ34.5 gene enables the virus to multiply and spread in the CNS but it is a not essential gene for viral replication (Chou et al., 1990) (Whitley and Roizman, 2001).

The γ34.5 gene is located in the inverted repeats flanking the long unique sequence (R_L) of viral DNA and therefore the gene is present in two copies per genome (see details in **Figure 11.**) (Dambach et al., 2006) (Markert et al., 2012) (Chou and Roizman, 1994) (Chou et al., 1990). It encodes the ICP34.5 protein, composed by 263 aminoacids and consisted of a large amino-terminal domain, a linker or swivel region with the triplet *Ala-Thr-Pro* (ATP codons) repeated 10-times (Chou et al., 1990).

ICP34.5 protein is the major HSV neurovirulence factor; thus, the deletion of a large portion of the gene encoding the ICP34.5 factor is responsible for the neuroattenuated phenotype exhibited by the virus. In addition, these deletions inhibit autophagy and block virus-induced host protein shutoff, improving the safety profile and minimizing the neurotoxicity of HSVs employed in oncolytic virotherapy (Dambach et al., 2006) (Kanai et al., 2010) (Aghi and Rabkin, 2005) (Markert et al., 2009).

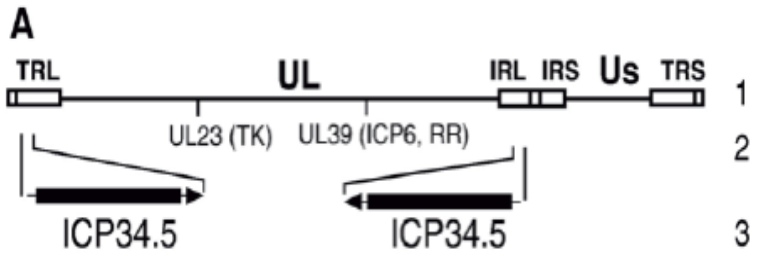

Figure 11. **Schematic diagram of the HSV1 genome** (line 1) indicating the relative locations of the genes encoding for ICP34.5. The unique long (U_L) and unique short (U_S) segments are indicated by lines. The open boxes represent the repeat regions of the genome. Above the repeat regions, the terminal and inverted repeats flanking the U_L region are indicated as TRL and IRL, while those flanking the US region are indicated as TRS and IRS. The γ34.5 gene encoding for ICP34.5 protein is located in the TRL and is thus present in two copies (filled rectangles, line 3).

2. MAIN AIMS OF THE STUDY

- **Isolation and characterization of human Bone Marrow (BM-) and Adipose Tissue (AT-) Mesenchymal Stem Cells (hMSCs) and cell culture.**
- **Characterization of primary GBM stem like cells (GSCs) and cell culture.**
- **Evaluation of killing and replication capability of R3616 virus in GSCs.**
- **Evaluation of pro-differentiating effects mediated by Bone Morphogenetic Protein 2 (BMP2) treatment in GSCs.**
- **Evaluation of *in vitro* migratory properties of BM-MSCs toward GSCs *per sè*, GSCs infected with HSV1 wild type and R3616 viruses or BMP2 pre-treated .**
- **Evaluation of the most suitable candidate for stem cell therapy between BM-MSCs and AT-MSCs to further genetically engineered to express therapeutic genes (BMP2) as well as conditionally replication competent viruses (R3616).**
- **Evaluation of combining hMSCs and virotherapy approach to obtain a more integrated and efficient strategy to selectively target GSCs.**

3.1 MATERIALS AND METHODS

Part I

3.1.1 Atmosphere-Controlled Incubation

For culture in 21% oxygen, cells were incubated in a Heraeus BBD 6220 Incubator (Thermo Scientific, Asheville, NC, http://www.thermoscientific.com). CO_2 was added to maintain a 21% O_2, 5% CO_2 75% N_2 balance.

For 2-5% oxygen culturing, cells were incubated in a INVIVO$_2$ 300 Ruskinn chamber (Ruskinn C300, Ruskinn Technology Ltd, Baker Company Bridgend UK, http://www.ruskinn.com), a hypoxia workstation able to maintain and to control temperature, humidity, oxygen and CO_2 levels. The system is provided of a chamber for maintaining cultures (**1.**); a gas mixer Q with a gas control software (**2.**) and a glove box to perform cell manipulation (**3.**) (**Figure 12.**).
During all phases of culturing and experimentation the following balance gas levels was observed: 2% O_2, 5% CO_2, 93% N_2.

Figure 12: **The Invivo2 300 Hypoxia Workstation (Ruskinn C300).** The system is provided of a chamber for maintaining cultures (**1.**); a gas mixer Q (**2.**) and a glove box (**3.**). In our experiments it has been programmed to observe 2% O_2, 5% CO_2, 93% N_2 gas levels balance.

3.1.2 Isolation and culture of Human GBM derived Cells (hGBMs)

In the first part of this study, Human Tumor Primary cultures of Glioblastoma (hGBM) were used. Samples were derived from 4 tumors taken at surgery (see **Table1**). hGBM10 and hGBM13 cells were used for both normoxic and hypoxic experimentation.

Written informed consent for the donation of tumor brain tissue was obtained from patients according to the protocol for the acquisition of human brain tissues obtained from the Ethical Committee board of the University of Padova and Padova Academic Hospital. Tissues were acquired following the tenets of the Declaration of Helsinki.

code	Tumor type	Age	Gender
hGBM01	**Glioblastoma**	**64**	**Male**
hGBM10	**Glioblastoma**	**75**	**Female**
hGBM13	**Glioblastoma**	**67**	**Male**
hGBM83	**Glioblastoma**	**54**	**Male**

Table 1.: Neurosurgical sample collection.

3.1.3 Tissue Dissociation

Tumor tissue was washed with 1X phosphate-buffered saline PBS (10X PBS solution: 0.58M sodium phosphate dibasic Na_2HPO_4, 0.17M sodium phosphate monobasic NaH_2PO_4, 0.68M sodium chloride NaCl; pH 7.4), gently minced with a scalpel, and resuspended in 1 mL of 1X Hanks' buffered saline solution (HBSS; Ca^{2+}/Mg^{2+}-free, plus Hepes and 1.55 g/L glucose, without bicarbonate, pH 7.2; GIBCO, Monza, MB, Italy, http://www.lifetechnologies.com) containing 200 U/ml DNase I (Roche, Indianapolis, IN, USA; https://www.roche-applied-science.com), 1 mM $MgCl_2$ and 200 μg/mL Liberase Blendzyme -1 (0.62 WU/ml Collagenase and 66.7 U/ml Dispase, Roche) for 1 hr at 37°C. Sample was then centrifuged at 1150 rpm for 7 minutes, resuspended in fresh HBSS/DNase/$MgCl_2$ without enzyme, and mechanically triturated. Upon properly trituration, tissue was centrifuged at 1150 rpm for 7 minutes and cells

were resuspended in medium appropriate for further use (Panchision et al., 2007) (Pistollato et al., 2007).

3.1.4 Cell Cultures

- **hGBM cells** were cultured on fibronectin/poly-l-ornithine (GE Healthcare, Little Chalfont, U.K.; http://www.gehealthcare.com) coated flasks in Dulbecco's modified Eagle's medium and Ham's nutrient mixture F-12 (DMEM-F12, GIBCO)) enriched with 10% of a serum substitute constituted by 1% Bovine Serum Albumin, 10 μg/mL rh-Insulin, 200 μg/mL Human Transferrin (BIT9500 Stem Cell Technologies, CA, USA; http://www.stemcell.com), 10 ng/ml epidermal growth factor (EGF, R&D Systems, Minneapolis, MN, USA, http://www.rndsystems.com) and 20 ng/ml basic fibroblast growth factor (bFGF; R&D Systems), 2mM L-Glutamine (GIBCO) and 10.000 U/ml streptomycin sulfate/ penicillin G (GIBCO). For continuous expansion, one-half of this medium was replaced three times per week and cultures were passaged using TrypLe Express (Invitrogen, http://www.lifetechnologies.com). To test pro-differentiating effects on Hutu cells, bone morphogenetic protein 2 (BMP2, R&D Systems Inc.) was supplemented in the medium at the concentration of 20 ng/mL/day for 5 days; whereas, Wnt3a (R&D Systems) treatment was performed at the final concentration of 30 ng/mL/day for 7 days.

- **human Mesenchymal Stem Cells** (hMSCs) from bone marrow (BM-MSCs) of healthy donors or from adipose tissue (AT-MSCs) of glioma patients, dissociated with the same protocol described above for hGBM specimens, were grown and maintained in DMEM medium containing 20% FBS (GIBCO). BM-MSCs and AT-MSCs were characterized by flow cytometry for the typical mesenchymal surface markers and their immuno-phenotype was also tested after 15 days. Further confirmation for mesenchymal lineage was performed by plating cells in adipogenic and osteogenic media, as request by literature (Doucette et al., 2011), (Pittenger et al., 1999), (Dominici et al., 2006), (Ayatollahi et al., 2012).

3.1.5 Flow cytometry analysis

hMSCs were passaged and resuspended in flow cytometry buffer, consisting of 1X Hank's buffer. Cells were counted and diluted at a density of 10×10^4 cells per 100 µL. For surface marker analysis, antibodies against human CD90 (FITC conjugated, BioLegend, Milano, Italy; www.biolegend.com), CD44 (FITC conjugated, BD Biosciences, San Jose, CA, USA; http://www.bdbiosciences.com), CD106 (FITC conjugated, BD Biosciences)**,** CD184 (FITC conjugated, BD Biosciences), CD73 (PE conjugated, BD Biosciences), CD105 (PE conjugated, BD Biosciences), CD29 (PE conjugated, BD Biosciences), CD166 (PE coniugated, Beckman Coulter), CD271 (PE conjugated, BD Biosciences), CD117 (PE coniugated, Beckman Coulter), CD14 (PE coniugated, Beckman Coulter), CD45 (ECD coniugated, Beckman Coulter), HLA-DR (PC7 coniugated, Beckman Coulter, Beckman Coulter Inc. Brea, CA, USA http://www.beckmancoulter.com), CD19 (PE-Cy7 coniugated, Beckman Coulter), were used. Cells were labeled and incubated at R.T. for 15 minutes, washed and resuspended in 400 µl Hank's buffer before being analyzed on a FACS Aria III flow cytometer (BD Biosciences).

3.1.6 hMSCs *in vitro* Differentiation Assay

The ability of BM-MSCs and AT-MSCs to differentiate into adipocytes and osteoblasts was assayed both in hypoxia and normoxia as following described.

- *Adipogenesis differentiation: QUALITATIVE assay*

Once cells had reached confluence, adipogenic differentiation was induced by three cycles of 72 hours/each in a adipogenic induction medium (dexamethasone, insulin, indomethacin, 3-isobutyl-1-methyl- Xanthine, pen/strep, L-glutamine in MSCs growth medium) (Lonza, Walkersville, MD, USA, http://www.lonza.com). Following each round of induction, cells were maintained in a adipogenic maintenance medium for other 72 hours (high glucose-DMEM plus insulin) (Lonza). After final induction, hMSCs were grown for others 3 days into maintenance medium before fixing. cells in 10% formalin for 15 minutes. Differentiated cells were identified by Oil Red O (Sigma-

Aldrich, St. Louis, USA; http://www.sigmaaldrich.com), stain for lipid vacuoles. Plates were washed three times with dH_2O to reduce non-specific staining.

- *Adipogenesis differentiation: QUANTITATIVE assay*

Quantitative analysis of Oil Red O staining can be performed by determining OD_{520} (Optical Density) values of a set of known Oil Red O concentrations to obtain a calibration curve and then comparing these values to those obtained from the unknown sample. After evaluation of lipid vacuoles by qualitative differentiation analysis, Oil Red O lipid droplets stained were eluted by adding 100% isopropanol and incubated for at least 10 minutes. Solution obtained were measured at 520 nm using spectrophotometric techniques (Lambda 20 Spectrophotometer, Perkin Elmer, Milano, Italy; http://www.perkinelmer.com).

Calibration curve was calculated using standard samples starting from an Oil Red O working solution properly diluted with dH_20 to obtain serial dilutions. Blank control was 100% isopropanol.

- *Osteogenesis differentiation assay: QUALITATIVE assay*

The same rounds of induction and maintenance used for adipogenesis assay were performed. Osteogenic activation has required the presence of β glycerol-phosphate, ascorbic acid, dexamethasone, pen/strep, L-glutamine in MSCs growth medium (Lonza). Cells were fixed in 4% Para-formaldehyde for 5 minutes and differentiated cells were identified by Alizarin Red S (Sigma-Aldrich), stain for deposition of a calcium-rich mineralized elements. Cultures were rinsed two or three times with dH_2O to reduce non-specific staining.

- *Osteogenesis differentiation assay: QUANTITATIVE assay*

Quantitative analysis of Alizarin Red Staining can be performed by determining OD_{405} values of a set of known Alizarin Red concentrations to obtain a calibration curve and then comparing these values to those obtained from the unknown sample. After evaluation of deposition of a calcium-rich mineralized elements by qualitative differentiation analysis, 800 µL 10% Acetic Acid to each well of a six well plate (diameter: 35mm) were added and incubated for 30 minutes shaking. Monolayer was detached using a cell scraper and transferred in a 1.5 mL microcentrifuge tube, vortexed

and incubated at 85°C for 10 minutes and then in ice for 5 minutes. After incubation in ice, sample was centrifuged at 20,000 rpm for 15 minutes. The pH of the sample solution was neutralized by adding 10% Ammonium hydroxide and the OD was measured at 405 nm using spectrophotometric techniques.
Calibration curve was calculated using standard samples starting from a solution 10X Alizarin Red properly diluted with dH20 to obtain serial dilutions.

3.1.7 hMSCs Growth Curves

After trypsinization, 2×10^4 hBM-MSCs and AT-MSCs were seeded in a 12-well plate in 1mL DMEM 20%FBS medium and cultured both in hypoxia and normoxia. Viable cells (trypan blue-excluding) were counted after 24, 48 and 72 hours on a Burker counting chamber.

3.1.8 Co-colture assay

To test the modulation of hGBM10 and hGBM13 cells markers expression under effect of hBM-MSCs, co-colture assays were performed at the same time both in normoxia and hypoxia.
hBM-MSCs were seeded and grown as monolayer in DMEM 20% FBS medium under normoxic conditions. Before adding to the hMSCs monolayer, Hutu cells, grown at 2% or 21% O_2, were properly labeled with PKH26 (PE conjugated, Sigma-Aldrich) or PKH67 (FITC conjugated, Sigma-Aldrich), two membrane dyes, at the final concentration of 2×10^{-6} M PKH-dye per 1×10^{-7}cell/mL as recommended by Fluorescent Cell Linker Kit manufacturer's instructions (Sigma). Co-coltures were incubated at 37°C under hypoxic and normoxic conditions. After 7 days, cells were detached, resuspended in flow cytometry buffer (as described above) and labeled following the StemFlow Human Neural Lineage Analysis Kit manufacturer's instructions (BD Biosciences). Briefly, samples were first labeled with CD-133/2-PE (MACS, Miltenyi Biotec, Bergisch Gladbach, Germany, http://www.miltenyibiotec.com) and CD44 (Alexa700 coniugated, BD Biosciences), two surface markers, incubated at R.T. for 20 minutes, washed and resuspended in 100µL fix-buffer, provided by the kit. After 15 minutes incubation at R.T., cells were washed, pelleted and resuspended in 100µL

perm-buffer before adding the following markers: Nestin (Alexa Fluor 647 mouse anti-Nestin), Sox-2 (PerCP-Cy 5.5 mouse anti-Sox2), βIII-tubulin (Alexa Fluor 488 mouse anti-βIII-tubulin), and GFAP (Alexa Fluor 647 mouse anti-GFAP). Samples were incubated at R.T. for 20 minutes, washed, resuspended in 400µL flow cytometry-buffer and analyzed on a FACS Aria III flow cytometer.

3.1.9 hMSCs "*in vitro*" Migration Assay

The tropism of BM-MSCs and AT-MSCs was valuated toward Hutu cells, growth factors and Hutu cells pre-treated with BMP2 and WNT3a biological agents, grown alternatively in hypoxia and normoxia, by an "*in vitro"* migration assay. Migratory properties of BM-MSCs and AT-MSCs towards Hutu pre-differentiated cells were performed treating tumor cells with BMP2 at the concentration of 20 ng/ml for five days or with the Wnt3a factor at 30 ng/ml concentration at for 7 days, before loading hMSCs on Transwell. Tumor cells were seeded in 12-well plates at a density of 4×10^4 cells/well in 1mL DMEM-F12 medium in the lower well of a tissue culture Transwell plate (BD Biosciences). hMSCs, pre-labeled with DiI (Invitrogen), a lipophilic viable cell tracer, were plated in the upper well of Transwell plate at a density of 5×10^4 cell per Transwell. Hutu cells and hMSCs were co-incubated for 7 days and then the number of hMSCs passed through the Transwell and therefore migrated toward Hutu cells and/or growth factors pre-treated cells into 180 seconds were counted by flow cytometer . The experiments were done in triplicate.

3.2 MATERIALS AND METHODS

Part II

3.2.1 Isolation and Expansion of GSCs

In the second part of this study Human GSCs cultures: GBM2, GBM3, GBM4, and GBM5 of primary GBM surgical specimens were described. GBM specimens were obtained during surgical procedures of tumor removal previous a patient informed consent.

3.2.2 Tissue Dissociation

GSCs have been kindly provided by the Department of Molecular Medicine (Dr. Sgubin, Prof. Palù`) and cultured in neural stem cell media, as described in literature (Sgubin et al., 2012) (Kanai et al., 2012) (Wakimoto et al., 2009).

3.2.3 Cell Cultures

- **GSCs** were cultured as spheres in EF20 medium: Neurobasal Medium (GIBCO) supplemented with 3 mmol/l L-glutamine (Mediatech, Manassas,VA, http://www.cellgro.com), 1X B27 supplement (Life Technologies), $0.5XN_2$ supplement (Life Technologies), 2 µg/ml heparin (Sigma-Aldrich), 20 ng/ml recombinant human EGF (R&D Systems Inc.), 20 ng/ml recombinant human FGF2 (Peprotech, Rocky Hill, NJ, http://www.peprotech.com), and 0.5X penicillin G-streptomycin sulfate-amphotericin B complex (Mediatech). The cultures were fed once a week with one-tenth volume of fresh medium. Cell passaging was performed by dissociation of spheres using NeuroCult chemical dissociation kit (StemCell) (Sgubin et al., 2012) (Kanai et al., 2012) (Wakimoto et al., 2009).

- VERO cells (African green monkey kidney) obtained from the Dept. of Microbiology and Virology of the University of Padova were grown and maintained in DMEM medium containing 10% FBS.

3.2.4 Viruses

- **HSV1 wild type strain F** is a prototype HSV-1 strain used in this study.
- **R3616,** derived from HSV1 wild-type strain F, contains 1 kilobase-pair (1kbp) deletion in both copies of the $\gamma_1$34.5 gene (Chou et al., 1990).

3.2.5 Virus titration plaque assay

Vero cells were seeded in 6-well plates at a density of 20×10^4 cells per well in 2mL DMEM 10% FBS medium and infected with serial dilutions of virus prepared in 0.7 ml of DMEM with 1%IFBS. After 2 hours virus inoculum was removed and cells were incubated in 1mL DMEM 1%IFBS supplemented with methylcellulose at 37°C until plaques were visible. Cells were fixed with methanol for Giemsa staining and plaques were counted to determine the viral titer as Plaque-Forming Unit (PFU)/mL (Kuroda et al., 2006).

3.2.6 Cell Growth Curves

After spheres dissociation, 2×10^4 GBM2 and GBM4 cells were seeded in a 24-well plate in 500 µL EF20 medium and cultured. Viable cells (trypan blue-excluding) were counted on days 3, 6 and 9 on a Burker counting chamber.

3.2.7 Virus Yield Assay

GBM2 and GBM4 cells were single cell dissociated, seeded in 500 µL EF20 medium at the density of 2×10^4 cells per well in 24-well plates and infected with HSV1 or R3616 at Multiplicity Of Infection (MOI) of 0.2 and 1.5 respectively. The cells were harvested with supernatant at 12, 24, 48 and 72 hours after infection and processed with three

freeze/thaw cycles and sonication. The titers of the viruses in the lysates were determined by plaque assay on Vero cells (Kuroda et al., 2006).
For BM-MSCs viral yield assay, cells were seeded at the same density in 500 µL DMEM 20% FBS medium and monolayers were scraped into the medium to collect supernatants at previously indicated time points.

3.2.8 Cell Killing Assay

Single-cell suspensions of GSCs or BM-MSCs were seeded in 24-well plates at a density of 2×10^4 cells per well and infected with HSV1 and R3616 at MOI of 0.2 and 0.5 respectively. The cells were harvested at days 3, 6 and 9 and dissociated with 0.25%/0.1% Trypsin/EDTA (GIBCO), and viable (trypan blue-excluding) cells were counted on a Burker counting chamber.

3.2.9 Flow cytometry analysis

Analysis of GBM2, GBM3, GBM4 and GBM5 phenotype was performed by using the Stemflow Neural Cell Lineage Kit following the manufacturer's instructions previously described.
Moreover for surface marker analysis, antibodies against human CD133 (clone AC133/2-PE, Miltenyi), CD90 (FITC conjugated, BioLegend), CD44 (FITC conjugated, BD Biosciences), CD24 (PC5 conjugated, Immunotech a.s., Praha, Czech Republic, http://www. immunotech.cz), CD105, CD29, and CD56 (all of them PE conjugated, BD Biosciences) were also been tested.

3.2.10 BM-MSCs "*in vitro*" Migration Assay toward GSCs

The BM-MSCs tropism towards GBM2 and GBM4 cells, toward the growth factors conditioned medium and GBM2 and GBM4 cells pre-treated with BMP2 was tested by "*in vitro*" migration assay under normoxic conditions using the same protocol previously described. GSCs were seeded in 12-well plates at a density of 4×10^4 cells/ well in 1mL EF20 medium in the lower well of a tissue culture Transwell plate. To

induce differentiation, GBM cells were supplemented with BMP2 at the final concentration of 50ng/mL/day for 7 days before loading hMSCs on Transwell.
To investigate BM-MSCs tropism toward GSCs previously HSV1 or R3616 infected, GBM2 and GBM4 cells were seeded at the same density, infected with HSV1 at MOI of 0.1 and R3616 virus at MOI of 0.25. Prelabeled DiI-BM-MSCs were loaded respectively after 48 and 72 hours infection, according to the viral replication. Migratory properties were evaluated after 7 days of incubation using the same protocol above described.

3.2.11 BMP2 and R3616 virus Combination Treatment Assay

To investigate whether the infection of R3616 virus and the treatment with BMP2 could exert a combination effect in induce GSCs differentiation, GBM2 and GBM4 cells were seeded at a density of 6×10^4 cells in 3 mL EF20 medium and infected with R3616 at MOI of 0.1. To induce differentiation, GBM cells were supplemented with BMP2 at the final concentration of 50ng/mL/day for 7 days before analyzing the expression of the Nestin, Sox2, βIII-tubulin and GFAP markers included by the Stemflow Neural Cell Lineage Kit using flow cytometric techniques. A mock control, GBM cells infected with R3616 or treated with BMP2 alone were also included.

3.2.12 Western Blots

Following proper treatment, cells were washed with 1X PBS, resuspended in RIPA buffer (Sigma-Aldrich) with Protease Inhibitors (Sigma-Aldrich), lysed on ice for 30 minutes, and centrifuged for 10 minutes to separate cell debris. Protein concentrations of each sample were determined using the Micro BCA Protein Assay Kit (Thermo Fisher Scientific Inc., Meridian Rd Rockford, IL, USA, http://www.piercenet.com). Twenty micrograms of proteins were separated on a 7.5%, 10% or 12% SDS-polyacrylamide electrophoresis gel, transferred to a Whatman membrane (GE Healthcare), and incubated with primary antibodies overnight at 4°C under shacking. The next day, membranes were incubated with secondary peroxidase-conjugated antibodies for 1 hour at R.T. Proteins were visualized using the ECL Advanced Western blotting detection Kit (GE Healthcare) on Kodak BioMax light (Sigma-Aldrich). The

primary antibodies were used as following: 1:1000 rabbit anti-CD133 (clone AC133/2, Miltenyi); 1:5000 goat anti-Nestin (Santa Cruz Biotechnology, Inc, Santa Cruz, CA, USA; http://www.scbt.com)); 1:1000 rabbit anti-Sox2 (Cell Signaling Technologies Inc. Danvers, MA, USA; www.cellsignaling.com); 1:500 mouse anti-GFAP (Sigma-Aldrich); 1:1000 rabbit anti-Tuj1 (Covance, Princeton, NJ, USA; www.covance.com); 1:1000 mouse Pi-Smad1/5/8 (S463/465; S463/465; S426/428; Cell Signaling); 1:300 rabbit Smad1/5/8 (Santa Cruz Biotechnology); 1:5000 mouse β-actin (Sigma-Aldrich) and 1:1000 mouse anti-α-Tubulin (Sigma Aldrich). Secondary antibodies were peroxidase-labeled 1:2000 goat anti-rabbit IgG (Sigma Aldrich) or peroxidase-labeled 1:2000 goat anti-murine IgG (Sigma Aldrich).

3.3 Statistical analysis

Graphs and statistical analyses were prepared using Prism 5 (Graph Pad Software, Inc., San Diego, USA; http://www.graphpad.com) or Excel. Values are presented as mean ± standard error (SD). Statistical significance was measured by two-tailored unpaired *t-test* or one-way ANOVA with post-hoc Newman-Keul's test, *P < 0.05, **P < 0.01, ***P < 0.001. P values less than 0.05 were considered statistically significant.

4.1 RESULTS

Part I

The following reported data have been obtained from the collaboration between two Departments of the University of Padova: the Laboratory of Oncohematology (Department of Woman and Child, Supervisor: Prof. G. Basso, MD) where I worked with Dr. Persano, PhD as tutor and the Microbiology and Virology Laboratory (Department of Molecular Medicine, Supervisor: Prof. G. Palù, MD) where my tutor was Dr. D. Sgubin, MD.

Results presented in the first part of the study report cell delivery experiments employing human Mesenchymal Stem Cells as delivery vehicles for therapeutic molecules for the treatment of GBM.
Data described in Part II focus on viral therapy experiments for GBM in GSCs primary cultures.

▪ 4.1.1 Isolation of human Mesenchymal Stem Cells (hMSCs) and cell culture

hMSCs were collected from remaining samples of clinical bone marrow (BM-MSCs) transplantation drawing from consenting healthy volunteer donors or were derived from adipose tissue of glioma patients biopsies (AT-MSCs). Both hMSCs were isolated as the adherent fraction of mononuclear part by DMEM medium containing 20% FBS and grown in normoxic (21% O_2) or hypoxic conditions (2% O_2). Indeed, it was important to verify whether hMSCs were able to efficiently grow at both O_2 levels once they reached the perivascular or the hypoxic GBM niche after delivering.

In **Figure 13.** is reported in example images of BM-MSCs at 48 hours (Panel **A.**) and 15 days (Panel **B.**) after plating and grown in normoxia.

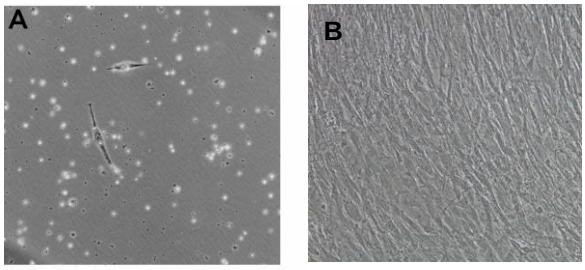

Figure 13. Characterization of isolated human Bone Marrow Mesenchymal Stem Cells (BM-MSCs). Cells were cultured from marrow after density fractionation and are shown at 48 hours after plating (Panel **A.**) and at 15 days after plating (Panel **B.**).

BM-MSCs as well as AT-MSCs retained the typical spindle shape, consistent with the mesenchymal morphology reported in literature (Zuk et al., 2002) (Pittenger et al., 1999) and no significant morphological differences between BM-MSCs and AT-MSCs neither in normoxia (**Figure 14.**), nor in hypoxia atmosphere were observed.

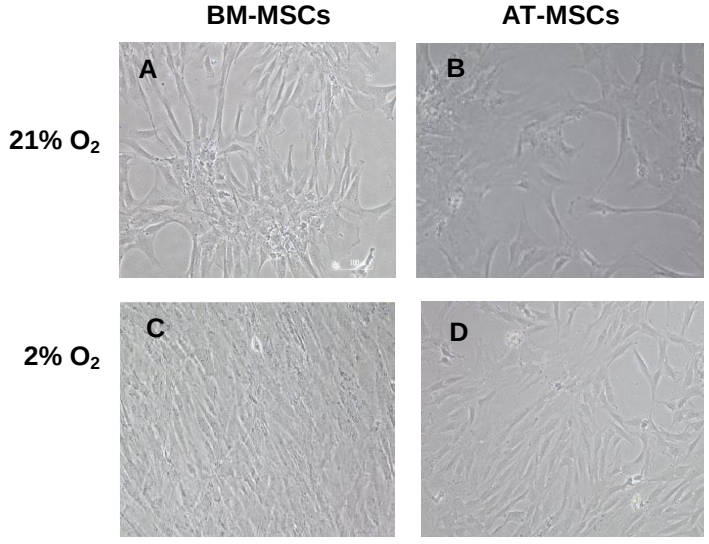

Figure 14. Morphological characterization of BM-MSCs and human Adipose Tissue Mesenchymal Stem Cells (AT-MSCs) isolated in DMEM medium containing 20% FBS and grown under normoxic (21% O_2) (Panel **A.** and Panel **B.** respectively) and hypoxic (2% O_2) (Panel **C.** and Panel **D.** respectively) conditions.

▪ 4.1.2 Characterization of stem like characteristics in AT- and BM-MSCs

The purity of the mesenchymal lineage of selected cells was assessed by a phenotypic characterization that was confirmed 15 days after isolation.

To evaluate hMSCs immune-phenotype, fifteen different cell surface markers were tested using cytofluorimetric techniques: CD90, HLA-DR, CD44, CD73, CD105, CD29, CD166; CD106, CD184, CD271, CD117, CD19, CD14, CD45, and CD133. Representative histograms are shown in **Figure 15.**.

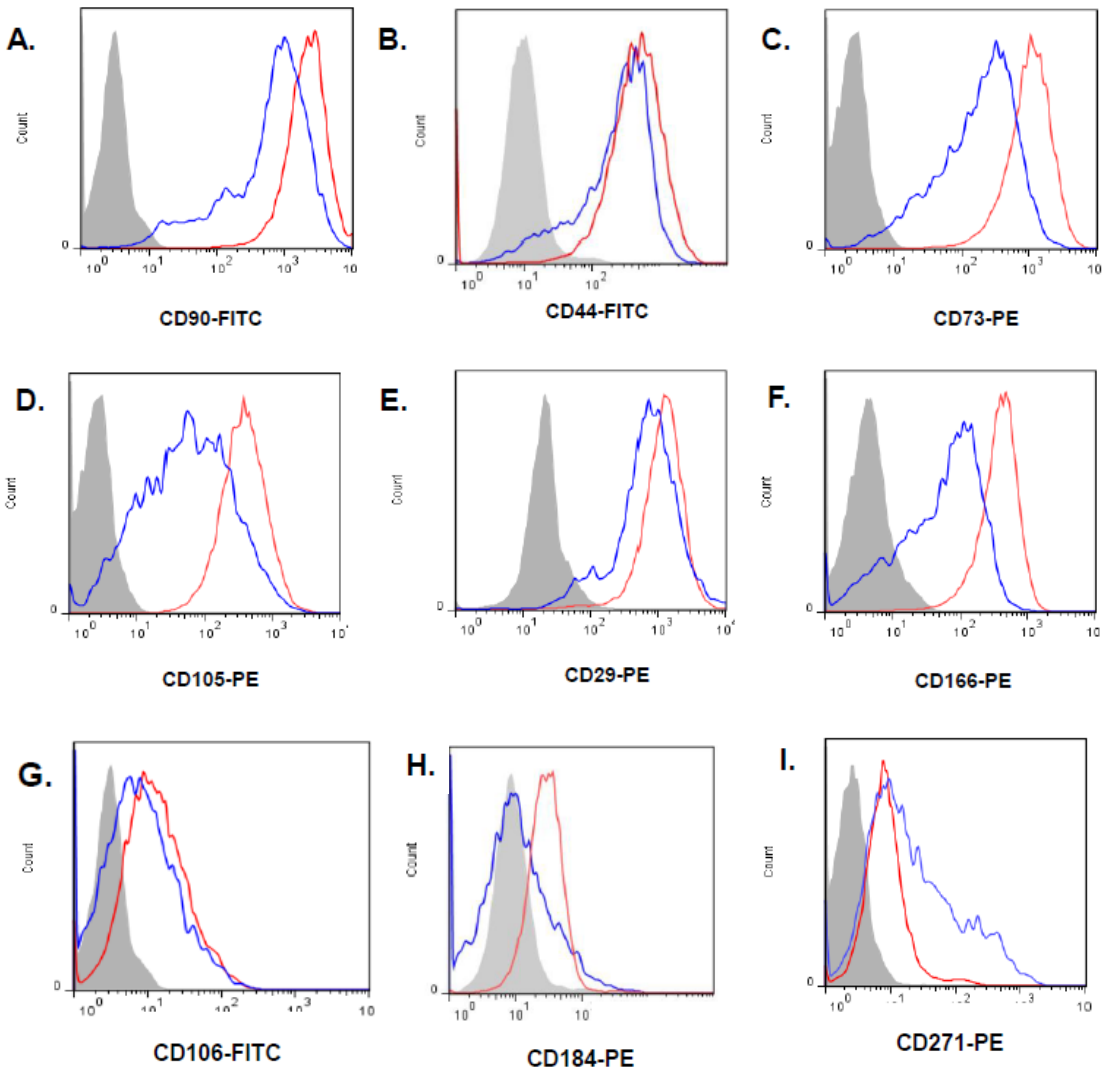

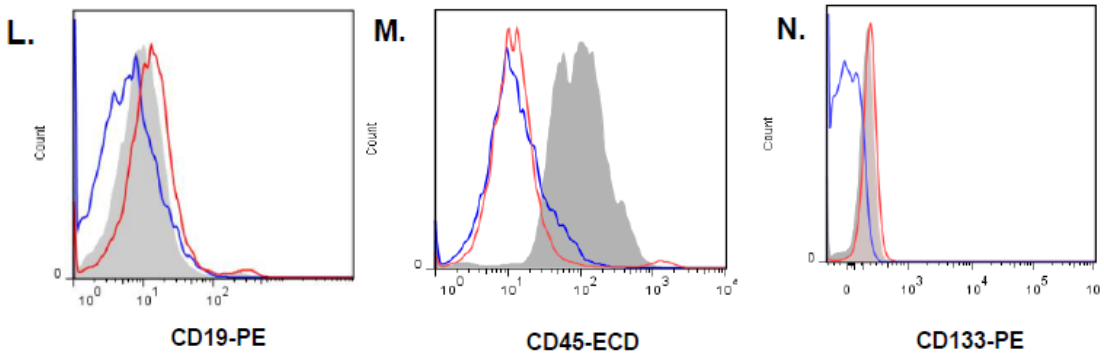

Figure 15. Immunophenotypic characterization of cell surface markers tested on hMSCs using cytofluorimetric techniques. BM-MSCs (red lines) and AT-MSCs (blue lines). Expression levels of CD90 (Panel **A.**), CD44 (Panel **B.**), CD73 (Panel **C.**), CD105 (Panel **D.**), CD29 (Panel **E.**), CD166 (Panel **F.**), CD106 (Panel **G.**), CD184 (Panel **H.**), CD271 (Panel **I.**), CD19 (Panel **L.**), CD45 (Panel **M.**) and CD133 (Panel **N.**) are shown. Flow cytometric analysis performed 15 days after isolation, confirmed that hMSCs retained the same surface molecules as those found on hMSCs from which they were derived. Grey lines represent unlabeled hMSCs.

According to criteria recommended by the International Society for Cellular Therapy (ISCT), our BM-MSCs and AT-MSCs positively expressed CD105 (endoglin receptor), CD73 (surface enzyme ecto-5'-nucleotidase), CD44 (hyaluronic receptor), CD90 (extracellular matrix protein), as well as the adhesion molecules CD29 (β_1-integrin), CD166 (activated leukocyte cell adhesion molecule) and CD271.

Conversely, they were negative for the most common hematopoietic surface antigens, such as: CD14, CD19, CD45 (Le Blanc et al., 2003; Pittenger et al., 1999) (Chamberlain et al., 2007).

Detailed percentages of each surface marker expression are reported in **Table2**.

Antibody	BM-MSCs	AT-MSCs
CD90	98,5±0.46	90 ± 1.8
HLA-DR	7.5 ±3.45	11 ± 4.1
CD44	94.33±0.87	92 ± 0.6
CD73	99.5± 0.06	91 ± 2.8
CD105	99.2± 1.13	89 ± 1
CD29	78.2± 37.50	99 ± 1.8
CD166	99.1± 0.65	81,5 ± 5.7
CD106	15.32 ± 2.6	13.4 ± 7.1
CD184	6.23 ± 3.80	negative
CD271	2.6 ±2.2	20 ± 2.8
CD117	negative	8 ± 2.8
CD19	negative	negative
CD14	negative	negative
CD45	negative	negative
CD133	1.33 ± 0.76	negative

Table 2. Phenotypic characterization of BM- and AT-MSCs: comparison of percentage of cell surface markers expressed by the two hMSC sources. Data acquired using cytofluorimetric thecniques. Each value represents the average percentage of at least three different experiments. ± is standard deviation (SD).

We tested several BM- and AT-derived MSCs lines and all our cell lineages displayed a stable phenotype. Flow cytometric analysis repeated 15 days after the first characterization, confirmed that hMSCs from both sources retained the same surface molecules as those found on hMSCs from which they were derived.

BM-MSCs was expected to be negative for CD106 expression, since CD106 is a vascular cell adhesion molecule associated with hematopoiesis (Zuk et al., 2002) (Chamberlain et al., 2007); accordingly, we found a low expression of CD106 both in BM-MSCs (15.3%) and in AT-MSCs (13.4%).

We also found slightly positive expression of the Human leukocyte antigen Class II (HLA-DR) antigen (7.5% on BM-MSCs and 11% on AT-MSCs), expected to be negative in adult hMSCs (Le Blanc et al., 2003) .

AT-MSCs demonstrated a positivity of 8% for the expression of CD117 (c-kit), marker associated to hematopoietic phenotype, thus expected to be negative, as retained in our BM-MSCs.

In general BM-MSCs expressed higher levels of selected cell surface markers in comparison to AT-MSCs, that could be related to the tissue source. Only CD271 expression was found higher in AT-MSCs than BM-MSCs, counting for 20% versus 2.6%.

Noteworthy, the study of CD133, a putative stem cell marker (Singh et al., 2004b), revealed that it was slightly expressed only in BM-MSCs, whilst it was totally absent in AT-MSCs, as reported in the last row of **Figure 15.**. A CD133-positive cell fraction was previously documented in hMSCs isolated from umbilical cord blood and in mobilized peripheral blood (Tondreau et al., 2005) (Doucette et al., 2011).

▪ 4.1.3 *In vitro* qualitative and quantitative differentiation of BM-MSCs and AT-MSCs under normoxic and hypoxic conditions

Upon the identification of mesenchymal lineage based on morphological and phenotypical characteristics, the stem cell nature of the BM-MSCs and AT-MSCs was *in vitro* confirmed by measuring their capacity to differentiate into multiple cell lineage.

Our BM-MSCs and AT-MSCs were tested for their ability to differentiate into adipocytes and osteoblasts when grown in appropriate conditioning media containing pro- adipogenic or pro-osteogenic factors. Since it is well reported that hypoxia increases stemness (Bar, 2011) (Heddleston et al., 2009), these properties were assessed both at 21% and 2% O_2. Representative results are reported in **Figure 16.**.

Adipogenesis (**Figure 16.** Panel **A.)** was detected through accumulation of lipid vacuoles within the cells and stained with Oil Red O. Cells adopted a round morphology and formed cytoplasmic droplets. Osteogenesis (**Figure 16.** Panel **B.)** was assessed by the mineralization of extracellular matrix and the accumulation of calcium depositions stained with Alizarin Red S dye.

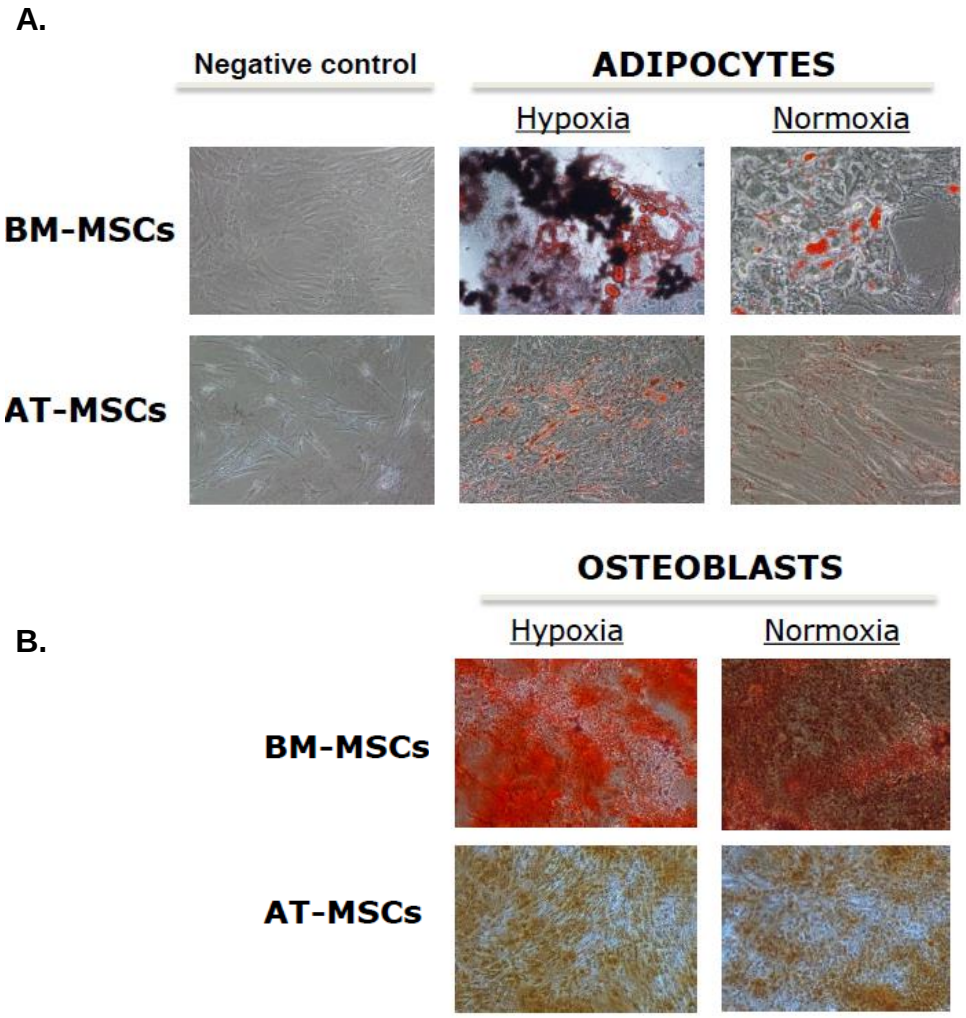

Figure 16. hMSCs differentiation assay. hMSCs isolated from BM- or AT- were tested for their ability to differentiate into adipocytes (Panel **A.**) or osteoblasts (Panel **B.**) when cultured under properly conditions for adipogenesis and osteogenesis both at 2% and 21% O_2. A negative control for both cell line was also included. Original magnification ×20.

BM-MSCs and AT-MSCs untreated control cultures, which were grown in regular medium without adipogenic or osteogenic differentiation stimuli, did not exhibit adipocyte or osteoblasts formation neither after 21 days of cultivation (see negative controls in **Figure 16.** Panel **A.**), thus confirming that our hMSCs did not differentiate spontaneously during culture expansion.

From the different assay conditions required for efficient differentiation, it is conceivable how basal nutrients, cell density, growth factors and cytokines can have a crucial role on hMSCs differentiation.

As shown in **Figure 16.**, BM-MSCs displayed more proliferative properties and a higher *in vitro* ability to differentiate into adipocytes or osteoblasts compared to AT-MSCs. In particular, this efficiency was found greatly increased at 2% O_2. Adipogenic differentiation demonstrated how AT-MSCs produced fewer and smaller lipid intracellular vacuoles than BM-MSCs, especially under normoxic conditions, suggesting that adipocytes in BM-MSCs could form earlier than in AT-MSCs and could be more mature. It is possible that a longer culture period could be necessary for adipogenic differentiation of AT-MSCs.

To further confirm these data, quantitative differentiation analysis of adipogenesis (**Figure 17.** Panel **A.**) and osteogenesis (**Figure 17.** Panel **B.**) based on spectrophotometric techniques were performed under normoxic and hypoxic conditions.

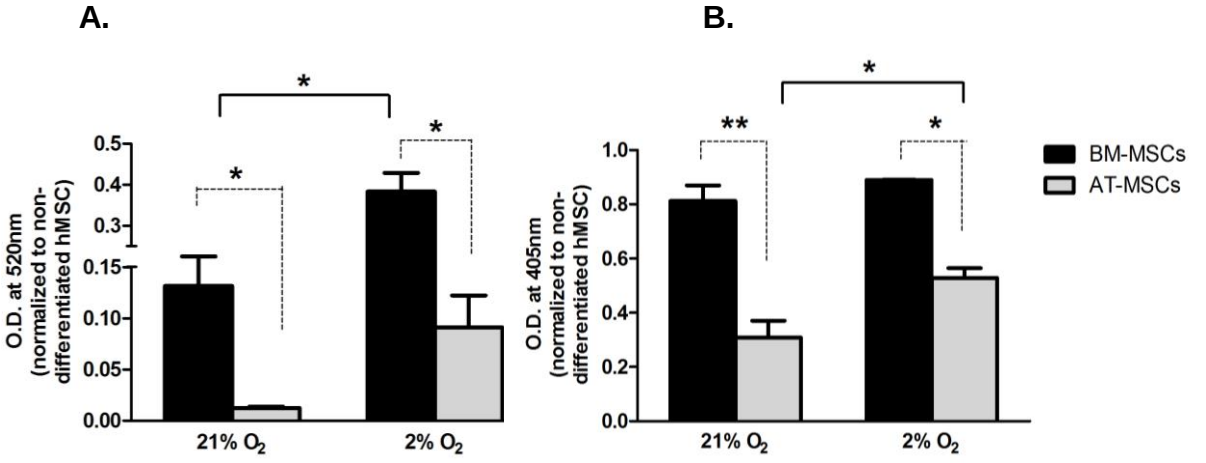

Figure 17. Histograms resembling BM-MSCs (black bars) and AT-MSCs (grey bars) quantitative adipogenic (Panel **A.**) and osteogenic (Panel **B.**) differentiation at 21% O_2 and 2% O_2 tension. After fixing and staining hMSCs with Oil Red O dye in the case of adipocytes or with Alizarin Red S dye for osteoblasts, the intensity of the dye was measured at 520 and 405 nm respectively using spectroscopic techniques. The Optical Density (O.D.) ratios reported are been normalized to non-differentiated proper hMSCs (negative control). * $P < 0.05$ (two-tailored unpaired *t-test*) between indicated bars. Panel **A.** It has been found significantly difference between BM- and AT-MSCs in normoxia and hypoxia (*$P < 0.05$) and between BM-MSCs grown at 21% and 2% O_2 (*$P < 0.05$). Panel **B.** It has been found significantly difference between BM- and AT-MSCs in normoxia (**$P < 0.01$) and hypoxia (*$P < 0.05$) and between BM-MSCs grown at 21% and 2% O_2 (*$P < 0.05$).

As shown in **Figure 17.**, BM-MSCs exhibited a statistically significant difference in ability to quantitative differentiate into adyposites and osteoblasts both under normoxic and hypoxic conditions compared to the AT-MSCs (*P < 0.05) confirming qualitative data reported in **Figure 16.**. Accordingly, in BM-MSCs quantitative adipogenic and osteogenic differentiation efficiency was found statistically increased in hypoxia (**P < 0.01).

▪ 4.1.4 Cell growth analyses

To verify whether BM-MSCs exhibited a more proliferative potential *per sè* in comparison to AT-MSCs, cells were grown under hypoxic and normoxic conditions and counted after 24, 48 and 72 hours **(Figure 18.)**.

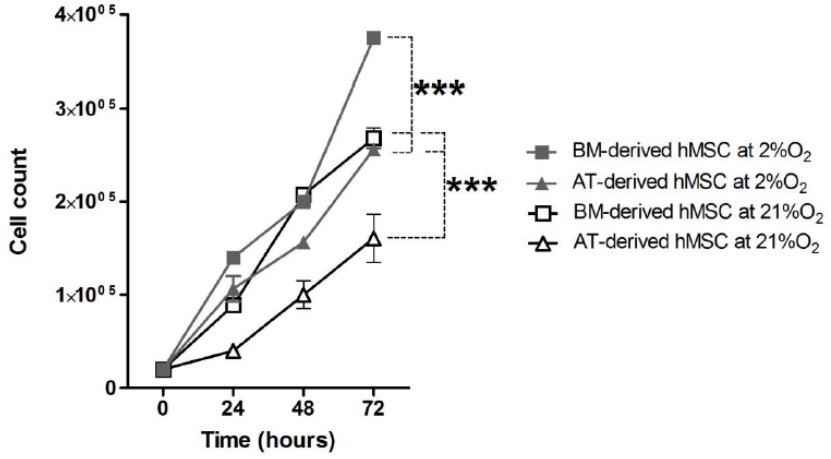

Figure 18. Growth kinetics of BM- and AT-MSCs under hypoxic (grey check and triangle respectively) and normoxic (white check and triangle respectively) conditions. *** P<0.001 (One-way ANOVA) indicated pairs are significantly different at 72h between BM- and AT-MSCs in hypoxia and normoxia. Error bars are standard deviations (SD).

A statistically significant difference in proliferation rate under hypoxic as well as under normoxic conditions was found at 72h after seeding both in BM-MSCs and AT-MSCs (P<0.001). BM-MSCs grew faster compared to AT-MSCs both in hypoxia and in normoxia (P<0.001). Indeed, BM-MSCs expanded 1.5-fold than AT-MSCs both in hypoxic and normoxic conditions after 72 hours, confirming an increased proliferative activity compared to AT-MSCs.

- **4.1.5 *In vitro* evaluation of migratory properties of BM-MSCs and AT-MSCs toward GBM derived stem like cells under HYPOXIC conditions**

Before evaluating migratory properties of BM- and AT-MSCs towards GBM derived cells, we verified that the selected medium for GBM cell cultures in which hMSCs should grow along the time of migration assay, did not modify their immunophenotype. Thus, cells were seeded alternatively in DMEM 20% FBS and in DMEM-F12 supplemented with BIT serum substitute and cultured for seven days before analyzing some of the most common mesenchymal surface markers using cytofluorimetric techniques. For this analysis performed in BM-MSCs following markers investigated: CD44, CD73, CD90, CD105, CD106 and CD166 (**Figure 19.**).

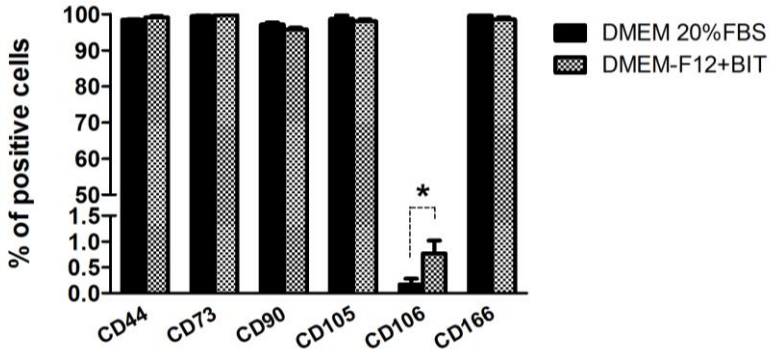

Figure 19. Immunophenotypic characterization of CD44, CD73, CD90, CD105, CD106 and CD166 cell surface markers tested on BM-MSCs grown in DMEM 20% FBS and DMEM-F12 BIT media seven days after seeding. Data acquired using cytofluorimetric techniques. Except for CD106, all other markers evaluated retained the same expression levels when grown in DMEM-F12 plus BIT. CD106 was found significantly increased when BM-MSCs were grown in DMEM-F12 medium plus BIT (*$P < 0.05$). Error bars are standard deviation (SD).

Except CD106 that demonstrated to be significantly increased when BM-MSCs were grown in DMEM-F12 medium supplemented with a serum substitute (*****$P < 0.05$), no significant variations in markers expression levels were observed, suggesting that BM-MSCs retained a stable phenotype even when grown along seven days.

BMP2 and WNT3a have been described in literature as astro-glial (Piccirillo et al., 2006) (Persano et al., 2013) and neuronal (Rampazzo et al., 2013) pro-differentiating factors respectively; therefore, we sought to preliminary test whether a BMP2 or WNT3a pro-differentiating treatment of GBM cells would increase hMSCs migratory properties. Additionally, with the final aim to employ genetically engineered hMSCs expressing therapeutic genes, as delivery vehicles for brain tumor therapy, we investigated whether BMP2 or WNT3a, as two potential suitable agents, would enhance hMSCs tropism when loaded at the same time of hMSCs.

By immunohistological analyses we previously verified GBM cells differentiation upon BMP2 and WNT 3a supplementation. Cells were treated with a single 20ng/mL BMP2 spike/die per five days or 30 ng/mL WNT3a spike/die per seven days. Repeated applications were needed due to the short half-life of both biological agents tested. BMP2 treated GBM-derived cells were stained with βIII-tubulin (red) and GFAP (green) according to the protocol described in recently published data (Persano et al., 2012) (Rampazzo et al., 2013). As shown in **Figure 20.**, Panel **A.** BMP2 pre-treatment induced a increment of βIII-tubulin and GFAP expression levels in GBM cells compared to the control not treated. Similar results were observed when GBM cells received WNT 3a treatment (**Figure 20.**, Panel **B.**).

A.

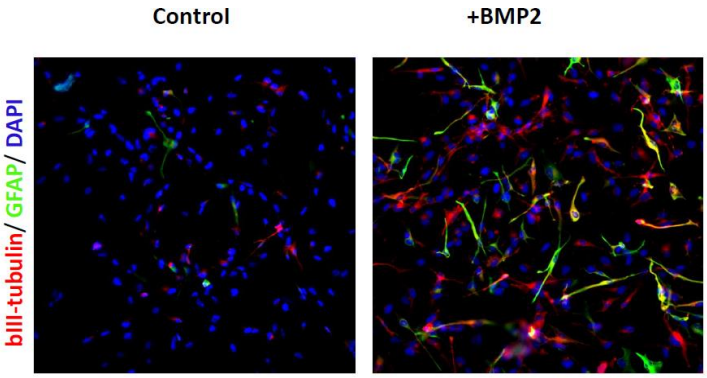

B.

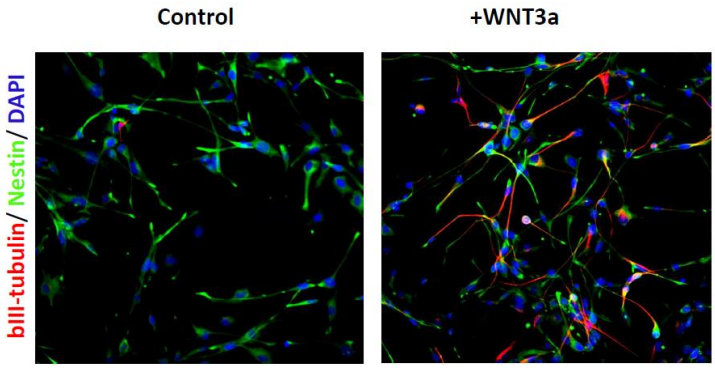

Figure 20. Images showing phenotypic analysis of GBM cells. In Panel **A.**: hGBM CTRL and hGBM cells BMP2 treated and stained for βIII-tubulin (red), GFAP (green) and DAPI (blue) were analyzed. In Panel **B.**: hGBM CTRL and hGBM cells WNT3a treated and stained for βIII-tubulin (red), Nestin (green) and DAPI (blue) were analyzed. 10X Magnification.

Hypoxia has been identified to play a critical role in promoting tropism of hMSCs toward GBM cells (Rochefort et al., 2006). Moreover, in order to assess whether cytokines released the GBM and other soluble factors, such as BMP2, as astro-glial pro-differentiating agent, or WNT3a, as neuronal pro-differentiating molecule or whether oxygen levels could influence the hMSCs inherent tropism toward GBM cells, *in vitro* migration assays were performed under hypoxic conditions.

To identify hMSCs migrated towards GBM-derived cells, hMSCs were previously labeled using the viable cell Tracer CM-DiI; then plated in the top well of a Transwell plate and counted using cytofluorimetric techniques seven days after seeding. To study the possible oxygen level effects exhibited on hMSCs tropism toward GBM-derived stem like cells, hGBM cells previously grown in hypoxia, were exposed at 21% O_2 for 15 days before loading hMSCs. Moreover, hMSCs *in vitro* migration was evaluated toward the hGBM cells conditioned medium; hGBM cells alone and hGBM cells added of 20ng/mL BMP2 or 30 ng/mL WNT3a at the same moment of hMSCs loading to monitor whether BMP2 or WNT3a presence could modulate hMSCs migration. A negative control (medium culture alone) was also included.

In **Figure 21.** is shown the *in vitro* migration profile retained by BM-MSCs and AT-MSCs toward GBM stem like cells, treated or not under hypoxic conditions.

Cells migration was calculated as a ratio, so-called migration index, normalizing the number of MSCs passed into 180 seconds in each conditions with the number of hMSCs passed to medium alone.

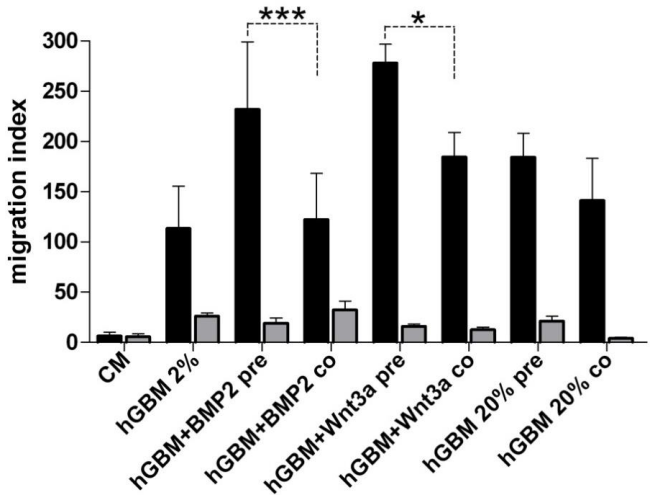

Figure 21. Migratory properties of BM-MSCs (black bars) and AT-MSCs (grey bars) toward GBM derived stem like cells under hypoxic conditions. **C.M.**: hGBM cells Conditioned Medium, **hGBM**: hGBM cells alone, **hGBM+BMP2 pre**: hGBM cells pre-differentiated with BMP2 treatment at the concentration of 20 ng/ml for 5 days, **hGBM+BMP2 co**: 20ng/ml BMP2 added to hGBM cells at the same moment of hMSCs, **hGBM+Wnt3a pre**: hGBM cells pre-differentiated with Wnt3a treatment at the concentration of 30 ng/ml for 7 days, **hGBM+Wnt3a co**: 30ng/ml Wnt3a added to hGBM cells at the same moment of hMSCs, **hGBM 20% O2 pre**: hGBM cells pre-differentiated at 20% O_2 treatment for 15 days. **hGBM 20% O2 co**: MI of hMSCs referred to hGBM cells pre-differentiated at 20% O_2 in normoxia. Migration index was calculated normalizing the number of hMSCs passed into 180 seconds in each conditions with the number of hMSCs passed to medium alone. Error bars are standard deviations (SD). *$P < 0.05$, ***$P < 0.001$ (one-way ANOVA) between indicated pairs in BM-MSCs. It has been found significantly difference between hGBM+Wnt3a pre and hGBM+Wnt3a co and between hGBM+BMP2 pre and hGBM+BMP2 co.

Our results suggest that under hypoxic conditions, BMP2- and WNT3a-differentiated GBM stem like cells dramatically enhanced the migratory properties of BM-MSCs when cells were pre-treated, likewise when biological agents were supplemented to GBM cells at the same moment of hMSCs loading.

AT-MSCs appeared much less sensitive to all biological agents screened displaying a weak and aspecific migratory ability compared to BM-MSCs.
For this reason we selected BM-MSCs as suitable cell carrier for further analyses.

To directly estimate how oxygen levels could modulate hMSCs migratory properties, hMSCs-DiI^{+} were simultaneously loaded on GBM cells cultured at 2% and 21% O_2 and counted seven days after seeding. In **Figure 22.** is reported the migratory properties of BM-MSCs toward hGBM cells (i.e. hGBM13) grown in hypoxia and normoxia. The *in vitro* migration was evaluated toward the GBM cells conditioned medium; GBM cells alone, GBM cells BMP2 pre-treated at the concentration of 20 ng/mL/die for 5 days and GBM cells added of 20ng/mL BMP2 at the same moment of hMSCs loading.

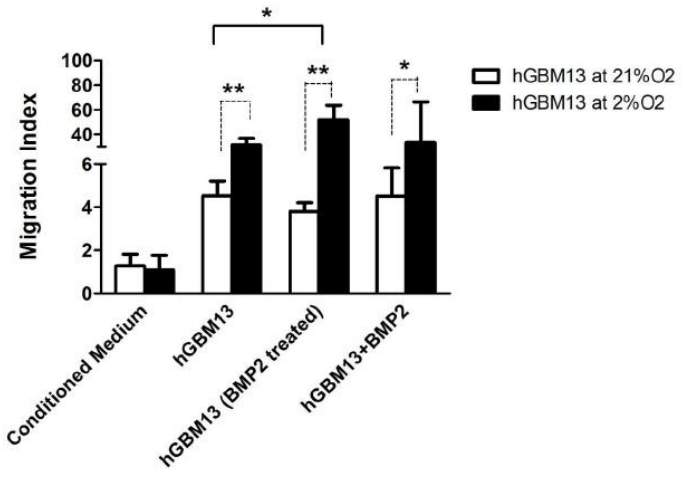

Figure 22. Comparison of *in vitro* migratory properties of BM-MSCs toward hGBM derived cells (i.e. hGBM13) under normoxic (white bars) and hypoxic (black bars) conditions. **Conditioned Medium**: GBM cells Conditioned Medium, **hGBM**: hGBM cells alone, **hGBM(BMP2 treated)**: GBM cells pre-differentiated with BMP2 treatment at the concentration of 20 ng/ml for 5 days, **hGBM+BMP2**: 20ng/ml BMP2 added to GBM cells at the same moment of hMSCs. Migration index was calculated normalizing the number of hMSCs passed into 180 seconds in each conditions with the number of hMSCs passed to medium alone. Error bars are standard deviations (SD). *P < 0.05, **P < 0.01 (two-tailored unpaired *t-test*) between indicated pairs. hGBM was found significantly different in normoxia and hypoxia (**P < 0.01). hGBM(BMP2 treated) was found significantly different in hypoxia and normoxia (**P < 0.01). hGBM+BMP2 was found significantly different in normoxia and hypoxia (*P < 0.05). Under hypoxic conditions it has been found significant difference between hGBM and hGBM(BMP2 treated) (*P < 0.05).

Results demonstrated that the inherent migratory properties of BM-MSCs toward GBM cells alone, GBM cells BMP2 pre-differentiated for 5 days or enriched with BMP2 at the moment of hMSCs loading were greatly increased in hypoxic conditions. Moreover, the significantly difference found between hGBM and hGBM (BMP2) treated confirmed the enhancer effect induced by hypoxia on hMSCs migration upon BMP2 treated cells of hGBM specimens (i.e. hGBM13). Conversely, GBM cells grown in normoxia did not exert any significant modulation on hMSCs homing.

Taken together all these findings suggest how hypoxia as well as the treatment with BMP2 as pro-differentiating agent for GBM stem like cells greatly enhance the migration properties of hMSCs.
BM-MSCs, displaying a more proliferative and growing properties, a greater ability to differentiate into multiple cell lineage and a higher inherent tropism toward GBM stem like cells in normoxia as well as in hypoxia compared to AT-MSCs, were selected the for future analyses of our study.

▪ 4.1.6 Direct modulation of GBM stem cell markers by BM-MSCs

To better understand the effects exerted by BM-MSCs once reached tumor bed, we analyzed the expression of the most common stemness markers, such as Nestin (neural stem cells), Sox2 (neural stem cells), CD133 and differentiation markers, such as, βIII-tubulin (neuronal), CD44 (astrocytes, astrocyte precursors) and GFAP (filament astrocytes) after co-culture with BM-MSCs in normoxia and hypoxia conditions, thus resembling both peculiar GBM niches. The BM-MSCs immunophenotypic characterization previously assessed in different media confirmed us that hMSCs retained a stable phenotype. To directly estimate how oxygen levels could modulate co-colture, BM-MSCs were simultaneously seeded with hGBM cells and cultured at 2% and 21% O2 for seven days until measuring markers expression on hGBM cells with cytofluorimetric techniques. To recognize GBM cells from BM-MSCs, hGBM cells were previously label with PKH-26 and PKH-67, two membrane staining and grown as monolayer.

Examples of BM-MSCs co-cultured with hGBM cells under normoxia (Panel **A.**) and hypoxia (Panel **B.**) are shown in **Figure 23.**.

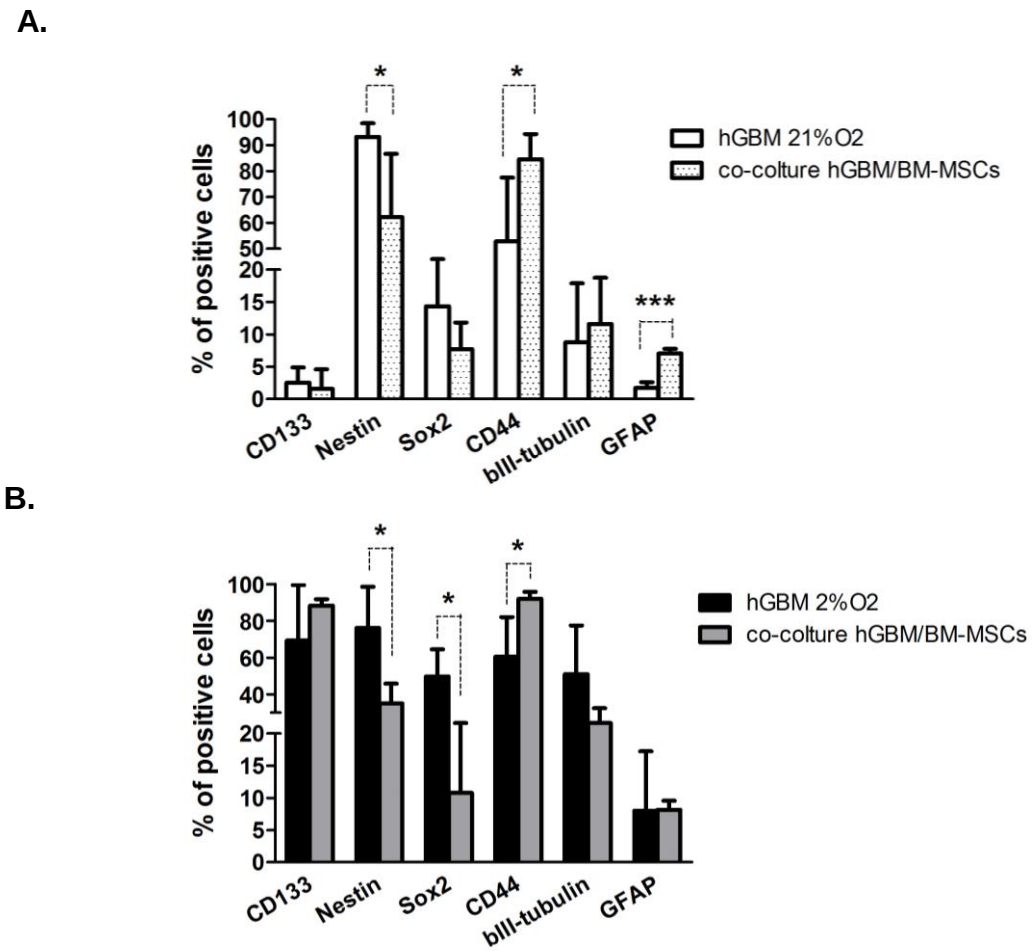

Figure 23. Modulation of hGBM cells and differentiation markers under effect of BM-MSCs in normoxia (Panel **A.**) and hypoxia (Panel **B.**). Bar graph reporting relative Nestin$^+$, Sox-2$^+$, CD133$^+$, βIII-tubulin$^+$, CD44$^+$ and GFAP$^+$ hGBM cells quantification according to the BD Stemflow Human Neural Lineage Analysis Kit's instructions. *P < 0.05, ***P < 0.001 between indicated pairs (two-tailored unpaired *t-test*). In Panel **A.** it has been found statistical decrease of Nestin levels (*P < 0.05) and statistical increase of CD44 (*P < 0.05) and GFAP (***P < 0.001) levels. In Panel **B.** it has been found statistical decrease of Nestin and Sox2, levels (*P < 0.05) and statistical increase of CD44 (*P < 0.05) expression when hGBM cells were co-cultured with BM-MSCs. Results represent the average of two different experiments performed in triplicate. Error bars are standard deviations (SD).

BM-MSCs in co-culture with hGBM cells under normoxic conditions (Panel **A.**) induced a statistical decrease of Nestin levels (*P < 0.05) with a concomitant statistical increase of GFAP (***P < 0.001) levels, suggesting how the presence of hMSCs could contribute to a more differentiated commitment in hGBM cells. Under hypoxic

conditions, (Panel **B.**) co-colture mediated a statistical decrease of Nestin and Sox2 (*P < 0.05) levels as well as a statistical increase of CD44 (*P < 0.05) levels, three stemness markers. Notably, CD133 was found dimly expressed at 21% O_2; whereas at 2% O_2 its expression was found increased, even in co colture, supporting studies that report how hypoxia promotes the expansion of $CD133^+$ population through the activation of HIFs (Soeda et al., 2009) (Seidel et al., 2010)

4. 2 RESULTS

Part II

- **4.2.1 Isolation and characterization of GBM stem like cell cultures from human GBM specimens**

In the second part of this study primary GSCs were grown as spheres under the culture conditions designed for selective expansion of neural stem cells (Sgubin et al., 2012) (Kanai et al., 2012) (Wakimoto et al., 2009). Representative images of the two different cultures mainly employed in our studies, GBM2 and GBM4 are shown in **Figure 24**.

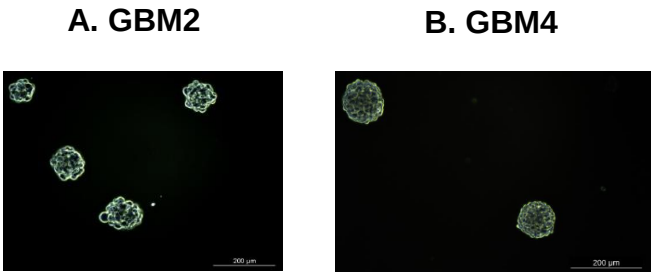

Figure 24. Phase contrast microscopic images of GBM2 (Panel **A.**) and GBM4 (Panel **B.**) spheres cultured in the serum free medium supplemented with EGF and bFGF. Original magnification ×10. Scale bar, 200 μm.

Cells were characterized for the following stemness expression markers: CD133, Nestin, Sox2 and CD44 using cyto-fluorimetric techniques.

Representative results of four different cultures phenotipically investigated: GBM2 (Panel **A.**), GBM3 (Panel **B.**), GBM4 (Panel **C.**) and GBM5 (Panel **D.**) are shown in **Figure 25.**.

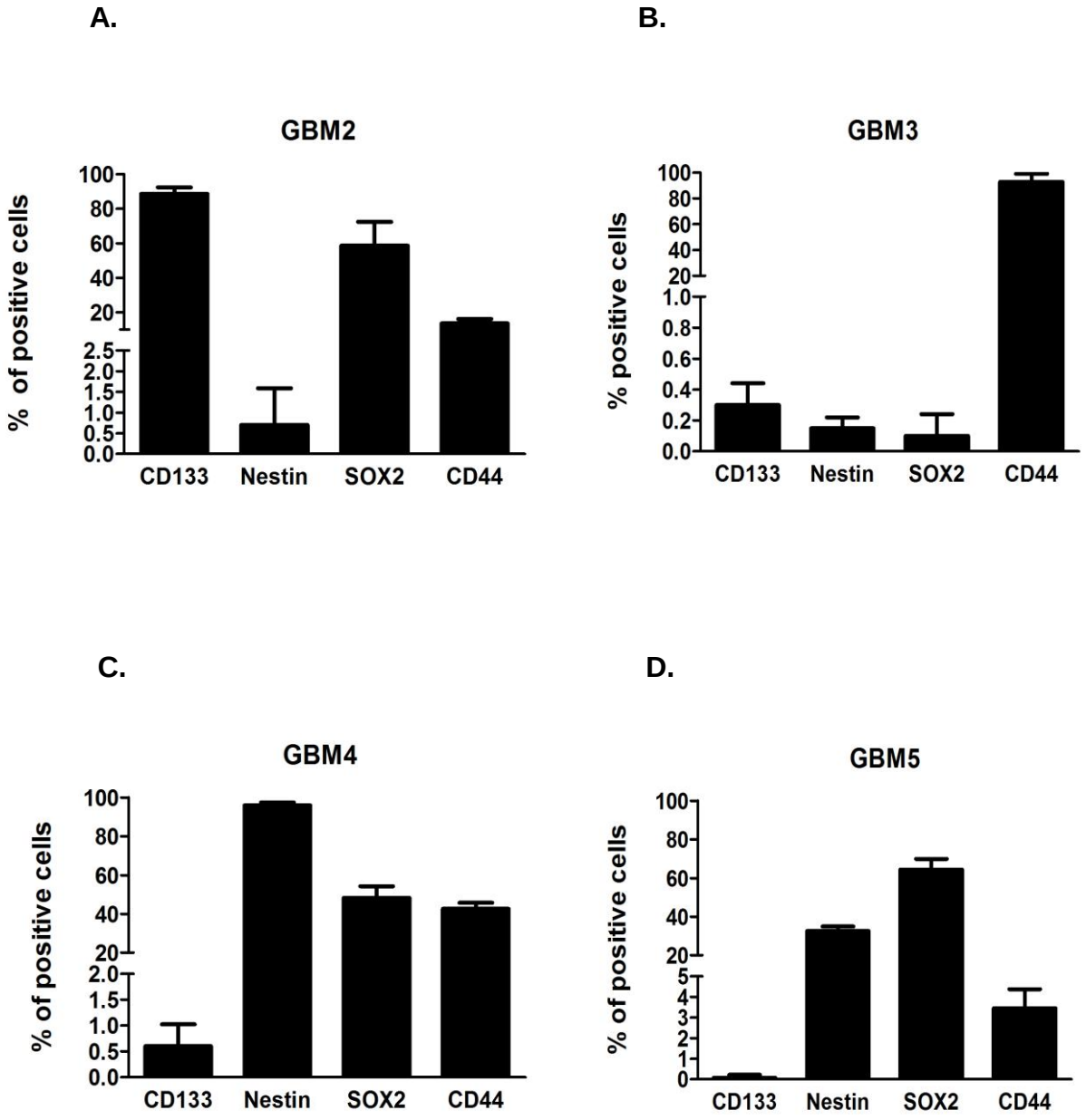

Figure 25. Phenotypic characterization of four different GSC cultures: GBM2 (Panel **A.**), GBM3 (Panel **B.**), GBM4 (Panel **C.**) and GBM5 (Panel **D.**). Percentage of some of the most common stemness markers expressed by GSCs after isolation is indicated. Data acquired using cyto fluorimetric techniques. Error bars are standard deviations (SD).

Flow cytometric analysis revealed that the levels of expression markers varied significantly among cultures. For example, CD133 antigen, a putative brain tumor stem-like cells marker (Singh et al., 2004b) (Uchida et al., 2000), was highly expressed only in GBM2 (Panel **A.**), where it retained an expression of 88.8%; whereas, the percentage

of CD133 positive cells in GBM3 (Panel **B.**), GBM4 (Panel **C.**) and in GBM5 (Panel **D.**) was less than 1%.

Nestin, marker for neural stem/progenitor cells (Uchida et al., 2000) (Tohyama et al., 1992) (Dahlstrand et al., 1992), reported the highest expression levels in GBM4 and GBM5, with a percentage of around 95.9% and 32.5% respectively. Conversely, Nestin was weakly expressed in GBM2 and in GBM3, counting less than 1%. Sox2, another neural stem cells marker (Cai et al., 2002) (Hemmati et al., 2003), was found expressed in GBM2 with a percentage of 58.7%, in GBM4 $Sox2^{+}$ cells were around 48%, and in GBM5 around 64%. Differently, Sox2 was weakly expressed in GBM3, counting for only a 0.1%.

CD44 is a transmembrane cell-surface adhesion protein (Ponta et al., 2003) assumed to be expressed in brain tumor stem cells (Singh et al., 2004a; Singh et al., 2004b). It's expression widely varied among the four tested cultures: the highest expression levels of CD44 were observed in GBM3, counting for 92.8%, followed by GBM4 with a percentage of 42.6% $CD44^{+}$ cells; whereas in GBM2 and GBM5 only the 13.5% and 3.4% respectively was found expressing CD44.

Taken together these results highlight how GSCs, as primary cultures, may be phenotypically more heterogeneous in comparison to their commercially obtained counterpart.

▪ 4.2.2 Glioma stem-like cells growth

In order to assess GSCs growth curves, GBM2 (Panel **A.**) and GBM4 (Panel **B.**) growing assays were performed **(Figure 26.)**.

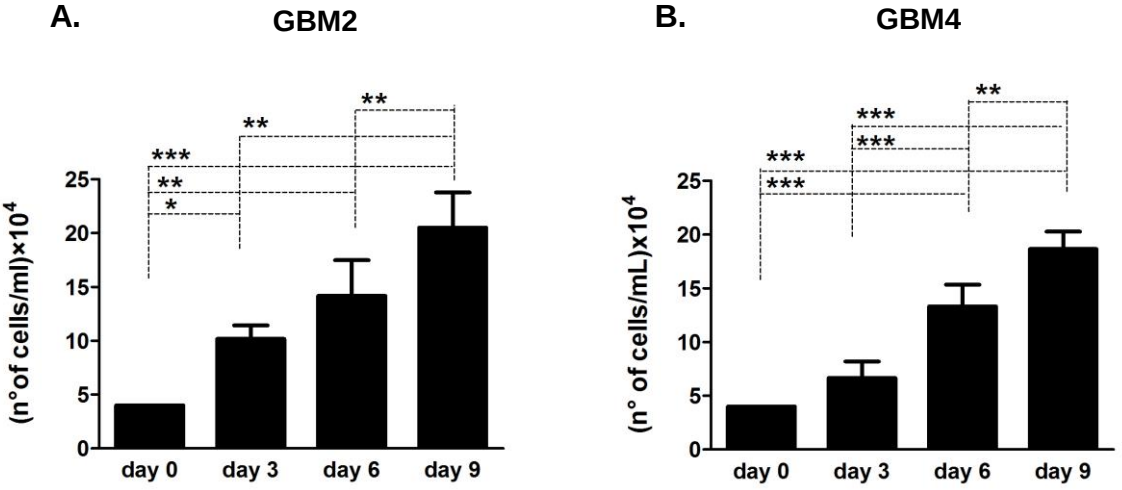

Figure 26. Growth kinetics of GBM2 (Panel **A.**) and GBM4 (Panel **B.**) cells under normoxic conditions. *P < 0.05, **P < 0.01, ***P < 0.001 between indicated pairs (one-way ANOVA). In Panel **A.** it has been found significantly difference between day 0 and day 3 (*P < 0.05), day 0 and day 6 (**P < 0.01), day 0 and day 9 (***P < 0.001); between day 3 and day 6 (**P < 0.01) and between day 3 and day 9 (***P < 0.001). In Panel **B.** it has been found significantly difference between day 0 and day 6 (***P < 0.001), day 0 and day 9 (***P < 0.001); between day 3 and day 6 (***P < 0.001), day 3 and day 9 (***P < 0.001) and between day 6 and day 9 (**P < 0.01). Error bars are standard deviations (SD).

GBM2 and GBM4 growth kinetics was monitored upon 9 days, cells were counted every three days.

Both GSC cultures demonstrated to grow well when cultured in serum free medium supplemented with proper growth factors EGF and bFGF (details in 3.2.3 "Material and Methods" section), reporting a statistical increment among days.

At day 3 after plating, GBM2 cells were found doubled and 5-fold increased at day 9. The mean viability of the GBM2 was slightly higher compared to GBM4, that retained 1.7-fold increased at day 3 and around 4.5-fold at day 9.

▪ 4.2.3 *In vitro* replication assay of wild type HSV1 and R3616

Critical for the selection of potential viral candidates for brain tumor therapy is their ability to replicate in human GSCs. Hence, GBM2 and GBM4 cells were first infected with HSV1 wild type at MOI of 0.2 and it's replication efficiency was then compared to the replication ability of R3616, γ34.5 deleted HSV1, employed for our investigation.
Supernatants were collected at 12, 24, 48 and 72 hours post infection. Cells became round, lost their morphological features, and detached from the culture plate since 90 minutes after inoculation with viral suspensions.
HSV1 wild type displayed a statistical significant ability to replicate in both GSCs tested, retaining a slightly higher replication ability in GBM2 compared to GBM4 cells. Indeed, in GBM2 72 hours after infection HSV1 wt viral titer was estimated increased around 1.8-fold (6.6 pfu/mL, log scale) than input (3.6 pfu/mL, log scale) (***P < 0.001); whereas, in GBM4 the increment was around 1.7 (6 pfu/mL, log scale) (***P < 0.001).
Representative results of HSV1 replication ability in GBM2 (Panel **A.**) and GBM4 (Panel **B.**) are shown in **Figure 27.**.

A. **GBM2**

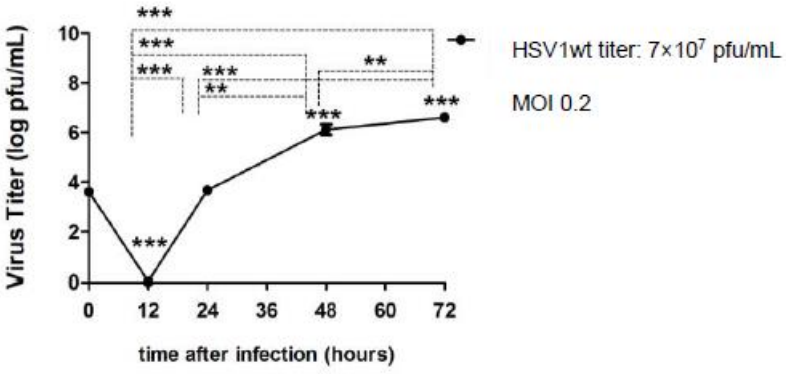

B. **GBM4**

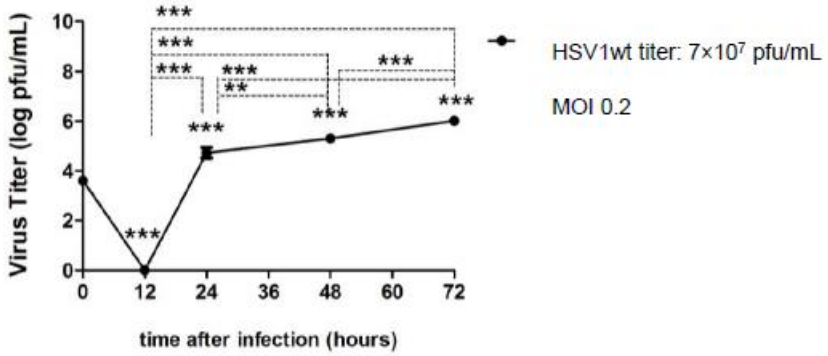

Figure 27. Replication of wild type HSV1 in infected GBM2 (Panel **A.**) and GBM4 cells (Panel **B.**). Cells were infected at an MOI of 0.2 and virus titer was determined at indicated times (hours) after infection. HSV1 displayed significant viral replication ability in both GBM2 and GBM4 cells. HSV1 input was $4*10^3$ pfu/mL (log scale). **P < 0.01; ***P < 0.001 between indicated points (one-way ANOVA).
In Panel **A.** time points at 12, 24, 48 and 72 hours after infection were found significantly different compared to the input (***P < 0.001). It has been found significant difference between 12 hours and 24, 48 and 72 hours after infection (***P < 0.001); between 24 hours and 48 and 72 hours after infection (***P < 0.001); between 48 and 72 hours after infection (**P < 0.01). In Panel **B.** time points at 12, 48 and 72 hours after infection were found significantly different compared to the input (***P < 0.001). It has been found significant difference between 12 hours and 24, 48 and 72 hours after infection (***P < 0.001); between 24 hours and 48 and 72 hours after infection (***P < 0.001); between 48 and 72 hours after infection (***P < 0.001). Error bars are standard deviations (SD).

R3616 was not able to efficiently replicate both in GBM2 and GBM4 cells, even at MOI of 1.5, with viral yields lower than input (3×10^4 pfu/mL) over the 72-h time course. Results are shown in **Figure 28.**.

A. **GBM2**

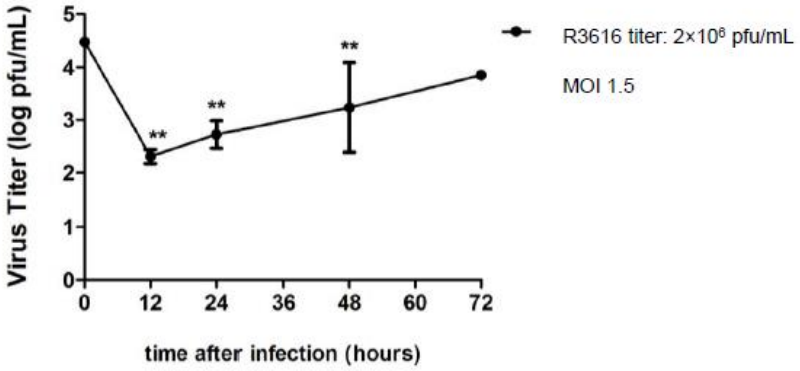

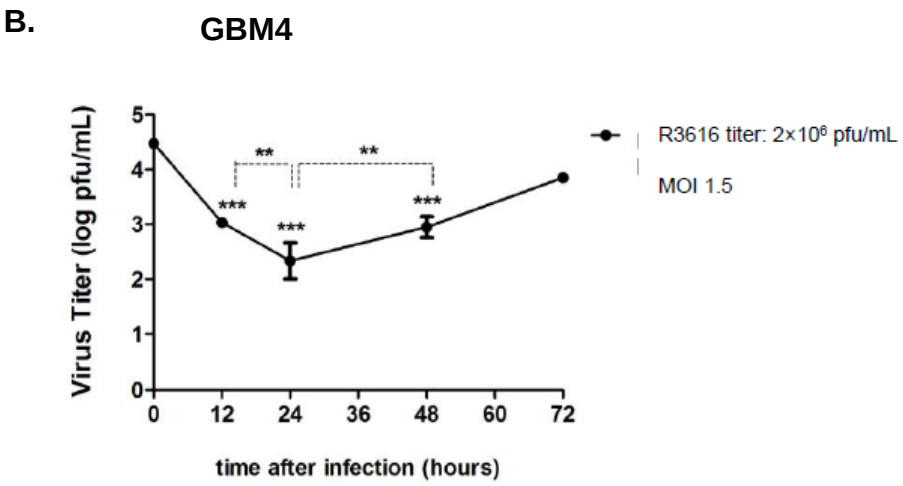

Figure 28. Replication of R3616 in GBM2 (Panel **A.**) and GBM4 (Panel **B.**). Cells were infected at MOI of 1.5. R3616 did not replicate both in GBM2 and GBM4 cells, with virus yields less than input (3×10^4 pfu/mL) over the 72-h time course. **P < 0.01 between indicated points (one-way ANOVA): in Panel **A.** time points at 12, 24 and 48 hours after infection were found significantly different compared to the input (**P < 0.01). In Panel **B.** time points at 12 and 48 hours after infection were found significantly different compared to the input (***P < 0.001). It has been found significant difference between 12 hours and 24 hours after infection (**P < 0.01) and between 24 hours and 48 hours after infection (**P < 0.01). Error bars are standard deviations (SD).

▪ 4.2.4 *In vitro* cell killing ability of wild type HSV1 and R3616

In order to assess wild type HSV1 cytotoxicity in GSCs, GBM2 and GBM4 were infected with an MOI of 0.2 and counted after 3, 6 and 9 days.

Wild type HSV1 exhibited significant killing effect in both GSCs tested. We observed an almost complete eradication of neurosphere cultures at day 9 after infection. In particular, GBM2 reported a fraction affected (FA) of 0.81 at day 6 and 0.94 at day 9 found statistically different compared to FA at day 3 (*******P < 0.001). In GBM4 cells FA resulted 0.69, 6 days after infection (*******P < 0.001) and 0.93 after 9 days (*******P < 0.001) as shown in **Figure 29.**.

No differences in killing ability were observed between tested GSCs and their FA values at day 9 were comparable.

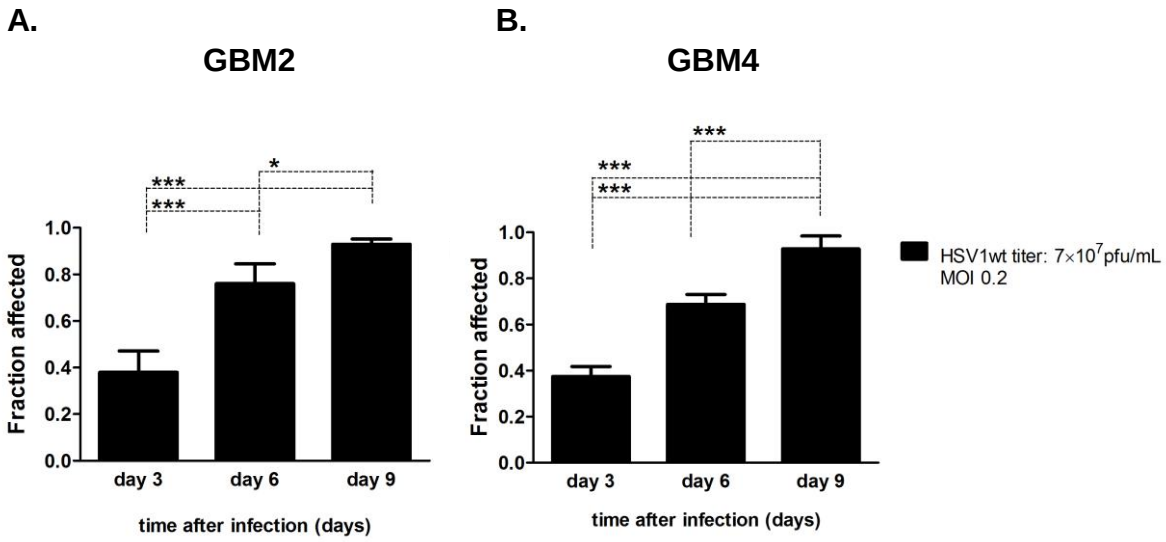

Figure 29. wtHSV1 killing ability in GBM2 (Panel **A.**) and GBM4 cells (Panel **B.**). 2×10^4 cells were infected at an MOI of 0.2 and viable cells were counted after 3, 6 and 9 days. *P < 0.05, ***P < 0.001 between indicated pairs (one-way ANOVA). In Panel **A.** FA has been found significantly difference between day 3 and day 6, between day 3 and day 9 (***P < 0.001) and between day 6 and day 9 (*P < 0.05). In Panel **B.** FA has been found significantly different between day 3 and day 6, between day 3 and day 9 and between day 6 and day 9 (***P < 0.001). Error bars are standard deviations (SD).

To verify whether R3616 was able to replicate in GCSs, GBM2 and GBM4 cells have been infected with R3616 at an MOI of 0.2 or 0.5. Results reported in **Figure 30.** show R3616 killing ability in GBM2 and GBM4 assessed at MOI of 0.5.

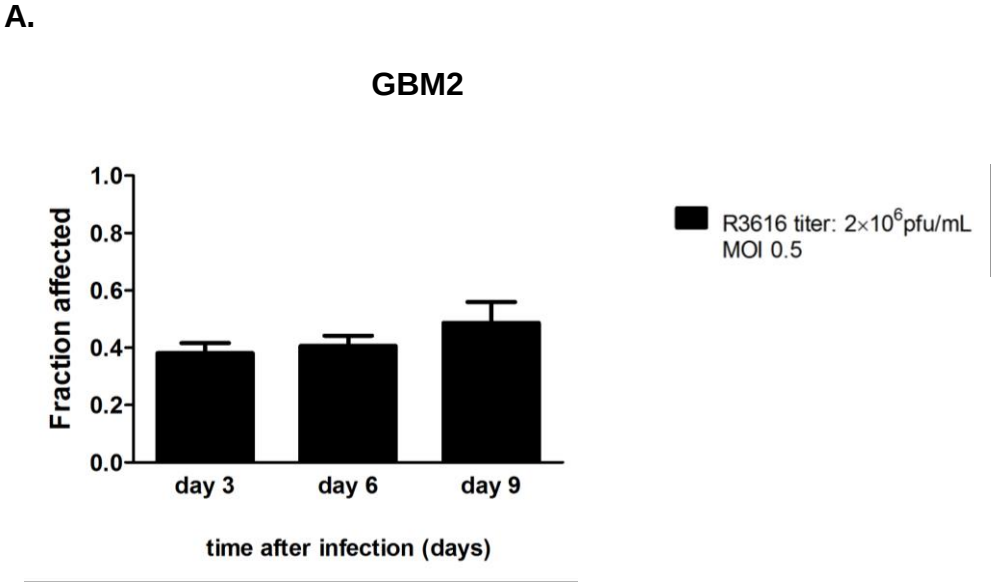

B.

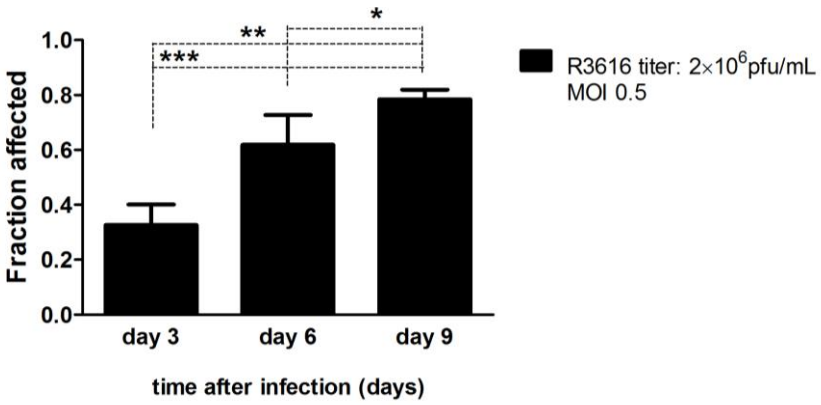

Figure 30. R3616 killing ability in GBM2 (Panel **A.**) and GBM4 (Panel **B.**) cells. 2×10^4 cells were infected at an MOI of 0.5 and viable cells were counted after 3, 6 and 9 days. *P < 0.05, **P < 0.01, ***P < 0.001 between indicated pairs (one-way ANOVA): in Panel **B.** FA between day 3 and day 6 (**P < 0.01), between day 3 and day 9 (***P < 0.001) and between day 6 and day 9 (*P < 0.05) was found significantly different in GBM4 cells infected with R3616. Error bars are standard deviations (SD).

R3616 exhibited a more efficient killing ability on GBM4 compare to GBM2 reporting a fraction affected of 0.65 in GBM4 at day 6 (**P < 0.01) and 0.78 at day 9 (***P < 0.001). Conversely, the R3616 FA in GBM2 attained to 0.4 at day 6 and did not exceed 0.5 at day 9 .

Taken together these findings indicated that both viruses were able to kill GSCs, albeit with significant different potency.

To examine the effect of the γ34.5 deletion on GSCs, we compared R3616 cytotoxicity to HSV1 killing efficiency. GBM2 cells were infected with R3616 at the same MOI of 0.2 used for HSV1 wt and viable cells were counted at day 3, 6 and 9 after infection. Obtained data are shown in **Figure 31.**

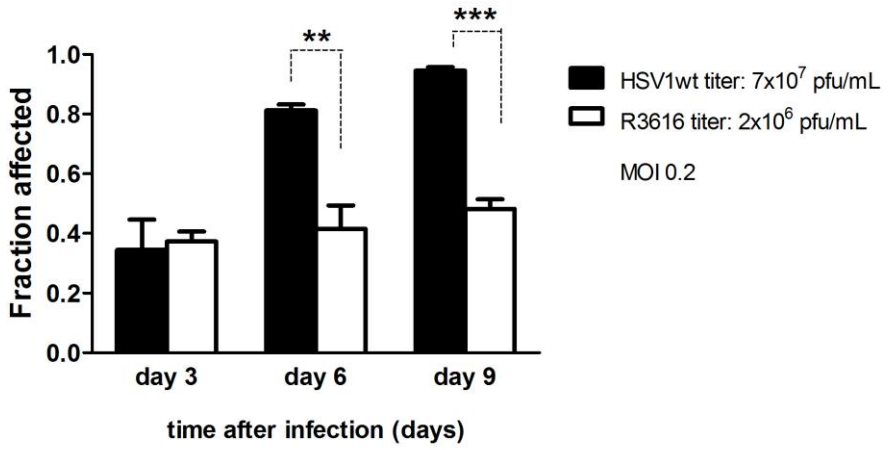

Figure 31. Comparison between HSV1 wt (black bars) and R3616 (white bars) cytotoxicity in GBM2. 2×10^4 cells were infected at an MOI of 0.2 and viable GBM2 cells were counted after 3, 6 and 9 days. ***P < 0.001, **P < 0.01 between indicated pairs (two-tailored unpaired *t-test*): FA between GBM2 cells HSV1wt infected and GBM2 cells R3616 infected at day 6 (**P < 0.01), and day 9 was found significantly different (***P < 0.001). Error bars are standard deviations (SD).

As might be expected, HSV1 wt demonstrated to be significantly more cytotoxic than R3616. Although HSV1 wt and R3616 exhibited only a marginal different cytotoxicity at day 3, reporting a FA of 0.34 and 0.37 respectively, wild type HSV1 was found very efficacious in killing GBM2 cells with a FA of 0.81 at day 6 and 0.94 after 9 days. Differently, R3616 killing ability was significantly less efficient compared to HSV1 wt reporting a FA of 0.41 at day 6 (**P < 0.01) and stabilized at 0.48 at day 9 (***P < 0.001).

▪ 4.2.5 *In vitro* evaluation of BMP2 treatment in GSCs

Following the published data in other GBM cell cultures (Piccirillo et al., 2006) (Persano et al., 2012) (Pistollato et al., 2009b), the BMP2 ability to promote astro-glial differentiation in GSCs has been tested. Dissociated spheres from GBM2 and GBM4 were supplemented with a single 50ng/mL BMP2 spike/die per seven days before analyzing the expression of the most common stemness (i.e. CD133, Nestin, Sox-2), neuronal differentiation (i.e. βIII-tubulin) and astrocytic differentiation (i.e. GFAP) markers using flow cytometric techniques. Since GCSc are slow replicating cells, BMP2 treatment was prolonged for 7 days. Daily repeated BMP2 applications were needed due to its short half-life.

In **Figure 32.** the phenotypic effects mediated by BMP2 treatment in GBM2 (Panel **A.**) and GBM4 cells (Panel **B.**) are shown.

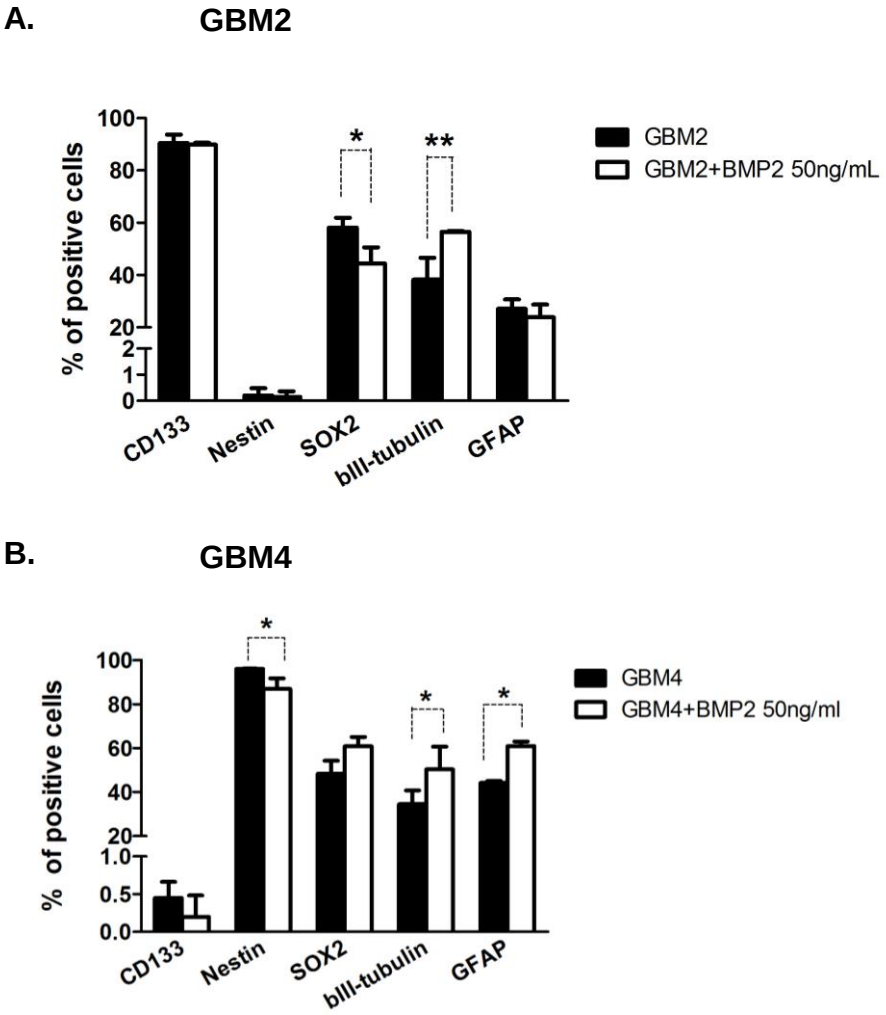

Figure 32. Modulation of expression markers in GBM2 (Panel **A.**) and GBM4 (Panel **B.**) cells alone (black bars) or pre-treated with BMP2 (white bars) supplemented at the concentration of 50ng/mL BMP2 spike/die upon seven days. Bar graphs report relative $CD133^+$, $Nestin^+$, $Sox2^+$, $GFAP^+$ and $\beta III\text{-}tubulin^+$ quantified according to the BD Stemflow Human Neural Lineage Analysis Kit's instructions using flow-cytometric techniques. $^*P < 0.05$, (two-tailored unpaired *t-test*) between indicated pairs. In Panel **A.** it has been found significantly difference in $Sox2^+$ ($^*P < 0.05$) and in $\beta III\text{-}tubulin^+$ ($^{**}P < 0.01$) between GBM2 and GBM2 -BMP2 treated cells. In Panel **B.** it has been found significantly difference in $Nestin^+$, $\beta III\text{-}tubulin^+$ and in $GFAP^+$ between GBM4 and GBM4 -BMP2 treated cells ($^*P < 0.05$). Results represent the average of two different experiments performed in triplicate. Error bars are standard deviations (SD).

Upon supplementation of BMP2 to GBM2 cells, a statistical reduction in Sox2 expression (from around 58% in GBM2 alone to 44.5% in GBM2-BMP2 treated cells) with a concomitant up-regulation of βIII-tubulin^{+} (from around 38% in GBM2 alone to 56,5% in GBM2-BMP2 treated cells), neuronal marker, was observed (*$P < 0.05$).
Conversely, no appreciable variation in CD133 and Nestin expression levels was found. CD133 positive cells remained very high, counting 90.5% in GBM2 and 89.9% in GBM2-BMP2 treated. Similarly, the GFAP positive population seemed not to be affected by BMP2 treatment, ranging from 27% to 23.85% upon BMP2 supplementation.

Following to the BMP2 treatment in GBM4 cells, flow cytometric analysis reported significantly increased in both expression levels of βIII-tubulin and GFAP (*$P < 0.05$); with the positive population ranging from 34.5% to 50.35% for the neuronal marker βIII-tubulin; while GFAP^{+} was around 44% in GBM4 alone and 60.9% in GBM4 BMP2-pretreated cells.
These data suggest that BMP2 treatment in GBM4 induce an increment of both neuronal and astroglial differentiation markers with concomitant significant decrement of Nestin levels. Indeed, Nestin was the only stemness marker decreased after BMP2 supplementation. CD133^{+} population remained weakly expressed. No statistical differences were found in Sox2^{+} cell population either.

Taken together, all these findings confirm that GBM2 and GBM4 cells do not retain the same aptitude to pro-differentiating effect modulated by BMP2. Moreover, in our analysis, beside an inter-cultures variability, there is an intra-culture variability, that typically occurs in primary cell lines, suggesting a possible variation in stem markers expression.

▪ 4.2.6 Evaluation of BMP2 treatment in GSCs by Western Blot analysis

The effects mediated by BMP2 in GSCs were evaluated through Western Blot assays. In **Figure 33.** are reported, as example, the expression of the proteins investigated in GBM4 lysates.

GSCs, grown in normoxia, were daily supplemented with medium alone or 50 ng/mL and 100 ng/mL BMP2 for seven days in order to tested whether BMP2 pro differentiation ability was modulated in a concentration dependent manner.

Proteins controlled were Nestin and Sox2, as stemness markers; βIII- tubulin and GFAP as differentiation markers. Additionally, it has been also preliminary evaluated in GBM4 the expression of Pi-Smad 1/5/8, downstream proteins of BMP2 signaling pathway, known to be activated in the phosphorylated state at 21% O2, whereas, it has been reported that hypoxia can repress BMP signaling pathway via Smad phosphorylation (Pistollato et al., 2007).

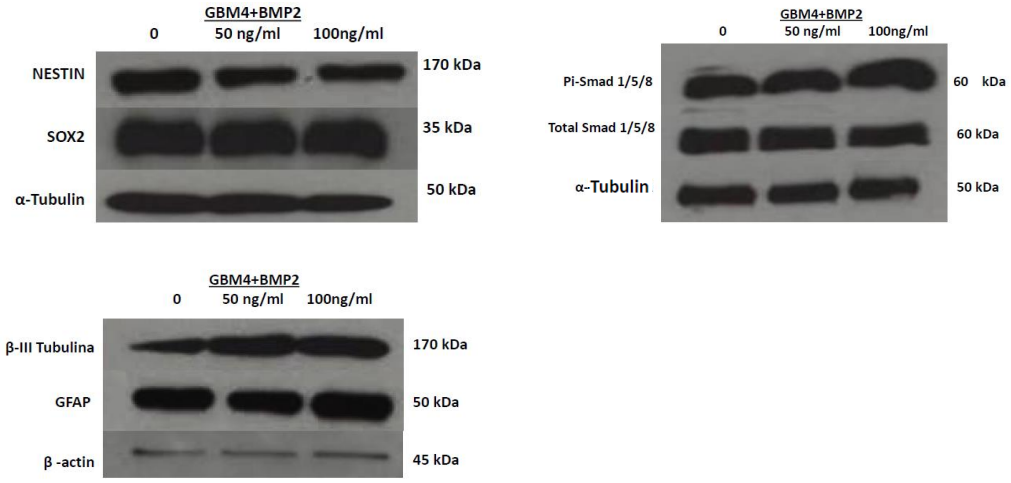

Figure 33. Representative western blot analyses in GBM4. Whole cell protein extracts were isolated following 7 days of medium or 50 and 100 ng/mL BMP2 treatment and subjected to western blot analysis. Proteins investigated were: Nestin, Sox-2, βIII-tubulin, GFAP, Pi-Smad 1/5/8 and Total Smad. α-tubulin and β-actin were alternatively used as loading control.

In GBM4 cells, analyses reported a modest downregulation of Nestin and concomitant up regulation of βIII-tubulin in a BMP2 concentration dependent manner. A slightly increase in GFAP levels is also appreciable when GBM4 cells were treated with 100 ng/mL BMP2.

BMPs pathway activity in GSCs was monitored by expression of the Pi-Smad 1/5/8 proteins. Our preliminary analyses performed in GBM4 revealed an expression of proteins in phosphorylated state even in the control, suggesting that these proteins were expressed at 21% O_2. Following BMP2 treatment Pi-Smad 1/5/8 were up regulated in a BMP2 concentration dependent manner.
Total-Smad proteins analysis indicated a homogenous expression among conditions.
Pi Smad 1/5/8 expression at 21% O_2 could be due to the presence of endogenously secreted BMPs; thus, BMP2 supplementation would increase Pi Smad 1/5/8 levels. Further analyses to understand how BMP2 signaling pathway on GSCs is regulated in normoxia needed to be investigated.

▪ 4.2.7 Evaluation of *in vitro* migratory properties of BM-MSCs toward GSCs in presence of BMP2

Before evaluating migratory properties of BM-MSCs towards GSCs, we verified that the selected medium for GSC cultures in which BM-MSCs should grow along the time of migration assay, did not impair their immunophenotype. Thus, hMSCs were seeded alternatively in DMEM 20% FBS and in EF 20 serum free media and cultured for seven days before analyzing some of the most common mesenchymal surface markers using cytofluorimetric techniques. For this analysis performed in BM-MSCs following markers investigated: CD44, CD73, CD90, CD105, CD106 and CD166 (**Figure 33.**).

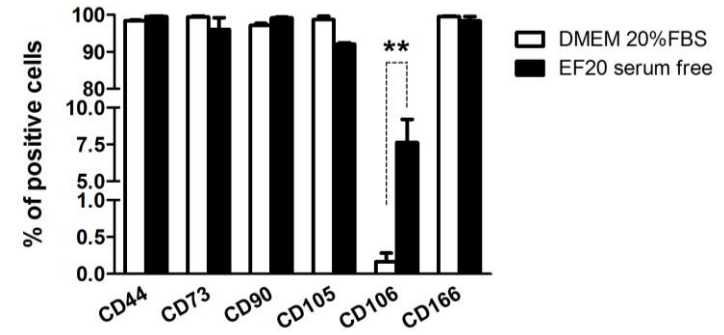

Figure 34. Immunophenotypic characterization of CD44, CD73, CD90, CD105, CD106 and CD166 cell surface markers tested on BM-MSCs grown in DMEM 20% FBS and EF20 serum free media seven days after seeding. Data acquired using cytofluorimetric techniques. Except for CD106, all other markers evaluated retained the same expression levels when grown in DMEM 20% FBS or EF20 media. CD106 was found significantly increased when BM-MSCs were grown in EF20 serum free medium selected for GSC cultures (**P < 0.01). Error bars are standard deviation (SD).

Except CD106 that demonstrated to be significantly increased when BM-MSCs were grown in EF20 serum free medium selected for GSC cultures (**P < 0.01), no significant variations in markers expression levels were observed, suggesting that BM-MSCs retained a stable phenotype even when grown along seven days.

In order to verify whether cytokines and chemokines released by GSCs were able to promote hMSCs inherent tumor homing, we performed *in vitro* migration assays employing GBM2 and GBM4 cells. Moreover, to understand whether GSCs pre-treated with biological soluble factors supposed to induce astro-glial differentiation, such as BMP2, might modulate BM-MSCs tropism, we supplemented GBM2 and GBM4 cells with BMP2 at the concentration of 50ng/mL/day for 7 days or we added 50ng/mL BMP2 one time at the same moment of BM-MSCs loading.

The *in vitro* migration assay was performed at 21% O_2. BM-MSCs migratory effect was evaluated using the same conditions already described for *in vitro* migration assays as reported in Results Part 1 (see section 4.1.5). After seven days of incubation BM-MSCs tropism was quantified by cyto-fluorimetric techniques.

Cells migration was calculated as a ratio, so-called migration index, normalizing the number of MSCs passed into 180 seconds in each conditions with the number of BM-MSCs passed to medium alone.

In **Figure 35.** is reported the BM-MSCs tropism towards GBM2 (Panel **A.**) and GBM4 (Panel **B.**).

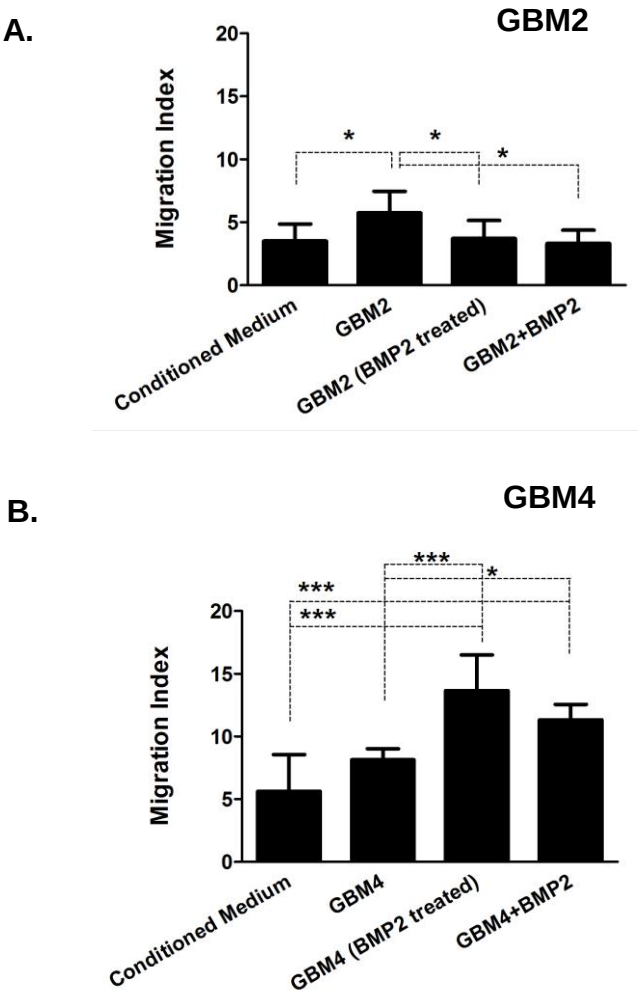

Figure 35. Migratory properties of BM-MSCs toward GBM2 (Panel **A.**) and GBM4 (Panel **B.**) under normoxic conditions. **Conditioned Medium**: GBM Conditioned Medium, **GBM2** and **GBM4**: GBM cells alone; **GBM2** or **GBM4 (BMP2 treated)**: GBM cells pre-differentiated with BMP2 treatment at the concentration of 50 ng/ml for 7 days; **GBM2** or **GBM4+BMP2**: 50ng/ml BMP2 added to GBM cells at the same moment of BM-MSCs, Migration index was calculated normalizing the number of BM-MSCs passed into 180 seconds in each conditions with the number of BM-MSCs passed to medium alone. *P < 0.05, ***P < 0.001 (one-way ANOVA) between indicated pairs in BM-MSCs. In Panel **A.** it has been found significantly difference between Conditioned Medium and GBM2; GBM2 and GBM2 (BMP2 treated) and GBM2 and GBM2+BMP2 (*P < 0.05). In Panel **B.** it has been found significantly difference between Conditioned Medium and GBM4 (BMP2 treated), Conditioned Medium and GBM4+BMP2 (***P < 0.001), GBM4 and GBM4 (BMP2 treated) (***P < 0.001) and between GBM4 and GBM4+BMP2 (*P < 0.05). Results represent the average of two different experiments performed in triplicate. Error bars are standard deviations (SD).

Our findings indicated that BM-MSCs migration was statistically enhanced toward GBM4 cells pre-treated with BMP2 in comparison to medium supplied of GBM4 released factors or GBM4 cells grown alone (*******P < 0.001). Significantly statistical was found the migratory effect exerted by GBM4 enriched one time with BMP2 in comparison to GBM4 conditioned medium (*******P < 0.001) or GBM4 cells alone (*****P < 0.05) as well.
Differently, in GBM2 we found statistically significant the BM-MSCs migration towards cells grown alone compared to supplemented medium and to GBM2 cells plus BMP2 (*****P < 0.05). Unlike of GBM4, BMP2 did not exert any effect on GBM2 cells neither when cells were exposed to treatment for 7 days.

GBM4 confirmed to be more responsive to BMP2 pro differentiating treatment than GBM2 and taken together our data suggest that GSCs more responsive to BMP2 treatment greatly enhanced the BM-MSCs inherent tropism.

▪ 4.2.8 Evaluation of *in vitro* migratory properties of BM-MSCs toward GSCs infected with HSV-1 wt or R3616

To investigate BM-MSCs tropism toward GSCs infected with wild type HSV1 and R3616, GBM2 or GBM4 cells were seeded at day 0; infected with HSV1 at MOI of 0.1 or with R3616 virus at MOI of 0.25. BM-MSCs-DiI^{+} were loaded respectively 48 and 72 hours post infection, according to the viral replication. Migratory properties were evaluated after 7 days of incubation at 21% O_2.

In **Figure 36.** is shown the migratory assay of BM-MSCs toward GBM2 (Panel **A.**) and GBM4 (Panel **B.**) infected with HSV1 wt.

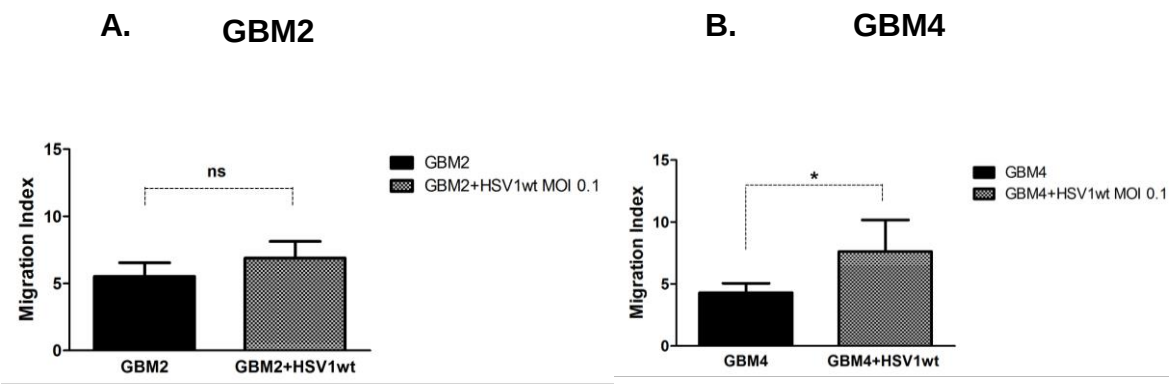

Figure 36. Migratory properties of BM-MSCs toward GBM2 (Panel **A.**) and GBM4 (Panel **A.**) in normoxic conditions. **GBM2** or **GBM4**: GSCs alone, **GBM2** or **GBM4+HSV1 wt**: GSCs infected with HSV1 wt at MOI 0.1. Two days after infection with HSV1, BM-MSCs-DiI^+ were added on the top well of a Transwell plate. After seven days the number of BM-MSCs passed through the Transwell into 180 seconds was counted using cytofluorimetric techniques. *P < 0.05 (two-tailored unpaired *t-test*). GBM4 results represent the average of two different experiments performed in triplicate. Error bars are standard deviations (SD).

Data obtained infecting GBM4 cells with HSV1 wt demonstrated to significantly increase the migration of BM-MSCs (*****P < 0.05). Conversely, there was no significant differences in hMSCs tropism when GBM2 cells were infected with HSV1 wt.

We next assessed the migration properties of BM-MSCs toward GBM2 and GBM4 when GSCs were been previously infected with R3616 at MOI 0.25. Interestingly, BM-MSCs exhibited a statistical enhanced efficiency in migratory properties when GBM4 cells were infected with R3616 (*******P < 0.001) increasing their inherent tropism of more than 3.5 fold. Likewise for GBM2 infected with HSV1 wt, no significant difference in BM-MSCs migration was seen even when cells were infected with R3616.

In **Figure 37.** are reported the *in vitro* migration assay of BM-MSCs toward GBM2 and GBM4 cells infected with R3616. Assays were performed under normoxic conditions.

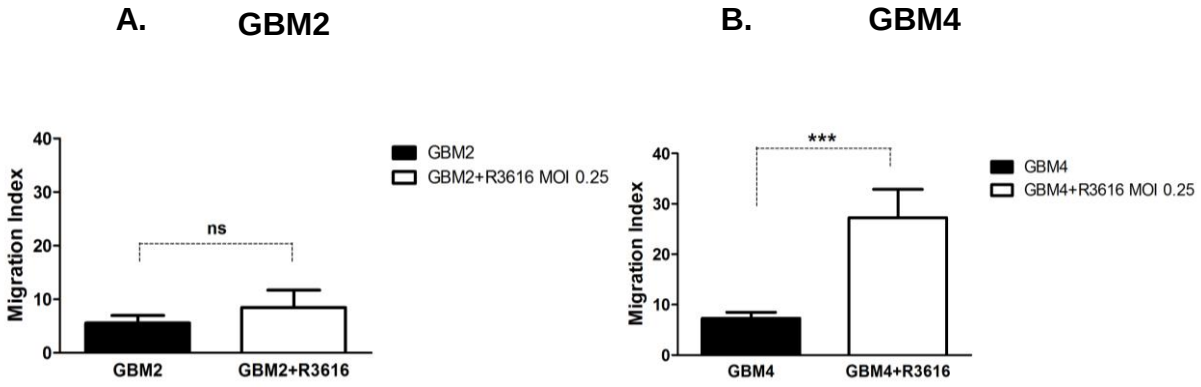

Figure 37. Migratory properties of BM-MSCs toward GBM2 (Panel **A.**) and GBM4 (Panel **A.**) in normoxic conditions. **GBM2** or **GBM4**: GSCs alone, **GBM2** or **GBM4+R3616**: GSCs infected with R3616 at MOI 0.25. Three days after infection, BM-MSCs-DiI$^+$ were added on the top well of a Transwell plate. After seven days the number of BM-MSCs passed through the Transwell into 180 seconds was counted using cytofluorimetric techniques. ***P < 0.001 (two-tailored unpaired *t-test*). GBM4 results represent the average of two different experiments performed in triplicate. Error bars are standard deviations (SD).

Together these data demonstrated how GBM4-infected cells significantly improve the inherent tumor tropism of BM-MSCs, especially when cells were infected with R3616. Conversely, no significative effect related to HSV1 or R3616-infection was able to modify MSCs migration ability towards GBM2 cells.

▪ 4.2.9 BMP2 and R3616 Combination treatment in GBM4

We previously showed that BMP2 treatment in GBM4 cells significantly enhanced βIII-tubulin$^+$ and GFAP$^+$ with concomitant decrement of Nestin$^+$ expression levels. *In vitro* migratory assays demonstrated that GBM4 cells pre-treated with BMP2 were significantly more attractive for BM-MSCs increasing their inherent tumor tropism. Conversely, the same effect was not retained in GBM2 cells. Moreover, we observed a greatly enhanced migration ability of BM-MSCs toward GBM4 cells infected with R3616. Taking into account all these findings, we next analyzed whether the combination treatment of BMP2 and R3616 promoted a stronger differentiation in GBM4 cells.

Cells were first infected with R3616 at MOI 0.1, according to the viral replication, and then treated with BMP2 at the concentration of 50ng/mL/day for 7 days before analyzing the cell phonotype through cyto fluorimetric techniques. GBM4 cells grown alone, supplemented only with BMP2 or infected with R3616 were also evaluated. To better understand the effects mediated by the co-treatment, Nestin, as representative marker of stemness and the two differentiation markers, βIII-tubulin and GFAP, found increased in GBM4-BMP2 treated cells, were analyzed for each conditions.

Representative results of are shown in **Figure 38.**

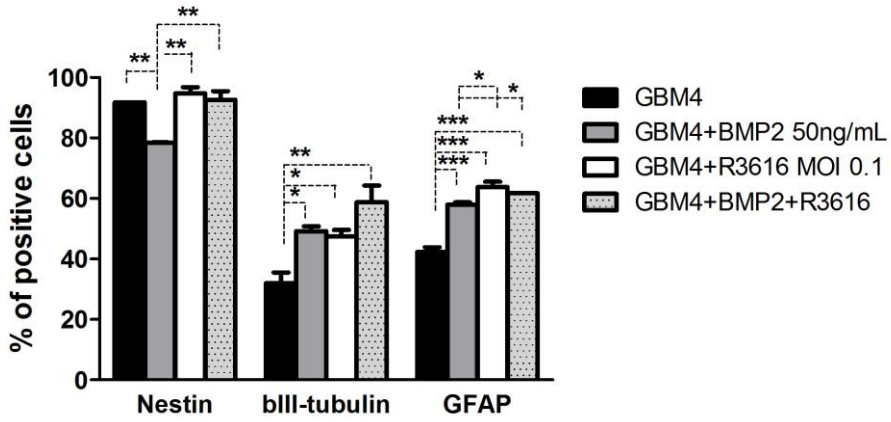

Figure 38. BMP2 and R3616 combination treatment in GBM4. Analysis performed using cyto-fluorimetric techniques. Cells were infected with R3616 at MOI 0.1 and treated with BMP2 at the concentration of 50ng/mL/day for 7 days. GBM4 cells grown alone, GBM4 cells supplemented only with BMP2 50ng/mL/day for 7 days and GBM4 cells infected with R3616 at MOI 0.1 were also evaluated.*P < 0.05, **P < 0.01, ***P < 0.001 (one-way ANOVA) between indicated pairs in GBM4 cells. It has been found significant difference in Nestin expression between GBM4 and GBM4-BMP2 treated; GBM4-BMP2 treated and GBM4+R3616; GBM4-BMP2 treated and GBM4+BMP2+R3616 (**P < 0.01); in βIII-tubulin expression between GBM4 and GBM4-BMP2 treated, GBM4+R3616 (*P < 0.05) and GBM4+BMP2+R3616 (**P < 0.01); in GFAP expression between GBM4 and GBM4-BMP2 treated, GBM4+R3616 and GBM4+BMP2+R3616 (***P < 0.001); between GBM4+BMP2 and GBM4+R3616 and between GBM4+BMP2 and GBM4+BMP2+R3616 (*P < 0.05). Error bars are standard deviations (SD).

Analysis of the combined treatment confirmed an up regulation of βIII-tubulin and GFAP with a concomitant down regulation of Nestin expression when GBM4 cells were supplemented with BMP2. Conversely, the R3616 infection seems do not to modify Nestin expression levels, even when cells received BMP2/R3616 co-treatment.
We also evaluated the effect of the combination treatment with BMP2 and R3616 in cell viability, analyzing the percentage of positive live cells in each condition tested by cytofluorimetric techniques.
A statistical decrease in percentage of live cells was observed when GBM4 cells were infected with R3616 alone in co-treatment with BMP2 and R3616 in comparison to GBM4 cells grown alone or BMP2-treated. Conversely any significative variation in cell viability was found when cells were treated only with BMP2.

Representative results are shown in **Figure 39.**.

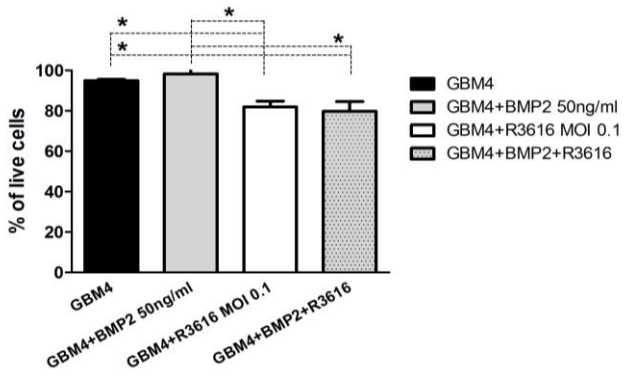

Figure 39. Percentage of GBM4 cell viability in BMP2 and R3616 combination treatment assay. Cell viability was monitored in GBM4 cells grown alone, GBM4 cells supplemented only with BMP2 50ng/mL/day for 7 days; GBM4 cells infected with R3616 at MOI 0.1 and in GBM4 cells infected with R3616 and treated with BMP2. *P < 0.05, (one-way ANOVA) between indicated pairs. It has been found significantly difference between GBM4 and GBM4+R3616; GBM4 and GBM4+BMP2+R3616; between GBM4+BMP2 and GBM4+R3616 and between GBM4+BMP2 and GBM4+BMP2+R3616 (*P < 0.05). Error bars are standard deviations (SD).

▪ 4.2.10 R3616 effect on BM-MSCs

With the final aim to exploit hMSCs inherent tumor tropism to deliver oncolytic virus, we preliminary tested the R3616 ability to replicate in and to kill BM-MSCs comparison to wild type HSV1. A suitable carrier must retain inherent tropism for

GSCs, must support the viral replication and release viral particles that subsequently will infect targeted cells.

- **4.2.10.1 *In vitro* replication assay of wild type HSV1 and R3616 in BM-MSCs**

We evaluated viral replication in BM-MSCs after HSV1 wt infection at MOI of 0.2 or at MOI 1.5 with R3616.

Representative results of HSV1 wt (Panel **A.**) and R3616 (Panel **B.**) growth curves are shown in **Figure 40.**.

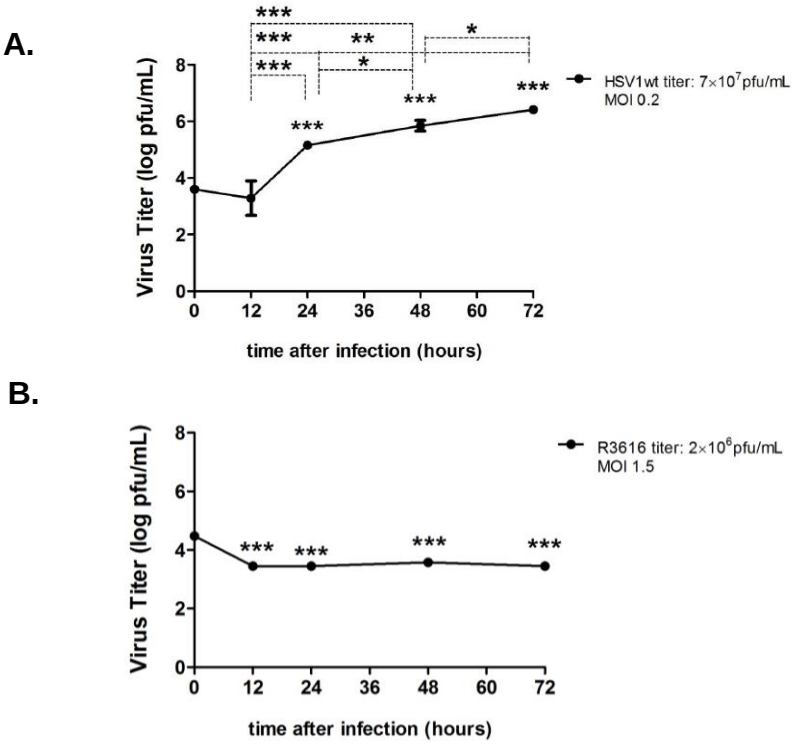

Figure 40. Replication curves of wild type HSV1 (Panel **A.**) and R3616 (Panel **B.**) in infected BM-MSCs. Cells were infected at an MOI of 0.2 with HSV1 or 1.5 with R3616. Virus titer was determined at indicated times (hours) after infection. HSV1 input was 4×10^3 pfu/ml; R3616 input was 3×10^4 pfu/ml. HSV1 and R3616 displayed significant (***P < 0.001) viral replication ability compared to the viral input (one-way ANOVA). In Panel **A.** It has been found significant difference between 12h and 24h; 12h and 48h, 12h and 72h (***P < 0.001); between 24h and 48h (*P < 0.05), 24h and 72h (**P < 0.01) and between 48h and 72h (*P < 0.05). Error bars are standard deviations (SD).

HSV1 demonstrated significative statistical replication efficiency in BM-MSCs reporting a viral titer more than 1.75 fold increased (6.42 pfu/mL, log scale) (*******P < 0.001) at 72 hours after infection.

Conversely, R3616 was not able to efficiently replicate in BM-MSCs retaining a viral yield lower than input (3×10^4 pfu/ml) over the 72-h time course.
Taken together these findings indicated that the deletion of γ34.5 in R3616 significantly attenuates the potency of R3616 in BM-MSCs.

- **4.2.10.2 *In vitro* cell killing ability of wild type HSV1 and R3616 in BM-MSCs**

In order to assess wild type HSV1 and R3616 cytotoxicity, BM-MSCs were infected with an MOI of 0.2 and 0.5 respectively and counted at day 3, 6 and 9 after infection.

Killing ability of HSV1 wt (Panel **A.**) and R3616 (Panel **B.**) retained by the two viruses are shown in **Figure 41.**

A.

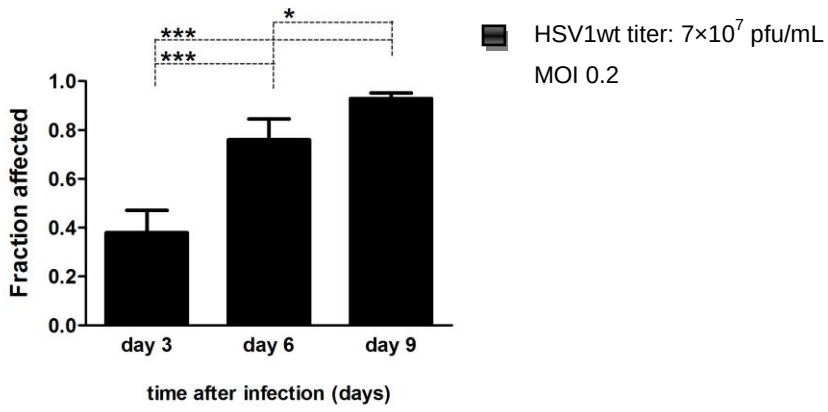

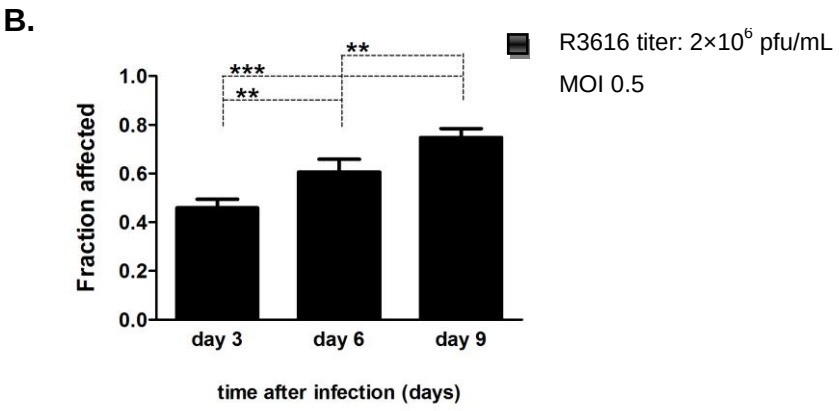

Figure 41. Killing ability of HSV1 wt (Panel **A.**) and R3616 (Panel **B.**) in BM-MSCs. 2×10^4 cells were infected at an MOI of 0.2 with HSV1 or 0.5 with R3616 and viable cells were counted after 3, 6 and 9 days. *P < 0.05, **P < 0.01, ***P < 0.001 between indicated pairs (one-way ANOVA): In Panel **A.** FA between day 3 and day 6, between day 3 and day 9 (***P < 0.001) and between day 6 and day 9 (*P < 0.05) was found significantly different. In Panel **B.** FA between day 3 and day 6 (**P < 0.01), between day 3 and day 9 (***P < 0.001) and between day 6 and day 9 (**P < 0.01) was found significantly different. Error bars are standard deviations (SD).

HSV1 wt demonstrated to be more cytotoxic than R3616 in BM-MSCs even if the cells were infected with R3616 using a MOI 2.5 fold higher.

Wild type HSV1 exhibited a greatly significative killing ability on BM-MSCs reporting a fraction affected of 0.76 at day 6 and 0.93 after 9 days.

R3616 demonstrated a significative killing ability on BM-MSCs with a FA of 0.6 at day 6 and 0.75 at day 9.

5. DISCUSSION

Glioblastoma Multiforme (GBM) is the most malignant primary brain tumor in adults (Wen and Kesari, 2008), displaying high heterogeneity, fast growth, vascular proliferation, diffuse infiltration into the brain parenchyma and necrosis areas (Wen and Kesari, 2008) (Rong et al., 2006). The prognosis remains still dismal, despite the current optimal multimodal therapy (Stupp et al., 2005; Stupp et al., 2009b) (Crocetti et al., 2012).

One hypothesis to explain the poor GBM outcome seem to be related to the existence of a population of Cancer Stem Cells (CSCs) (Galli et al., 2004) (Dirks, 2008), recently reported to be involved in tumor initiation and progression (Hemmati et al., 2003; Ignatova et al., 2002; Singh et al., 2003) in the GBM as well as in other tumors (Bonnet and Dick, 1997) (Al-Hajj et al., 2003) (Esposito et al., 2002) (Ricci-Vitiani et al., 2007). These so-called Glioma stem cells (GSCs) are described as a sub-population of undifferentiated tumor-cells with stem-like properties including self-renewal capability, multi-lineage differentiation and highly tumorigenic potential when transplanted in immune-deficient mice (Galli et al., 2004) (Crocetti et al., 2012; Visvader and Lindeman, 2008) (Dirks, 2008). GSCs have been reported to express stemness markers (i.e. CD133, Sox2 and Nestin) and to exhibit multipotency when placed in defined serum-free stem cell medium (Hemmati et al., 2003; Ignatova et al., 2002; Singh et al., 2003). Notably, accumulating evidence suggested that GSCs are important in tumor recurrence and in resistance to radiotherapy and chemotherapy (Wang et al., 2009) (Alcantara Llaguno et al., 2009).

A parameter we considered with particular attention in our study was the tumor microenvironment. Indeed, the biology of GBM is characterized by a continuous change in the microenvironment that greatly influences tumor growth and response to therapies (Bleau et al., 2008). In particular, hypoxia plays a pivotal role in normal homeostasis of stem cells likewise in the initiation, development and aggressiveness of gliomas by modulating GBM derived cells phenotype (Li et al., 2009) (Wong and Brem, 2008) (Azuma et al., 2003; Jogi et al., 2002) (Gillespie et al., 2007). Recently, our group

described a novel concentric model of the tumour stem cells niche indicating that the more immature cells are localized in the inner core and in the intermediate layer of the tumour mass (Pistollato et al., 2010a) (Persano et al., 2011), highlighting how GBM nature is strictly linked to hypoxia and its peculiar microenvironment. Therefore, targeting GSCs located in the GBM niches may be critical.
In our study we focused on two different therapeutic approaches to selectively target GSCs.

a.) By taking advantage of the well known ability of Mesenchymal Stem Cells (MSCs) to migrate towards tumor sites (Nakamizo et al., 2005) (Doucette et al., 2011) (Sasportas et al., 2009), we *in vitro* investigated hMSCs migratory properties with the final aim to genetically engineer them in order to express therapeutic genes thus exploiting hMSCs as delivery vehicles for brain tumor therapy.

b.) We used the neuroattenuated herpes simplex virus type 1 vector, R3616, as a tool to selectively kill GSCs, sparing normal neural cells (Martuza et al., 1991).

c.) We sought to exploit hMSCs tropism to tumor sites as delivery vehicles for R3616, possibly combining both strategies.

Our laboratory has already reported the role of BMPs in promoting astro-glial differentiation in GBM stem like cells (Piccirillo et al., 2006) (Pistollato et al., 2009a) (Pistollato et al., 2009b) (Persano et al., 2011). Additionally, it is known the involvement of signaling molecules, such as bone morphogenetic proteins (BMPs) as crucial mediators of stem cell self-renewal and cell fate determination, which appear instead disrupted in brain cancers (Dirks, 2008). Piccirillo et al. (Piccirillo et al., 2006) showed that BMP4 (and analogously BMP2) can modulate glial differentiation through increase in GFAP expression in GBM primary cultures; in particular in the brain tumor inducing population, thus indicating BMPs as potentially useful candidate molecules to promote differentiation of the tumor-initiating cells.
With the final aim to further transduce hMSCs with a vector harboring therapeutic genes, such as BMP2, to be released once cells have reached GBM site, we sought to

unravel whether BMP2 had some effect on hMSCs inherent tropism towards GBM stem like cells. Alternatively, we also pre-treated GBM-derived cells with BMP2 to verify whether pre-differentiated GSCs, become more permissive to hMSCs migration.

Primary GBM-derived cells employed in this study were grown and cultured alternatively in adhesion (Conti et al., 2005) (Sun et al., 2008) (Pistollato et al., 2011) or in neurosphere suspension conditions (Reynolds and Weiss, 1992; Reynolds and Weiss, 1996). In particular, GSC cultures as spheres were characterized for some of the most common stemness markers, such as CD133, (Singh et al., 2004b) (Uchida et al., 2000), Nestin (Uchida et al., 2000) (Tohyama et al., 1992) (Dahlstrand et al., 1992), Sox2 (Cai et al., 2002) (Hemmati et al., 2003) and CD44 (Singh et al., 2004a; Singh et al., 2004b). According to literature (Dirks, 2008) (Galli et al., 2004) (Gursel et al., 2011), our results clearly demonstrated that primary GSC cultures employed, expressed stemness markers with variable percentages, thus resembling GBM samples heterogeneity. These results highlight once again how GSCs, as primary cultures, may be phenotypically more heterogeneous in comparison to the commercially obtained counterpart. For example, CD133 was not always found highly expressed. Accordingly, recent publications provided evidence that GSCs can exist in the CD133-negative population (Beier et al., 2007) (Chen et al., 2012) (Ogden et al., 2008).

Concerning hMSCs, preliminary studies focused on the choice for the best hMSC candidate, between bone marrow- (BM-MSCs) and adipose tissue (AT-MSCs) derived hMSCs, for cell delivery experiments. According to criteria recommended by the International Society for Cellular Therapy (ISCT), our BM-MSCs and AT-MSCs positively expressed CD105, CD73, CD44, CD90, CD29, CD166, CD271 and were dimly positive for CD106, expected to be negative (Zuk et al., 2002) (Chamberlain et al., 2007). Conversely, they were negative for the most common hematopoietic surface antigens, such as CD14, CD19, CD45 (Le Blanc et al., 2003; Pittenger et al., 1999) (Chamberlain et al., 2007). We also found slightly positive expression of the Human leukocyte antigen Class II (HLA-DR) antigen expected to be negative in adult hMSCs (Le Blanc et al., 2003). Except for CD117 and CD271 expression, BM-MSCs more positively expressed cell surface markers in comparison to AT-MSCs. Noteworthy, analysis of CD133 expression revealed that it was slightly expressed only in BM-MSCs, whilst it was totally absent in AT-MSCs, in agreement to CD133 expression reported in

MSCs isolated from peripheral and umbilical cord blood (Tondreau et al., 2005) (Doucette et al., 2011).

Human stem cell-based therapy have already shown to be a promising therapeutic approach for brain cancer (Aboody et al., 2000) (Aboody et al., 2000) (Tyler et al., 2009) (Yuan et al., 2006). hMSCs have been used as delivery vehicles for therapeutic molecules in human gliomas (Lamfers et al., 2009) (Pierdomenico et al., 2005) (Huang et al., 2010), exhibiting selective tropism and migrating significant distances to target gliomas (Nakamizo et al., 2005). Indeed tumor cells, and in particular GBM cells (Zhou et al., 2002), secrete cytokines and chemokines that enhance hMSCs migration. hMSCs can be readily harvested from a broad range of sources, including adipose tissue (Zuk et al., 2001) (Zuk et al., 2002) and bone marrow (Bruder et al., 1997). AT-MSCs and BM-MSCs derived hMSCs have extensively evaluated over last years as both of them offer the most accessible source of hMSCs for use in research and clinical applications. Adipose tissue is less invasive and less expensive than bone marrow to obtain (Locke et al., 2011) (Yoo et al., 2009). Additionally, unmodified AT-MSCs remain free of oncogenic transformation, demonstrating more oncogenic resistance than BM-MSCs (Momin et al., 2010).

We isolated AT-MSCs from brain adipose tissue of glioma-bearing patient with the final aim to employed the same cells as therapeutic delivery vehicles for the treatment of GBM, thus presumably minimizing patient morbidity during cell harvesting, as already documented by Momin (Momin et al., 2010).

To mimic the peculiar GBM microenvironment and to compare the growing efficiency of the two different sources within, we cultured hMSCs both in normoxic, at 21% O2, and hypoxic, at 2% O2, conditions. Clearly, the use of MSCs for the treatment of gliomas requires a population of cells with a doubling time and proliferation rate rapid enough to allow timely expansion of autologous cells for clinical applications. Although BM- and AT-MSCs resulted immunophenotypically quite similar, AT-MSCs had a significantly shorter doubling time, expanding around 1.5-fold less than BM-MSCs in 72 hours both in hypoxic and normoxic conditions. These data were in agreement with data published by Ikegame et al. (Ikegame et al., 2011). Moreover, as demonstrated by *in vitro* multilineage developmental potential into adipocytes or osteoblasts assays, BM-MSCs exhibited an significative increased proliferative activity compared to AT-MSCs, especially under hypoxic conditions. Harvest efficiency for AT-MSCs and BM-MSCs

have been reported to partially depend also on donor age (Strem et al., 2005): the hMSC population has been shown to decrease substantially with age, casting further doubt on the use of autologous hMSCs as a therapeutic delivery vehicle in patient-bearing glioma (Kern et al., 2006) taking into account the elderly median age of GBM patients (Crocetti et al., 2012) (Wen and Kesari, 2008).
Finally, Pendleton et al. (Pendleton et al., 2013) in a study comparing the *in vitro* efficacy and specificity of AT-MSCs and BM-MSCs glioma tropism demonstrated how both sources retained similar homing. Differently, our studies reported that AT-MSCs showed a less efficient and aspecific migration toward GBM cells compared to BM-MSCs, both in normoxia and in hypoxia; thus confirming BM-MSCs as the most efficient candidate for cell delivery. For this reason, we decided to employ BM-MSCs for our next experiments.

Beside in normoxia and hypoxia, hMSCs migratory properties were investigated in the presence or absence of BMP2, WNT3a or after GBM derived cells were pre-treated with the two pro- differentiation factors. Wnt3a ligand mediates neuronal differentiation and proliferation inhibition of GBM cells and this phenomenon is enhanced under hypoxic conditions (Rampazzo et al., 2013).
Under hypoxic conditions, BM-MSCs demonstrated to migrate preferentially toward both BMP2 or WNT3a pre-treated GBM cells or either when BMP2 and WNT 3a have been added at the same time of BM-MSCs loading, thus suggesting that hMSCs migration could be preferential toward more differentiated cells, or either differentiated GSCs are more permissive to hMSC migration. Under normoxic conditions BMP2 treated cells not always increased hMSCs tropism. The exposure of stem cells to hypoxia increased hMSCs migration rate (Campos et al., 2010). Accordingly, we observed a significant increased hMSCs migration towards GBM cells grown under hypoxic conditions compared to normoxia. Notably, migratory properties were found more increased when hMSCs were loaded with BMP2 or WNT3a and were found dramatically increased when GBM cells have been pre-differentiated with these agents. This could be explained by considering a positive combination effect exerted by hypoxia and BMP2/WNT3a pro-differentiating agents able to efficiently enhance the hMSCs. Our results suggest that BMP2 can greatly increase the mesenchymal tropism

towards GBM site, even at lowered O_2 levels. Interestingly we observed a scale migration manner ranging from normoxia to hypoxia.

Such effect could be explain considering that hypoxia may enhance hMSCs migratory properties by upregulating chemotactic cytokines and by activating other signaling pathways that could involve also hMSCs (Fehrer et al., 2007). Further experiments need to be performed in order to elucidate this issue, but targeting GSCs exploiting BM-MSCs inherent homing, seems to be a promising approach to deliver therapeutic agents, such as BMP2 to the tumor site, especially in hypoxia. Noteworthy, GSCs expressing high levels of CD133 did not modulate BM-MSCs migration when pre-treated with BMP2; conversely, the most efficient migration was observed versus GBM cells alone. Such effect can be explained by hypothesizing that stemness could impair in some ways hMSCs migratory properties, although this hypothesis should be better confirmed before we could consider it as realistic.

Another approach we pursued to selectively targeting GSCs was represented by oncolytic viruses. Genetically engineered viruses have been widely investigated due to their capacity to selectively replicate in and kill cancer cells, while sparing normal neural cells (Martuza et al., 1991). For our studies we tested the therapeutical effect of the R3616, deleted for both copies of gene γ34.5, important for the virus replication and neurovirulence. Indeed, HSV wt can cause life-threatening encephalitis; thus attenuation is a prerequisite for a oHSVs. R3616 has already been demonstrated to *in vitro* replicate in and kill different human glioma cells (Martuza et al., 1991) (Andreansky et al., 1997). In order to evaluate such ability in GSCs selected for our study, we tested R3616 replication properties and cytotoxicity in comparison to HSV1 wild type. Analogously to Wakimoto et al., (Wakimoto et al., 2009) we found that the deletions of γ34.5 occurred in R3616 negatively affected viral replication and attenuated cell killing ability in comparison to HSV wt.

BM-MSCs migratory properties towards GSCs previously infected with HSV1 wt and R3616 under normoxic conditions were also evaluated.

Notably, when we infected GSCs with HSV1 wt and R3616, we found an increased in BM-MSCs migratory properties, In particular, R3616 infection consistent enhanced hMSCs tropism retaining a the migration index 3.5-fold higher compared to HSV1 wild

type. This could be related to the enhancing effect exerted by oHSVs on chemoattractant receptors expression (Willmon et al., 2009).

Differently, GSCs with high CD133 levels alternatively infected with HSV1 wt and R3616 seemed to impair hMSCs migration.

Our data show that hMSCs could contribute to GBM cells differentiation *per se*. This was observed by co-culturing BM-MSCs with GBM derived cells. Interestingly, we noted that under both normoxic and hypoxic conditions hMSCs increased the expression of GBM differentiation markers and decreased the stemness markers percentage. Differently from data reported McLean et al. in a similar study on ovarian carcinoma (McLean et al., 2011) and by Prockop et al. (Prockop et al., 2010) for hematopoietic stem cells, our data do not suggest that hMSCs promote a cancer stem cell supporting milieu. A new study of Schichor (Schichor et al., 2012) on the interactions between glioma cells and hMSCs grown in co-culture revealed fusion between the two different cell types, resulting as multinucleated cells. Conversely, other studies have reported an inhibitory effect of the mesenchymal stem cells on the growth of the tumor (Schichor et al., 2012). However, hMSCs direct effect on tumor cells could be different and, in some way opposite, depending on tumor type.

Finally, we sought to employ BM-MSCs as delivery vehicle for R3616. Cell-mediated vector delivery has been widely explored over last years for GBM (Short et al., 1990) (Kramm et al., 1995) (Nakamizo et al., 2005) (Doucette et al., 2011). It is possible to deliver viral particles to distant parts of the tumor exploiting tumor-tropic migratory cells as oncolytic virus carriers. Thus, the viral particles within cells may be protected from the host immune system and reach tumor site without be neutralized before exerting any effect (Yamamoto and Curiel, 2010) (Herrlinger et al., 2000). An ideal carrier should maintain the inherent tropism for the tumor site even after loading with the oncolytic virus and would support high levels of viral replication with concomitant minimal collateral damage to itself .

Unfortunately, our data indicated that R3616 was not able to efficiently replicate in BM-MSCs, while it retained an efficient killing ability. For this reason we excluded the potential use of BM-MSCs as delivery vehicle for R3616.

In summary, in this study we sought to point out which was the most pursuable therapeutic approach to selectively target GBM derived cells, by analyzing between

virotherapy, employing R3616 and the hMSCs as delivery vehicles to be further genetically engineered to express oHSVs as well as pro-differentiating molecules such as BMP2. We found that BM-MSCs were not possible to use as useful delivery vehicle of R3616 due to the hindered replication. Nevertheless, hMSCs demonstrated to efficiently migrate towards tumor site both in normoxia and hypoxia. In particular, hypoxia was confirmed to increase hMSCs migratory properties toward tumor site, showing an enhancing effect in presence of pro-differentiating molecules. Beside hypoxia, our data suggest other two different components as hMSCs migration enhancers: the R3616 as well as the BMP2 pro-differentiation treatment.

This is the reason why we aim to combine both methods and, upon GSCs infection with R3616 and treatment with BMP2, estimate how hMSCs tropism is enhanced. Preliminary data collected in normoxia have already indicated that combination treatment increase differentiation markers more than BMP2 treatment alone. BM-MSCs employed for our studies seem to contribute to a GBM cells differentiation per sè; therefore our further efforts will direct to evaluate whether the combining treatment can improve hMSCs migratory properties as well.

References

Aboody, K. S., Brown, A., Rainov, N. G., Bower, K. A., Liu, S., Yang, W., Small, J. E., Herrlinger, U., Ourednik, V., Black, P. M., *et al.* (2000). Neural stem cells display extensive tropism for pathology in adult brain: evidence from intracranial gliomas. Proceedings of the National Academy of Sciences of the United States of America *97*, 12846-12851.

Aboody, K. S., Najbauer, J., and Danks, M. K. (2008). Stem and progenitor cell-mediated tumor selective gene therapy. Gene therapy *15*, 739-752.

Aghi, M., and Rabkin, S. (2005). Viral vectors as therapeutic agents for glioblastoma. Current opinion in molecular therapeutics *7*, 419-430.

Aghi, M. K., Liu, T. C., Rabkin, S., and Martuza, R. L. (2009). Hypoxia enhances the replication of oncolytic herpes simplex virus. Molecular therapy : the journal of the American Society of Gene Therapy *17*, 51-56.

Ahmed, A. U., Tyler, M. A., Thaci, B., Alexiades, N. G., Han, Y., Ulasov, I. V., and Lesniak, M. S. (2011). A comparative study of neural and mesenchymal stem cell-based carriers for oncolytic adenovirus in a model of malignant glioma. Molecular pharmaceutics *8*, 1559-1572.

Al-Hajj, M., Wicha, M. S., Benito-Hernandez, A., Morrison, S. J., and Clarke, M. F. (2003). Prospective identification of tumorigenic breast cancer cells. Proceedings of the National Academy of Sciences of the United States of America *100*, 3983-3988.

Alcantara Llaguno, S., Chen, J., Kwon, C. H., Jackson, E. L., Li, Y., Burns, D. K., Alvarez-Buylla, A., and Parada, L. F. (2009). Malignant astrocytomas originate from neural stem/progenitor cells in a somatic tumor suppressor mouse model. Cancer cell *15*, 45-56.

Allen, C., Opyrchal, M., Aderca, I., Schroeder, M. A., Sarkaria, J. N., Domingo, E., Federspiel, M. J., and Galanis, E. (2013). Oncolytic measles virus strains have significant antitumor activity against glioma stem cells. Gene therapy *20*, 444-449.

Altaner, C. (2008). Prodrug cancer gene therapy. Cancer letters *270*, 191-201.

Amano, S., Li, S., Gu, C., Gao, Y., Koizumi, S., Yamamoto, S., Terakawa, S., and Namba, H. (2009). Use of genetically engineered bone marrow-derived mesenchymal stem cells for glioma gene therapy. International journal of oncology *35*, 1265-1270.

Amberger-Murphy, V. (2009). Hypoxia helps glioma to fight therapy. Current cancer drug targets *9*, 381-390.

Andreansky, S., Soroceanu, L., Flotte, E. R., Chou, J., Markert, J. M., Gillespie, G. Y., Roizman, B., and Whitley, R. J. (1997). Evaluation of genetically engineered herpes simplex viruses as oncolytic agents for human malignant brain tumors. Cancer research *57*, 1502-1509.

Ayatollahi, M., Salmani, M. K., Geramizadeh, B., Tabei, S. Z., Soleimani, M., and Sanati, M. H. (2012). Conditions to improve expansion of human mesenchymal stem cells based on rat samples. World journal of stem cells *4*, 1-8.

Azuma, Y., Chou, S. C., Lininger, R. A., Murphy, B. J., Varia, M. A., and Raleigh, J. A. (2003). Hypoxia and differentiation in squamous cell carcinomas of the uterine cervix: pimonidazole and involucrin. Clin Cancer Res *9*, 4944-4952.

Bao, S., Wu, Q., McLendon, R. E., Hao, Y., Shi, Q., Hjelmeland, A. B., Dewhirst, M. W., Bigner, D. D., and Rich, J. N. (2006a). Glioma stem cells promote radioresistance by preferential activation of the DNA damage response. Nature *444*, 756-760.

Bao, S., Wu, Q., Sathornsumetee, S., Hao, Y., Li, Z., Hjelmeland, A. B., Shi, Q., McLendon, R. E., Bigner, D. D., and Rich, J. N. (2006b). Stem cell-like glioma cells promote tumor angiogenesis through vascular endothelial growth factor. Cancer research *66*, 7843-7848.

Bar, E. E. (2011). Glioblastoma, cancer stem cells and hypoxia. Brain Pathol *21*, 119-129.

Batterson, W., and Roizman, B. (1983). Characterization of the herpes simplex virion-associated factor responsible for the induction of alpha genes. Journal of virology *46*, 371-377.

Beier, D., Hau, P., Proescholdt, M., Lohmeier, A., Wischhusen, J., Oefner, P. J., Aigner, L., Brawanski, A., Bogdahn, U., and Beier, C. P. (2007). CD133(+) and CD133(-) glioblastoma-derived cancer stem cells show differential growth characteristics and molecular profiles. Cancer research *67*, 4010-4015.

Benedetti, S., Pirola, B., Pollo, B., Magrassi, L., Bruzzone, M. G., Rigamonti, D., Galli, R., Selleri, S., Di Meco, F., De Fraja, C., *et al.* (2000). Gene therapy of experimental brain tumors using neural progenitor cells. Nature medicine *6*, 447-450.

Bexell, D., Svensson, A., and Bengzon, J. (2013). Stem cell-based therapy for malignant glioma. Cancer treatment reviews *39*, 358-365.

Birnbaum, T., Roider, J., Schankin, C. J., Padovan, C. S., Schichor, C., Goldbrunner, R., and Straube, A. (2007). Malignant gliomas actively recruit bone marrow stromal cells by secreting angiogenic cytokines. Journal of neuro-oncology *83*, 241-247.

Bleau, A. M., Howard, B. M., Taylor, L. A., Gursel, D., Greenfield, J. P., Lim Tung, H. Y., Holland, E. C., and Boockvar, J. A. (2008). New strategy for the analysis of phenotypic marker antigens in brain tumor-derived neurospheres in mice and humans. Neurosurgical focus *24*, E28.

Bonnet, D., and Dick, J. E. (1997). Human acute myeloid leukemia is organized as a hierarchy that originates from a primitive hematopoietic cell. Nature medicine *3*, 730-737.

Boviatsis, E. J., Chase, M., Wei, M. X., Tamiya, T., Hurford, R. K., Jr., Kowall, N. W., Tepper, R. I., Breakefield, X. O., and Chiocca, E. A. (1994). Gene transfer into experimental brain tumors mediated by adenovirus, herpes simplex virus, and retrovirus vectors. Human gene therapy *5*, 183-191.

Braidwood, L., Dunn, P. D., Hardy, S., Evans, T. R., and Brown, S. M. (2009). Antitumor activity of a selectively replication competent herpes simplex virus (HSV) with enzyme prodrug therapy. Anticancer research *29*, 2159-2166.

Bruder, S. P., Jaiswal, N., and Haynesworth, S. E. (1997). Growth kinetics, self-renewal, and the osteogenic potential of purified human mesenchymal stem cells during extensive subcultivation and following cryopreservation. Journal of cellular biochemistry *64*, 278-294.

Cai, J., Wu, Y., Mirua, T., Pierce, J. L., Lucero, M. T., Albertine, K. H., Spangrude, G. J., and Rao, M. S. (2002). Properties of a fetal multipotent neural stem cell (NEP cell). Developmental biology *251*, 221-240.

Calvi, L. M., Adams, G. B., Weibrecht, K. W., Weber, J. M., Olson, D. P., Knight, M. C., Martin, R. P., Schipani, E., Divieti, P., Bringhurst, F. R., *et al.* (2003). Osteoblastic cells regulate the haematopoietic stem cell niche. Nature *425*, 841-846.

Campos, B., Wan, F., Farhadi, M., Ernst, A., Zeppernick, F., Tagscherer, K. E., Ahmadi, R., Lohr, J., Dictus, C., Gdynia, G., *et al.* (2010). Differentiation therapy exerts antitumor effects on stem-like glioma cells. Clinical cancer research : an official journal of the American Association for Cancer Research *16*, 2715-2728.

Chamberlain, G., Fox, J., Ashton, B., and Middleton, J. (2007). Concise review: mesenchymal stem cells: their phenotype, differentiation capacity, immunological features, and potential for homing. Stem Cells *25*, 2739-2749.

Chen, J., McKay, R. M., and Parada, L. F. (2012). Malignant glioma: lessons from genomics, mouse models, and stem cells. Cell *149*, 36-47.

Chiocca, E. A., Abbed, K. M., Tatter, S., Louis, D. N., Hochberg, F. H., Barker, F., Kracher, J., Grossman, S. A., Fisher, J. D., Carson, K., *et al.* (2004). A phase I open-label, dose-escalation, multi-institutional trial of injection with an E1B-Attenuated adenovirus, ONYX-015, into the peritumoral region of recurrent malignant gliomas, in the adjuvant setting. Molecular therapy : the journal of the American Society of Gene Therapy *10*, 958-966.

Choi, S. A., Hwang, S. K., Wang, K. C., Cho, B. K., Phi, J. H., Lee, J. Y., Jung, H. W., Lee, D. H., and Kim, S. K. (2011). Therapeutic efficacy and safety of TRAIL-producing human adipose tissue-derived mesenchymal stem cells against experimental brainstem glioma. Neuro-oncology *13*, 61-69.

Chou, J., Kern, E. R., Whitley, R. J., and Roizman, B. (1990). Mapping of herpes simplex virus-1 neurovirulence to gamma 134.5, a gene nonessential for growth in culture. Science *250*, 1262-1266.

Chou, J., and Roizman, B. (1994). Herpes simplex virus 1 gamma(1)34.5 gene function, which blocks the host response to infection, maps in the homologous domain of the genes expressed during growth arrest and DNA damage. Proceedings of the National Academy of Sciences of the United States of America *91*, 5247-5251.

Cohrs, R. J., and Gilden, D. H. (2001). Human herpesvirus latency. Brain Pathol *11*, 465-474.

Conti, L., Pollard, S. M., Gorba, T., Reitano, E., Toselli, M., Biella, G., Sun, Y., Sanzone, S., Ying, Q. L., Cattaneo, E., and Smith, A. (2005). Niche-independent symmetrical self-renewal of a mammalian tissue stem cell. PLoS biology *3*, e283.

Crocetti, E., Trama, A., Stiller, C., Caldarella, A., Soffietti, R., Jaal, J., Weber, D. C., Ricardi, U., Slowinski, J., and Brandes, A. (2012). Epidemiology of glial and non-glial brain tumours in Europe. Eur J Cancer *48*, 1532-1542.

Curtis, M. A., Kam, M., Nannmark, U., Anderson, M. F., Axell, M. Z., Wikkelso, C., Holtas, S., van Roon-Mom, W. M., Bjork-Eriksson, T., Nordborg, C., *et al.* (2007). Human neuroblasts migrate to the olfactory bulb via a lateral ventricular extension. Science *315*, 1243-1249.

Dahlstrand, J., Collins, V. P., and Lendahl, U. (1992). Expression of the class VI intermediate filament nestin in human central nervous system tumors. Cancer research *52*, 5334-5341.

Dambach, M. J., Trecki, J., Martin, N., and Markovitz, N. S. (2006). Oncolytic viruses derived from the gamma34.5-deleted herpes simplex virus recombinant R3616 encode a truncated UL3 protein. Molecular therapy : the journal of the American Society of Gene Therapy *13*, 891-898.

Darefsky, A. S., King, J. T., Jr., and Dubrow, R. (2012). Adult glioblastoma multiforme survival in the temozolomide era: a population-based analysis of Surveillance, Epidemiology, and End Results registries. Cancer *118*, 2163-2172.

Dirks, P. B. (2008). Brain tumour stem cells: the undercurrents of human brain cancer and their relationship to neural stem cells. Philosophical transactions of the Royal Society of London Series B, Biological sciences *363*, 139-152.

Dirks, P. B. (2010). Brain tumor stem cells: the cancer stem cell hypothesis writ large. Molecular oncology *4*, 420-430.

Dolecek, T. A., Propp, J. M., Stroup, N. E., and Kruchko, C. (2012). CBTRUS statistical report: primary brain and central nervous system tumors diagnosed in the United States in 2005-2009. Neuro-oncology *14 Suppl 5*, v1-49.

Dominici, M., Le Blanc, K., Mueller, I., Slaper-Cortenbach, I., Marini, F., Krause, D., Deans, R., Keating, A., Prockop, D., and Horwitz, E. (2006). Minimal criteria for defining multipotent mesenchymal stromal cells. The International Society for Cellular Therapy position statement. Cytotherapy *8*, 315-317.

Doucette, T., Rao, G., Yang, Y., Gumin, J., Shinojima, N., Bekele, B. N., Qiao, W., Zhang, W., and Lang, F. F. (2011). Mesenchymal stem cells display tumor-specific tropism in an RCAS/Ntv-a glioma model. Neoplasia *13*, 716-725.

Ehtesham, M., Kabos, P., Gutierrez, M. A., Chung, N. H., Griffith, T. S., Black, K. L., and Yu, J. S. (2002a). Induction of glioblastoma apoptosis using neural stem cell-mediated delivery of tumor necrosis factor-related apoptosis-inducing ligand. Cancer research *62*, 7170-7174.

Ehtesham, M., Kabos, P., Kabosova, A., Neuman, T., Black, K. L., and Yu, J. S. (2002b). The use of interleukin 12-secreting neural stem cells for the treatment of intracranial glioma. Cancer research *62*, 5657-5663.

Erecinska, M., and Silver, I. A. (2001). Tissue oxygen tension and brain sensitivity to hypoxia. Respiration physiology *128*, 263-276.

Erices, A., Conget, P., and Minguell, J. J. (2000). Mesenchymal progenitor cells in human umbilical cord blood. British journal of haematology *109*, 235-242.

Esposito, I., Kleeff, J., Bischoff, S. C., Fischer, L., Collecchi, P., Iorio, M., Bevilacqua, G., Buchler, M. W., and Friess, H. (2002). The stem cell factor-c-kit system and mast cells in human pancreatic cancer. Laboratory investigation; a journal of technical methods and pathology *82*, 1481-1492.

Evans, S. M., Jenkins, K. W., Jenkins, W. T., Dilling, T., Judy, K. D., Schrlau, A., Judkins, A., Hahn, S. M., and Koch, C. J. (2008). Imaging and analytical methods as applied to the evaluation of vasculature and hypoxia in human brain tumors. Radiation research *170*, 677-690.

Fehrer, C., Brunauer, R., Laschober, G., Unterluggauer, H., Reitinger, S., Kloss, F., Gully, C., Gassner, R., and Lepperdinger, G. (2007). Reduced oxygen tension attenuates differentiation capacity of human mesenchymal stem cells and prolongs their lifespan. Aging cell *6*, 745-757.

Fisher, J. L., Schwartzbaum, J. A., Wrensch, M., and Wiemels, J. L. (2007). Epidemiology of brain tumors. Neurologic clinics *25*, 867-890, vii.

Fleming, A. B., and Saltzman, W. M. (2002). Pharmacokinetics of the carmustine implant. Clinical pharmacokinetics *41*, 403-419.

Forsyth, P., Roldan, G., George, D., Wallace, C., Palmer, C. A., Morris, D., Cairncross, G., Matthews, M. V., Markert, J., Gillespie, Y., *et al.* (2008). A phase I trial of intratumoral administration of reovirus in patients with histologically confirmed recurrent malignant gliomas. Molecular therapy : the journal of the American Society of Gene Therapy *16*, 627-632.

Freeman, A. I., Zakay-Rones, Z., Gomori, J. M., Linetsky, E., Rasooly, L., Greenbaum, E., Rozenman-Yair, S., Panet, A., Libson, E., Irving, C. S., *et al.* (2006). Phase I/II trial of intravenous NDV-HUJ oncolytic virus in recurrent glioblastoma multiforme. Molecular therapy : the journal of the American Society of Gene Therapy *13*, 221-228.

Friedman, G. K., Haas, M. C., Kelly, V. M., Markert, J. M., Gillespie, G. Y., and Cassady, K. A. (2012). Hypoxia Moderates gamma(1)34.5-Deleted Herpes Simplex Virus Oncolytic Activity in Human Glioma Xenoline Primary Cultures. Translational oncology *5*, 200-207.

Gage, F. H. (1998). Stem cells of the central nervous system. Current opinion in neurobiology *8*, 671-676.

Galli, R., Binda, E., Orfanelli, U., Cipelletti, B., Gritti, A., De Vitis, S., Fiocco, R., Foroni, C., Dimeco, F., and Vescovi, A. (2004). Isolation and characterization of tumorigenic, stem-like neural precursors from human glioblastoma. Cancer research *64*, 7011-7021.

Germano, I., Swiss, V., and Casaccia, P. (2010). Primary brain tumors, neural stem cell, and brain tumor cancer cells: where is the link? Neuropharmacology *58*, 903-910.

Gillespie, D. L., Whang, K., Ragel, B. T., Flynn, J. R., Kelly, D. A., and Jensen, R. L. (2007). Silencing of hypoxia inducible factor-1alpha by RNA interference attenuates human glioma cell growth in vivo. Clinical cancer research : an official journal of the American Association for Cancer Research *13*, 2441-2448.

Gunther, H. S., Schmidt, N. O., Phillips, H. S., Kemming, D., Kharbanda, S., Soriano, R., Modrusan, Z., Meissner, H., Westphal, M., and Lamszus, K. (2008). Glioblastoma-derived stem cell-enriched cultures form distinct subgroups according to molecular and phenotypic criteria. Oncogene *27*, 2897-2909.

Gursel, D. B., Shin, B. J., Burkhardt, J. K., Kesavabhotla, K., Schlaff, C. D., and Boockvar, J. A. (2011). Glioblastoma Stem-Like Cells-Biology and Therapeutic Implications. Cancers *3*, 2655-2666.

Harris, A. L. (2002). Hypoxia--a key regulatory factor in tumour growth. Nature reviews Cancer *2*, 38-47.

Hayry, V., Tynninen, O., Haapasalo, H. K., Wolfer, J., Paulus, W., Hasselblatt, M., Sariola, H., Paetau, A., Sarna, S., Niemela, M., *et al.* (2008). Stem cell protein BMI-1 is an independent marker for poor prognosis in oligodendroglial tumours. Neuropathology and applied neurobiology *34*, 555-563.

Heddleston, J. M., Li, Z., McLendon, R. E., Hjelmeland, A. B., and Rich, J. N. (2009). The hypoxic microenvironment maintains glioblastoma stem cells and promotes reprogramming towards a cancer stem cell phenotype. Cell Cycle *8*, 3274-3284.

Hegi, M. E., Diserens, A. C., Gorlia, T., Hamou, M. F., de Tribolet, N., Weller, M., Kros, J. M., Hainfellner, J. A., Mason, W., Mariani, L., *et al.* (2005). MGMT gene silencing and benefit from temozolomide in glioblastoma. The New England journal of medicine *352*, 997-1003.

Heldin, C. H., Miyazono, K., and ten Dijke, P. (1997). TGF-beta signalling from cell membrane to nucleus through SMAD proteins. Nature *390*, 465-471.

Hemmati, H. D., Nakano, I., Lazareff, J. A., Masterman-Smith, M., Geschwind, D. H., Bronner-Fraser, M., and Kornblum, H. I. (2003). Cancerous stem cells can arise from pediatric brain tumors. Proceedings of the National Academy of Sciences of the United States of America *100*, 15178-15183.

Herrlinger, U., Woiciechowski, C., Sena-Esteves, M., Aboody, K. S., Jacobs, A. H., Rainov, N. G., Snyder, E. Y., and Breakefield, X. O. (2000). Neural precursor cells for delivery of replication-conditional HSV-1 vectors to intracerebral gliomas. Molecular therapy : the journal of the American Society of Gene Therapy *1*, 347-357.

Hong, X., Miller, C., Savant-Bhonsale, S., and Kalkanis, S. N. (2009). Antitumor treatment using interleukin- 12-secreting marrow stromal cells in an invasive glioma model. Neurosurgery *64*, 1139-1146; discussion 1146-1137.

Huang, Q., Liu, X. Z., Kang, C. S., Wang, G. X., Zhong, Y., and Pu, P. Y. (2010). The anti-glioma effect of suicide gene therapy using BMSC expressing HSV/TK combined with overexpression of Cx43 in glioma cells. Cancer gene therapy *17*, 192-202.

Hunter, W. D., Martuza, R. L., Feigenbaum, F., Todo, T., Mineta, T., Yazaki, T., Toda, M., Newsome, J. T., Platenberg, R. C., Manz, H. J., and Rabkin, S. D. (1999). Attenuated, replication-competent herpes simplex virus type 1 mutant G207: safety evaluation of intracerebral injection in nonhuman primates. Journal of virology *73*, 6319-6326.

Ignatova, T. N., Kukekov, V. G., Laywell, E. D., Suslov, O. N., Vrionis, F. D., and Steindler, D. A. (2002). Human cortical glial tumors contain neural stem-like cells expressing astroglial and neuronal markers in vitro. Glia *39*, 193-206.

Ikegame, Y., Yamashita, K., Hayashi, S., Mizuno, H., Tawada, M., You, F., Yamada, K., Tanaka, Y., Egashira, Y., Nakashima, S., *et al.* (2011). Comparison of mesenchymal stem cells from adipose tissue and bone marrow for ischemic stroke therapy. Cytotherapy *13*, 675-685.

Jogi, A., Ora, I., Nilsson, H., Lindeheim, A., Makino, Y., Poellinger, L., Axelson, H., and Pahlman, S. (2002). Hypoxia alters gene expression in human neuroblastoma cells toward an immature and neural crest-like phenotype. Proc Natl Acad Sci U S A *99*, 7021-7026.

Kanai, R., Rabkin, S. D., Yip, S., Sgubin, D., Zaupa, C. M., Hirose, Y., Louis, D. N., Wakimoto, H., and Martuza, R. L. (2012). Oncolytic virus-mediated manipulation of DNA damage responses: synergy with chemotherapy in killing glioblastoma stem cells. Journal of the National Cancer Institute *104*, 42-55.

Kanai, R., Wakimoto, H., Cheema, T., and Rabkin, S. D. (2010). Oncolytic herpes simplex virus vectors and chemotherapy: are combinatorial strategies more effective for cancer? Future Oncol *6*, 619-634.

Keith, B., and Simon, M. C. (2007). Hypoxia-inducible factors, stem cells, and cancer. Cell *129*, 465-472.

Kern, S., Eichler, H., Stoeve, J., Kluter, H., and Bieback, K. (2006). Comparative analysis of mesenchymal stem cells from bone marrow, umbilical cord blood, or adipose tissue. Stem Cells *24*, 1294-1301.

Keung, E. Z., Nelson, P. J., and Conrad, C. (2013). Concise review: genetically engineered stem cell therapy targeting angiogenesis and tumor stroma in gastrointestinal malignancy. Stem Cells *31*, 227-235.

Kieff, E. D., Bachenheimer, S. L., and Roizman, B. (1971). Size, composition, and structure of the deoxyribonucleic acid of herpes simplex virus subtypes 1 and 2. Journal of virology *8*, 125-132.

Kolenda, J., Jensen, S. S., Aaberg-Jessen, C., Christensen, K., Andersen, C., Brunner, N., and Kristensen, B. W. (2011). Effects of hypoxia on expression of a panel of stem cell and chemoresistance markers in glioblastoma-derived spheroids. Journal of neuro-oncology *103*, 43-58.

Koshiji, M., To, K. K., Hammer, S., Kumamoto, K., Harris, A. L., Modrich, P., and Huang, L. E. (2005). HIF-1alpha induces genetic instability by transcriptionally downregulating MutSalpha expression. Molecular cell *17*, 793-803.

Kosztowski, T., Zaidi, H. A., and Quinones-Hinojosa, A. (2009). Applications of neural and mesenchymal stem cells in the treatment of gliomas. Expert review of anticancer therapy *9*, 597-612.

Kramm, C. M., Sena-Esteves, M., Barnett, F. H., Rainov, N. G., Schuback, D. E., Yu, J. S., Pechan, P. A., Paulus, W., Chiocca, E. A., and Breakefield, X. O. (1995). Gene therapy for brain tumors. Brain Pathol *5*, 345-381.

Kuroda, T., Martuza, R. L., Todo, T., and Rabkin, S. D. (2006). Flip-Flop HSV-BAC: bacterial artificial chromosome based system for rapid generation of recombinant herpes simplex virus vectors using two independent site-specific recombinases. BMC biotechnology *6*, 40.

Kwong, A. D., and Frenkel, N. (1989). The herpes simplex virus virion host shutoff function. Journal of virology *63*, 4834-4839.

Lamfers, M., Idema, S., van Milligen, F., Schouten, T., van der Valk, P., Vandertop, P., Dirven, C., and Noske, D. (2009). Homing properties of adipose-derived stem cells to intracerebral glioma and the effects of adenovirus infection. Cancer letters *274*, 78-87.

Le Blanc, K., Tammik, C., Rosendahl, K., Zetterberg, E., and Ringden, O. (2003). HLA expression and immunologic properties of differentiated and undifferentiated mesenchymal stem cells. Experimental hematology *31*, 890-896.

Lei, L., Sonabend, A. M., Guarnieri, P., Soderquist, C., Ludwig, T., Rosenfeld, S., Bruce, J. N., and Canoll, P. (2011). Glioblastoma models reveal the connection between adult glial progenitors and the proneural phenotype. PloS one *6*, e20041.

Li, V. S., Ng, S. S., Boersema, P. J., Low, T. Y., Karthaus, W. R., Gerlach, J. P., Mohammed, S., Heck, A. J., Maurice, M. M., Mahmoudi, T., and Clevers, H. (2012). Wnt signaling through inhibition of beta-catenin degradation in an intact Axin1 complex. Cell *149*, 1245-1256.

Li, Z., Bao, S., Wu, Q., Wang, H., Eyler, C., Sathornsumetee, S., Shi, Q., Cao, Y., Lathia, J., McLendon, R. E., *et al.* (2009). Hypoxia-inducible factors regulate tumorigenic capacity of glioma stem cells. Cancer cell *15*, 501-513.

Liu, T. C., Galanis, E., and Kirn, D. (2007). Clinical trial results with oncolytic virotherapy: a century of promise, a decade of progress. Nature clinical practice Oncology *4*, 101-117.

Locke, M., Feisst, V., and Dunbar, P. R. (2011). Concise review: human adipose-derived stem cells: separating promise from clinical need. Stem Cells *29*, 404-411.

Louis, D. N., Ohgaki, H., Wiestler, O. D., Cavenee, W. K., Burger, P. C., Jouvet, A., Scheithauer, B. W., and Kleihues, P. (2007). The 2007 WHO classification of tumours of the central nervous system. Acta neuropathologica *114*, 97-109.

Mackem, S., and Roizman, B. (1982). Structural features of the herpes simplex virus alpha gene 4, 0, and 27 promoter-regulatory sequences which confer alpha regulation on chimeric thymidine kinase genes. Journal of virology *44*, 939-949.

Markert, J. M., Cody, J. J., Parker, J. N., Coleman, J. M., Price, K. H., Kern, E. R., Quenelle, D. C., Lakeman, A. D., Schoeb, T. R., Palmer, C. A., *et al.* (2012). Preclinical evaluation of a genetically engineered herpes simplex virus expressing interleukin-12. Journal of virology *86*, 5304-5313.

Markert, J. M., Liechty, P. G., Wang, W., Gaston, S., Braz, E., Karrasch, M., Nabors, L. B., Markiewicz, M., Lakeman, A. D., Palmer, C. A., *et al.* (2009). Phase Ib trial of mutant herpes simplex virus G207 inoculated pre-and post-tumor resection for recurrent GBM. Molecular therapy : the journal of the American Society of Gene Therapy *17*, 199-207.

Markert, J. M., Medlock, M. D., Rabkin, S. D., Gillespie, G. Y., Todo, T., Hunter, W. D., Palmer, C. A., Feigenbaum, F., Tornatore, C., Tufaro, F., and Martuza, R. L. (2000). Conditionally replicating herpes simplex virus mutant, G207 for the treatment of malignant glioma: results of a phase I trial. Gene therapy *7*, 867-874.

Martuza, R. L., Malick, A., Markert, J. M., Ruffner, K. L., and Coen, D. M. (1991). Experimental therapy of human glioma by means of a genetically engineered virus mutant. Science *252*, 854-856.

Massague, J., Seoane, J., and Wotton, D. (2005). Smad transcription factors. Genes & development *19*, 2783-2810.

Masui, K., Cloughesy, T. F., and Mischel, P. S. (2012). Review: molecular pathology in adult high-grade gliomas: from molecular diagnostics to target therapies. Neuropathology and applied neurobiology *38*, 271-291.

Maugeri-Sacca, M., Di Martino, S., and De Maria, R. (2013). Biological and clinical implications of cancer stem cells in primary brain tumors. Frontiers in oncology *3*, 6.

McCord, A. M., Jamal, M., Shankavaram, U. T., Lang, F. F., Camphausen, K., and Tofilon, P. J. (2009). Physiologic oxygen concentration enhances the stem-like properties of CD133+ human glioblastoma cells in vitro. Molecular cancer research : MCR *7*, 489-497.

McLean, K., Gong, Y., Choi, Y., Deng, N., Yang, K., Bai, S., Cabrera, L., Keller, E., McCauley, L., Cho, K. R., and Buckanovich, R. J. (2011). Human ovarian carcinoma-associated mesenchymal stem cells

regulate cancer stem cells and tumorigenesis via altered BMP production. The Journal of clinical investigation *121*, 3206-3219.

Mineta, T., Rabkin, S. D., Yazaki, T., Hunter, W. D., and Martuza, R. L. (1995). Attenuated multi-mutated herpes simplex virus-1 for the treatment of malignant gliomas. Nature medicine *1*, 938-943.

Momin, E. N., Vela, G., Zaidi, H. A., and Quinones-Hinojosa, A. (2010). The Oncogenic Potential of Mesenchymal Stem Cells in the Treatment of Cancer: Directions for Future Research. Current immunology reviews *6*, 137-148.

Mullen, J. T., and Tanabe, K. K. (2002). Viral oncolysis. The oncologist *7*, 106-119.

Mundra, V., Gerling, I. C., and Mahato, R. I. (2013). Mesenchymal stem cell-based therapy. Molecular pharmaceutics *10*, 77-89.

Nager, M., Bhardwaj, D., Canti, C., Medina, L., Nogues, P., and Herreros, J. (2012). beta-Catenin Signalling in Glioblastoma Multiforme and Glioma-Initiating Cells. Chemotherapy research and practice *2012*, 192362.

Nakamizo, A., Marini, F., Amano, T., Khan, A., Studeny, M., Gumin, J., Chen, J., Hentschel, S., Vecil, G., Dembinski, J., *et al.* (2005). Human bone marrow-derived mesenchymal stem cells in the treatment of gliomas. Cancer research *65*, 3307-3318.

Nakamura, K., Ito, Y., Kawano, Y., Kurozumi, K., Kobune, M., Tsuda, H., Bizen, A., Honmou, O., Niitsu, Y., and Hamada, H. (2004). Antitumor effect of genetically engineered mesenchymal stem cells in a rat glioma model. Gene therapy *11*, 1155-1164.

Nakashima, H., Kaur, B., and Chiocca, E. A. (2010). Directing systemic oncolytic viral delivery to tumors via carrier cells. Cytokine & growth factor reviews *21*, 119-126.

Newcomb, W. W., Homa, F. L., Thomsen, D. R., Trus, B. L., Cheng, N., Steven, A., Booy, F., and Brown, J. C. (1999). Assembly of the herpes simplex virus procapsid from purified components and identification of small complexes containing the major capsid and scaffolding proteins. Journal of virology *73*, 4239-4250.

Nigro, J. M., Misra, A., Zhang, L., Smirnov, I., Colman, H., Griffin, C., Ozburn, N., Chen, M., Pan, E., Koul, D., *et al.* (2005). Integrated array-comparative genomic hybridization and expression array profiles identify clinically relevant molecular subtypes of glioblastoma. Cancer research *65*, 1678-1686.

Noushmehr, H., Weisenberger, D. J., Diefes, K., Phillips, H. S., Pujara, K., Berman, B. P., Pan, F., Pelloski, C. E., Sulman, E. P., Bhat, K. P., *et al.* (2010). Identification of a CpG island methylator phenotype that defines a distinct subgroup of glioma. Cancer cell *17*, 510-522.

Ogden, A. T., Waziri, A. E., Lochhead, R. A., Fusco, D., Lopez, K., Ellis, J. A., Kang, J., Assanah, M., McKhann, G. M., Sisti, M. B., *et al.* (2008). Identification of A2B5+CD133- tumor-initiating cells in adult human gliomas. Neurosurgery *62*, 505-514; discussion 514-505.

Ohgaki, H., and Kleihues, P. (2005a). Epidemiology and etiology of gliomas. Acta neuropathologica *109*, 93-108.

Ohgaki, H., and Kleihues, P. (2005b). Population-based studies on incidence, survival rates, and genetic alterations in astrocytic and oligodendroglial gliomas. Journal of neuropathology and experimental neurology *64*, 479-489.

Panchision, D. M., Chen, H. L., Pistollato, F., Papini, D., Ni, H. T., and Hawley, T. S. (2007). Optimized flow cytometric analysis of central nervous system tissue reveals novel functional relationships among cells expressing CD133, CD15, and CD24. Stem Cells *25*, 1560-1570.

Papanastassiou, V., Rampling, R., Fraser, M., Petty, R., Hadley, D., Nicoll, J., Harland, J., Mabbs, R., and Brown, M. (2002). The potential for efficacy of the modified (ICP 34.5(-)) herpes simplex virus HSV1716 following intratumoural injection into human malignant glioma: a proof of principle study. Gene therapy *9*, 398-406.

Parsons, D. W., Jones, S., Zhang, X., Lin, J. C., Leary, R. J., Angenendt, P., Mankoo, P., Carter, H., Siu, I. M., Gallia, G. L., *et al.* (2008). An integrated genomic analysis of human glioblastoma multiforme. Science *321*, 1807-1812.

Pendleton, C., Li, Q., Chesler, D. A., Yuan, K., Guerrero-Cazares, H., and Quinones-Hinojosa, A. (2013). Mesenchymal stem cells derived from adipose tissue vs bone marrow: in vitro comparison of their tropism towards gliomas. PloS one *8*, e58198.

Persano, L., Pistollato, F., Rampazzo, E., Della Puppa, A., Abbadi, S., Frasson, C., Volpin, F., Indraccolo, S., Scienza, R., and Basso, G. (2012). BMP2 sensitizes glioblastoma stem-like cells to Temozolomide by affecting HIF-1alpha stability and MGMT expression. Cell death & disease *3*, e412.

Persano, L., Rampazzo, E., Basso, G., and Viola, G. (2013). Glioblastoma cancer stem cells: role of the microenvironment and therapeutic targeting. Biochemical pharmacology *85*, 612-622.

Persano, L., Rampazzo, E., Della Puppa, A., Pistollato, F., and Basso, G. (2011). The three-layer concentric model of glioblastoma: cancer stem cells, microenvironmental regulation, and therapeutic implications. TheScientificWorldJournal *11*, 1829-1841.

Piccirillo, S. G., Combi, R., Cajola, L., Patrizi, A., Redaelli, S., Bentivegna, A., Baronchelli, S., Maira, G., Pollo, B., Mangiola, A., *et al.* (2009). Distinct pools of cancer stem-like cells coexist within human glioblastomas and display different tumorigenicity and independent genomic evolution. Oncogene *28*, 1807-1811.

Piccirillo, S. G., Reynolds, B. A., Zanetti, N., Lamorte, G., Binda, E., Broggi, G., Brem, H., Olivi, A., Dimeco, F., and Vescovi, A. L. (2006). Bone morphogenetic proteins inhibit the tumorigenic potential of human brain tumour-initiating cells. Nature *444*, 761-765.

Pierdomenico, L., Bonsi, L., Calvitti, M., Rondelli, D., Arpinati, M., Chirumbolo, G., Becchetti, E., Marchionni, C., Alviano, F., Fossati, V., *et al.* (2005). Multipotent mesenchymal stem cells with immunosuppressive activity can be easily isolated from dental pulp. Transplantation *80*, 836-842.

Pistollato, F., Abbadi, S., Rampazzo, E., Persano, L., Della Puppa, A., Frasson, C., Sarto, E., Scienza, R., D'Avella, D., and Basso, G. (2010a). Intratumoral hypoxic gradient drives stem cells distribution and MGMT expression in glioblastoma. Stem Cells *28*, 851-862.

Pistollato, F., Abbadi, S., Rampazzo, E., Viola, G., Della Puppa, A., Cavallini, L., Frasson, C., Persano, L., Panchision, D. M., and Basso, G. (2010b). Hypoxia and succinate antagonize 2-deoxyglucose effects on glioblastoma. Biochemical pharmacology *80*, 1517-1527.

Pistollato, F., Chen, H. L., Rood, B. R., Zhang, H. Z., D'Avella, D., Denaro, L., Gardiman, M., te Kronnie, G., Schwartz, P. H., Favaro, E., *et al.* (2009a). Hypoxia and HIF1alpha repress the differentiative effects of BMPs in high-grade glioma. Stem Cells *27*, 7-17.

Pistollato, F., Chen, H. L., Schwartz, P. H., Basso, G., and Panchision, D. M. (2007). Oxygen tension controls the expansion of human CNS precursors and the generation of astrocytes and oligodendrocytes. Molecular and cellular neurosciences *35*, 424-435.

Pistollato, F., Persano, L., Puppa, A. D., Rampazzo, E., and Basso, G. (2011). Isolation and expansion of regionally defined human glioblastoma cells in vitro. Current protocols in stem cell biology *Chapter 3*, Unit 3 4.

Pistollato, F., Rampazzo, E., Abbadi, S., Della Puppa, A., Scienza, R., D'Avella, D., Denaro, L., Te Kronnie, G., Panchision, D. M., and Basso, G. (2009b). Molecular mechanisms of HIF-1alpha modulation induced by oxygen tension and BMP2 in glioblastoma derived cells. PloS one *4*, e6206.

Pittenger, M. F., Mackay, A. M., Beck, S. C., Jaiswal, R. K., Douglas, R., Mosca, J. D., Moorman, M. A., Simonetti, D. W., Craig, S., and Marshak, D. R. (1999). Multilineage potential of adult human mesenchymal stem cells. Science *284*, 143-147.

Pollard, S. M., Yoshikawa, K., Clarke, I. D., Danovi, D., Stricker, S., Russell, R., Bayani, J., Head, R., Lee, M., Bernstein, M., *et al.* (2009). Glioma stem cell lines expanded in adherent culture have tumor-specific phenotypes and are suitable for chemical and genetic screens. Cell stem cell *4*, 568-580.

Ponta, H., Sherman, L., and Herrlich, P. A. (2003). CD44: from adhesion molecules to signalling regulators. Nature reviews Molecular cell biology *4*, 33-45.

Prockop, D. J., Kota, D. J., Bazhanov, N., and Reger, R. L. (2010). Evolving paradigms for repair of tissues by adult stem/progenitor cells (MSCs). Journal of cellular and molecular medicine *14*, 2190-2199.

Ramasamy, R., Lam, E. W., Soeiro, I., Tisato, V., Bonnet, D., and Dazzi, F. (2007). Mesenchymal stem cells inhibit proliferation and apoptosis of tumor cells: impact on in vivo tumor growth. Leukemia *21*, 304-310.

Rampazzo, E., Persano, L., Pistollato, F., Moro, E., Frasson, C., Porazzi, P., Della Puppa, A., Bresolin, S., Battilana, G., Indraccolo, S., *et al.* (2013). Wnt activation promotes neuronal differentiation of glioblastoma. Cell death & disease *4*, e500.

Reya, T., Morrison, S. J., Clarke, M. F., and Weissman, I. L. (2001). Stem cells, cancer, and cancer stem cells. Nature *414*, 105-111.

Reynolds, B. A., and Rietze, R. L. (2005). Neural stem cells and neurospheres--re-evaluating the relationship. Nature methods *2*, 333-336.

Reynolds, B. A., and Weiss, S. (1992). Generation of neurons and astrocytes from isolated cells of the adult mammalian central nervous system. Science *255*, 1707-1710.

Reynolds, B. A., and Weiss, S. (1996). Clonal and population analyses demonstrate that an EGF-responsive mammalian embryonic CNS precursor is a stem cell. Developmental biology *175*, 1-13.

Ricci-Vitiani, L., Lombardi, D. G., Pilozzi, E., Biffoni, M., Todaro, M., Peschle, C., and De Maria, R. (2007). Identification and expansion of human colon-cancer-initiating cells. Nature *445*, 111-115.

Robert, M., and Wastie, M. (2008). Glioblastoma multiforme: a rare manifestation of extensive liver and bone metastases. Biomedical imaging and intervention journal *4*, e3.

Rochefort, G. Y., Delorme, B., Lopez, A., Herault, O., Bonnet, P., Charbord, P., Eder, V., and Domenech, J. (2006). Multipotential mesenchymal stem cells are mobilized into peripheral blood by hypoxia. Stem Cells *24*, 2202-2208.

Rong, Y., Durden, D. L., Van Meir, E. G., and Brat, D. J. (2006). 'Pseudopalisading' necrosis in glioblastoma: a familiar morphologic feature that links vascular pathology, hypoxia, and angiogenesis. J Neuropathol Exp Neurol *65*, 529-539.

Sanai, N., Tramontin, A. D., Quinones-Hinojosa, A., Barbaro, N. M., Gupta, N., Kunwar, S., Lawton, M. T., McDermott, M. W., Parsa, A. T., Manuel-Garcia Verdugo, J., *et al.* (2004). Unique astrocyte ribbon in adult human brain contains neural stem cells but lacks chain migration. Nature *427*, 740-744.

Sant, M., Allemani, C., Santaquilani, M., Knijn, A., Marchesi, F., and Capocaccia, R. (2009). EUROCARE-4. Survival of cancer patients diagnosed in 1995-1999. Results and commentary. Eur J Cancer *45*, 931-991.

Sasportas, L. S., Kasmieh, R., Wakimoto, H., Hingtgen, S., van de Water, J. A., Mohapatra, G., Figueiredo, J. L., Martuza, R. L., Weissleder, R., and Shah, K. (2009). Assessment of therapeutic efficacy and fate of engineered human mesenchymal stem cells for cancer therapy. Proceedings of the National Academy of Sciences of the United States of America *106*, 4822-4827.

Schichor, C., Albrecht, V., Korte, B., Buchner, A., Riesenberg, R., Mysliwietz, J., Paron, I., Motaln, H., Turnsek, T. L., Jurchott, K., *et al.* (2012). Mesenchymal stem cells and glioma cells form a structural as well as a functional syncytium in vitro. Experimental neurology *234*, 208-219.

Seidel, S., Garvalov, B. K., Wirta, V., von Stechow, L., Schanzer, A., Meletis, K., Wolter, M., Sommerlad, D., Henze, A. T., Nister, M., *et al.* (2010). A hypoxic niche regulates glioblastoma stem cells through hypoxia inducible factor 2 alpha. Brain : a journal of neurology *133*, 983-995.

Semenza, G. L. (2010). Defining the role of hypoxia-inducible factor 1 in cancer biology and therapeutics. Oncogene *29*, 625-634.

Semenza, G. L., Wang, G. L., and Kundu, R. (1995). DNA binding and transcriptional properties of wild-type and mutant forms of the homeodomain protein Msx2. Biochemical and biophysical research communications *209*, 257-262.

Senzer, N. N., Kaufman, H. L., Amatruda, T., Nemunaitis, M., Reid, T., Daniels, G., Gonzalez, R., Glaspy, J., Whitman, E., Harrington, K., *et al.* (2009). Phase II clinical trial of a granulocyte-macrophage colony-stimulating factor-encoding, second-generation oncolytic herpesvirus in patients with unresectable metastatic melanoma. Journal of clinical oncology : official journal of the American Society of Clinical Oncology *27*, 5763-5771.

Sgubin, D., Wakimoto, H., Kanai, R., Rabkin, S. D., and Martuza, R. L. (2012). Oncolytic herpes simplex virus counteracts the hypoxia-induced modulation of glioblastoma stem-like cells. Stem cells translational medicine *1*, 322-332.

Short, M. P., Choi, B. C., Lee, J. K., Malick, A., Breakefield, X. O., and Martuza, R. L. (1990). Gene delivery to glioma cells in rat brain by grafting of a retrovirus packaging cell line. Journal of neuroscience research *27*, 427-439.

Shou, J., Ali-Osman, F., Multani, A. S., Pathak, S., Fedi, P., and Srivenugopal, K. S. (2002). Human Dkk-1, a gene encoding a Wnt antagonist, responds to DNA damage and its overexpression sensitizes brain tumor cells to apoptosis following alkylation damage of DNA. Oncogene *21*, 878-889.

Singec, I., Knoth, R., Meyer, R. P., Maciaczyk, J., Volk, B., Nikkhah, G., Frotscher, M., and Snyder, E. Y. (2006). Defining the actual sensitivity and specificity of the neurosphere assay in stem cell biology. Nature methods *3*, 801-806.

Singh, S. K., Clarke, I. D., Hide, T., and Dirks, P. B. (2004a). Cancer stem cells in nervous system tumors. Oncogene *23*, 7267-7273.

Singh, S. K., Clarke, I. D., Terasaki, M., Bonn, V. E., Hawkins, C., Squire, J., and Dirks, P. B. (2003). Identification of a cancer stem cell in human brain tumors. Cancer Res *63*, 5821-5828.

Singh, S. K., Hawkins, C., Clarke, I. D., Squire, J. A., Bayani, J., Hide, T., Henkelman, R. M., Cusimano, M. D., and Dirks, P. B. (2004b). Identification of human brain tumour initiating cells. Nature *432*, 396-401.

Soeda, A., Park, M., Lee, D., Mintz, A., Androutsellis-Theotokis, A., McKay, R. D., Engh, J., Iwama, T., Kunisada, T., Kassam, A. B., *et al.* (2009). Hypoxia promotes expansion of the CD133-positive glioma stem cells through activation of HIF-1alpha. Oncogene *28*, 3949-3959.

Stopschinski, B. E., Beier, C. P., and Beier, D. (2013). Glioblastoma cancer stem cells - From concept to clinical application. Cancer letters *338*, 32-40.

Strem, B. M., Hicok, K. C., Zhu, M., Wulur, I., Alfonso, Z., Schreiber, R. E., Fraser, J. K., and Hedrick, M. H. (2005). Multipotential differentiation of adipose tissue-derived stem cells. The Keio journal of medicine *54*, 132-141.

Stupp, R., Hegi, M. E., Mason, W. P., van den Bent, M. J., Taphoorn, M. J., Janzer, R. C., Ludwin, S. K., Allgeier, A., Fisher, B., Belanger, K., *et al.* (2009a). Effects of radiotherapy with concomitant and adjuvant temozolomide versus radiotherapy alone on survival in glioblastoma in a randomised phase III study: 5-year analysis of the EORTC-NCIC trial. The lancet oncology *10*, 459-466.

Stupp, R., Mason, W. P., van den Bent, M. J., Weller, M., Fisher, B., Taphoorn, M. J., Belanger, K., Brandes, A. A., Marosi, C., Bogdahn, U., *et al.* (2005). Radiotherapy plus concomitant and adjuvant temozolomide for glioblastoma. The New England journal of medicine *352*, 987-996.

Stupp, R., Mayer, M., Kann, R., Weder, W., Zouhair, A., Betticher, D. C., Roth, A. D., Stahel, R. A., Majno, S. B., Peters, S., *et al.* (2009b). Neoadjuvant chemotherapy and radiotherapy followed by surgery in selected patients with stage IIIB non-small-cell lung cancer: a multicentre phase II trial. The lancet oncology *10*, 785-793.

Sulman, E. P., Guerrero, M., and Aldape, K. (2009). Beyond grade: molecular pathology of malignant gliomas. Seminars in radiation oncology *19*, 142-149.

Sun, Y., Pollard, S., Conti, L., Toselli, M., Biella, G., Parkin, G., Willatt, L., Falk, A., Cattaneo, E., and Smith, A. (2008). Long-term tripotent differentiation capacity of human neural stem (NS) cells in adherent culture. Molecular and cellular neurosciences *38*, 245-258.

Suslov, O. N., Kukekov, V. G., Ignatova, T. N., and Steindler, D. A. (2002). Neural stem cell heterogeneity demonstrated by molecular phenotyping of clonal neurospheres. Proceedings of the National Academy of Sciences of the United States of America *99*, 14506-14511.

Tate, C. M., Pallini, R., Ricci-Vitiani, L., Dowless, M., Shiyanova, T., D'Alessandris, G. Q., Morgante, L., Giannetti, S., Larocca, L. M., di Martino, S., *et al.* (2012). A BMP7 variant inhibits the tumorigenic potential of glioblastoma stem-like cells. Cell death and differentiation *19*, 1644-1654.

Todo, T., Martuza, R. L., Rabkin, S. D., and Johnson, P. A. (2001). Oncolytic herpes simplex virus vector with enhanced MHC class I presentation and tumor cell killing. Proceedings of the National Academy of Sciences of the United States of America *98*, 6396-6401.

Tohyama, T., Lee, V. M., Rorke, L. B., Marvin, M., McKay, R. D., and Trojanowski, J. Q. (1992). Nestin expression in embryonic human neuroepithelium and in human neuroepithelial tumor cells. Laboratory investigation; a journal of technical methods and pathology *66*, 303-313.

Tondreau, T., Meuleman, N., Delforge, A., Dejeneffe, M., Leroy, R., Massy, M., Mortier, C., Bron, D., and Lagneaux, L. (2005). Mesenchymal stem cells derived from CD133-positive cells in mobilized peripheral blood and cord blood: proliferation, Oct4 expression, and plasticity. Stem Cells *23*, 1105-1112.

Tropepe, V., Sibilia, M., Ciruna, B. G., Rossant, J., Wagner, E. F., and van der Kooy, D. (1999). Distinct neural stem cells proliferate in response to EGF and FGF in the developing mouse telencephalon. Developmental biology *208*, 166-188.

Turcotte, S., Letellier, J., and Lippe, R. (2005). Herpes simplex virus type 1 capsids transit by the trans-Golgi network, where viral glycoproteins accumulate independently of capsid egress. Journal of virology *79*, 8847-8860.

Tyler, M. A., Ulasov, I. V., Sonabend, A. M., Nandi, S., Han, Y., Marler, S., Roth, J., and Lesniak, M. S. (2009). Neural stem cells target intracranial glioma to deliver an oncolytic adenovirus in vivo. Gene therapy *16*, 262-278.

Tyminski, E., Leroy, S., Terada, K., Finkelstein, D. M., Hyatt, J. L., Danks, M. K., Potter, P. M., Saeki, Y., and Chiocca, E. A. (2005). Brain tumor oncolysis with replication-conditional herpes simplex virus type 1 expressing the prodrug-activating genes, CYP2B1 and secreted human intestinal carboxylesterase, in combination with cyclophosphamide and irinotecan. Cancer research *65*, 6850-6857.

Uccelli, A., Moretta, L., and Pistoia, V. (2008). Mesenchymal stem cells in health and disease. Nature reviews Immunology *8*, 726-736.

Uchida, N., Buck, D. W., He, D., Reitsma, M. J., Masek, M., Phan, T. V., Tsukamoto, A. S., Gage, F. H., and Weissman, I. L. (2000). Direct isolation of human central nervous system stem cells. Proceedings of the National Academy of Sciences of the United States of America *97*, 14720-14725.

Valenta, T., Hausmann, G., and Basler, K. (2012). The many faces and functions of beta-catenin. The EMBO journal *31*, 2714-2736.

Vaupel, P. (2004). Tumor microenvironmental physiology and its implications for radiation oncology. Seminars in radiation oncology *14*, 198-206.

Vescovi, A. L., Galli, R., and Reynolds, B. A. (2006). Brain tumour stem cells. Nature reviews Cancer *6*, 425-436.

Visvader, J. E., and Lindeman, G. J. (2008). Cancer stem cells in solid tumours: accumulating evidence and unresolved questions. Nature reviews Cancer *8*, 755-768.

Wagner, E. K., and Bloom, D. C. (1997). Experimental investigation of herpes simplex virus latency. Clinical microbiology reviews *10*, 419-443.

Wakimoto, H., Johnson, P. R., Knipe, D. M., and Chiocca, E. A. (2003). Effects of innate immunity on herpes simplex virus and its ability to kill tumor cells. Gene therapy *10*, 983-990.

Wakimoto, H., Kesari, S., Farrell, C. J., Curry, W. T., Jr., Zaupa, C., Aghi, M., Kuroda, T., Stemmer-Rachamimov, A., Shah, K., Liu, T. C., *et al.* (2009). Human glioblastoma-derived cancer stem cells: establishment of invasive glioma models and treatment with oncolytic herpes simplex virus vectors. Cancer research *69*, 3472-3481.

Wang, Y., Yang, J., Zheng, H., Tomasek, G. J., Zhang, P., McKeever, P. E., Lee, E. Y., and Zhu, Y. (2009). Expression of mutant p53 proteins implicates a lineage relationship between neural stem cells and malignant astrocytic glioma in a murine model. Cancer cell *15*, 514-526.

Weiss, S., Dunne, C., Hewson, J., Wohl, C., Wheatley, M., Peterson, A. C., and Reynolds, B. A. (1996). Multipotent CNS stem cells are present in the adult mammalian spinal cord and ventricular neuroaxis. The Journal of neuroscience : the official journal of the Society for Neuroscience *16*, 7599-7609.

Weller, M., Wick, W., Hegi, M. E., Stupp, R., and Tabatabai, G. (2010). Should biomarkers be used to design personalized medicine for the treatment of glioblastoma? Future Oncol *6*, 1407-1414.

Wen, P. Y., and Kesari, S. (2008). Malignant gliomas in adults. The New England journal of medicine *359*, 492-507.

Westphal, M., Hilt, D. C., Bortey, E., Delavault, P., Olivares, R., Warnke, P. C., Whittle, I. R., Jaaskelainen, J., and Ram, Z. (2003). A phase 3 trial of local chemotherapy with biodegradable carmustine (BCNU) wafers (Gliadel wafers) in patients with primary malignant glioma. Neuro-oncology *5*, 79-88.

Westphal, M., and Lamszus, K. (2011). The neurobiology of gliomas: from cell biology to the development of therapeutic approaches. Nature reviews Neuroscience *12*, 495-508.

Whitley, R. J., and Roizman, B. (2001). Herpes simplex virus infections. Lancet *357*, 1513-1518.

Willmon, C., Harrington, K., Kottke, T., Prestwich, R., Melcher, A., and Vile, R. (2009). Cell carriers for oncolytic viruses: Fed Ex for cancer therapy. Molecular therapy : the journal of the American Society of Gene Therapy *17*, 1667-1676.

Wong, E. T., and Brem, S. (2008). Antiangiogenesis treatment for glioblastoma multiforme: challenges and opportunities. Journal of the National Comprehensive Cancer Network : JNCCN *6*, 515-522.

Woolard, K., and Fine, H. A. (2009). Glioma stem cells: better flat than round. Cell stem cell *4*, 466-467.

Xu, G., Jiang, X. D., Xu, Y., Zhang, J., Huang, F. H., Chen, Z. Z., Zhou, D. X., Shang, J. H., Zou, Y. X., Cai, Y. Q., *et al.* (2009). Adenoviral-mediated interleukin-18 expression in mesenchymal stem cells effectively suppresses the growth of glioma in rats. Cell biology international *33*, 466-474.

Yamamoto, M., and Curiel, D. T. (2010). Current issues and future directions of oncolytic adenoviruses. Molecular therapy : the journal of the American Society of Gene Therapy *18*, 243-250.

Yang, B., Wu, X., Mao, Y., Bao, W., Gao, L., Zhou, P., Xie, R., Zhou, L., and Zhu, J. (2009). Dual-targeted antitumor effects against brainstem glioma by intravenous delivery of tumor necrosis factor-related, apoptosis-inducing, ligand-engineered human mesenchymal stem cells. Neurosurgery *65*, 610-624; discussion 624.

Yoo, K. H., Jang, I. K., Lee, M. W., Kim, H. E., Yang, M. S., Eom, Y., Lee, J. E., Kim, Y. J., Yang, S. K., Jung, H. L., *et al.* (2009). Comparison of immunomodulatory properties of mesenchymal stem cells derived from adult human tissues. Cellular immunology *259*, 150-156.

Yuan, X., Hu, J., Belladonna, M. L., Black, K. L., and Yu, J. S. (2006). Interleukin-23-expressing bone marrow-derived neural stem-like cells exhibit antitumor activity against intracranial glioma. Cancer research *66*, 2630-2638.

Zhang, Y. F., and Wagner, E. K. (1987). The kinetics of expression of individual herpes simplex virus type 1 transcripts. Virus genes *1*, 49-60.

Zheng, F., Li, X., Zhang, L., Kong, X., Guo, L. Y., Yang, J. Y., Huang, Y. Z., Tang, J. M., and Wang, J. N. (2012). [Effect of conditioned medium of mesenchymal stem cells on proliferation, migration and adhesion of human umbilical vein endothelial cells]. Zhongguo shi yan xue ye xue za zhi / Zhongguo bing li sheng li xue hui = Journal of experimental hematology / Chinese Association of Pathophysiology *20*, 154-158.

Zhou, Y., Larsen, P. H., Hao, C., and Yong, V. W. (2002). CXCR4 is a major chemokine receptor on glioma cells and mediates their survival. The Journal of biological chemistry *277*, 49481-49487.

Zuk, P. A., Zhu, M., Ashjian, P., De Ugarte, D. A., Huang, J. I., Mizuno, H., Alfonso, Z. C., Fraser, J. K., Benhaim, P., and Hedrick, M. H. (2002). Human adipose tissue is a source of multipotent stem cells. Molecular biology of the cell *13*, 4279-4295.

Zuk, P. A., Zhu, M., Mizuno, H., Huang, J., Futrell, J. W., Katz, A. J., Benhaim, P., Lorenz, H. P., and Hedrick, M. H. (2001). Multilineage cells from human adipose tissue: implications for cell-based therapies. Tissue engineering *7*, 211-228.

Personal Scientific Education during the PhD

Abstracts presented at Congresses:

XVI National Meeting on Neuro Oncology, November 2011, Milano, Italy
"Cellule Staminali Mesenchimali guidano il rilascio di BMP2 su cellule primarie derivate da GBM *in vitro*."
S. Bianco, L. Persano, E. Rampazzo, A. Della Puppa, R. Scienza, D. d'Avella, G.Basso

3° Meeting Stem Cell Reaserch Italy Society, June 2012, Ferrara, Italy
"Bone Morphogenetic Protein-2 Enhances the Mesenchymal Stem Cells Migration towards Glioma Cells."
S. Bianco, E. Rampazzo, C. Frasson, A. Della Puppa, L. Persano, G. Basso

Italian Experience in biomedical research: young minds at work, November 2013, Desenzano Sul Garda (BS), Italy
"Set up of different strategies to selectively target Glioblastoma cells."
S. Bianco, D. Sgubin, L. Persano, C. Frasson, Prof. G. Basso, Prof. G. Palù

Oral Presentation:

XVI National Meeting on Neuro Oncology, November 2011, Milano (Italy)
"Cellule Staminali Mesenchimali guidano il rilascio di BMP2 su cellule primarie derivate da GBM in vitro."
S. Bianco, L. Persano, E. Rampazzo, A. Della Puppa, R. Scienza, D. d'Avella, G. Basso

3° Meeting Stem Cell Reaserch Italy Society, June 2012, Ferrara (Italy)
"Bone Morphogenetic Protein-2 Enhances the Mesenchymal Stem Cells Migration towards Glioma Cells."
S. Bianco, E. Rampazzo, C. Frasson, A. Della Puppa, L. Persano, G. Basso

Pubblication:

"Phenotypic and functional characterization of Glioblastoma cancer stem cells identified through 5 aminolevulinic acid-assisted surgery."
E. Rampazzo A. Della Puppa C. Frasson G. Battilana S. Bianco R. Scienza G. Basso L. Persano.
J Neurooncol. 2014